Mechanisms of Inhibitory Synaptic Plasticity: the Regulation of KCC2

by

Brooke Ashley Acton

A thesis submitted in conformity with the requirements
for the degree of Doctor of Philosophy

Department of Cell & Systems Biology
University of Toronto

Mechanisms of Inhibitory Synaptic Plasticity: the Regulation of KCC2

Brooke Ashley Acton
Doctor of Philosophy
Department of Cell & Systems Biology
University of Toronto
2013

Abstract

The mechanisms that regulate the activity of the neuron specific K^+Cl^- cotransporter (KCC2) remain poorly understood, despite the critical importance of this transporter in inhibitory synaptic transmission and plasticity. In this thesis I describe three novel discoveries which reveal the cellular and molecular mechanisms of KCC2 regulation. First, I assayed the K^+Cl^- cotransport function of KCC2 under isotonic conditions and determined the molecular domain of the cotransporter required for constitutive Cl^- transport in hippocampal neurons (Acton et al 2012). Specifically, I identified the 15 amino acid domain of the C-terminus in neurons that is responsible for the ability of KCC2 to cotransport K^+Cl^- under basal isotonic conditions, allowing it to remain constitutively active to create the steep Cl^- gradient across the neuronal membrane required for synaptic inhibition. Secondly, I investigated a novel KCC2-interacting protein named Neto2 and determined its effect on the postsynaptic action of GABA (Ivakine et al 2013). I have found that Neto2, which is also an auxiliary protein of kainate-type ionotropic receptors, can also regulate the activity of the KCC2. Neto2 is required for neurons to maintain low $[Cl^-]_i$ and strong synaptic inhibition. Third, I examined the functional relevance of the KCC2:Neto2:KAR multiprotein complex and found that this complex regulates the surface level membrane expression pattern of KCC2 and the stability of the cotransporter in the membrane.

Moreover, I have provided the first evidence that the interactions of KCC2:Neto2:GluK2 regulate KCC2 via a PKC-mediated phosphorylation of the cotransporter. Taken together, these results resolve three novel mechanisms of KCC2 regulation: the identity of the key C-terminal domain of KCC2 required for isotonic transport, the functional significance of the KCC2:Neto2 interaction, and the potential mechanisms by which the KCC2:Neto2:KAR complex regulates KCC2 expression and mobility in the neuronal membrane.

Acknowledgements

I would like to express my deepest appreciation to my supervisor, Dr. Melanie A. Woodin, who gave me my first opportunity in research and who has generously provided several experiences for me to grow both a scientist and as a person over the last six years in the Woodin Lab. Thank you for being a strong, successful female role model.

As always, tremendous thanks to my parents for the love and the support you have provided throughout the years. Dad, you were my very first role model, teaching me to work hard and to go after what I want in life. Mom, there is not a more patient and accepting person in my world. Thank you for your counsel during all of my stages of self-discovery. And finally, thanks to Will, Rob and Elise, who consistently find ways to enlighten their older sister. Love you all.

List of Contributions

The results presented in Chapter 3 of this thesis have been published in the *Journal of Neuroscience* (2012; 32(25):8746-51). The findings from Chapter 4 have been published in the *Proceedings of the National Academy of Sciences USA* (2013; 2:110(9):3561-6). Finally, the results from Chapter 5 have been submitted to *Cell Reports* (submission #418). All data presented in this thesis are results from experiments that I performed. In addition, a Statement of Authorship is provided at the beginning of each chapter outlining the details of the contributions.

During the course of my work, I have been generously funding by NSERC CGS-M and NSERC CGS-D Vanier Awards.

List of Abbreviations

AMPAR	alpha-amino-3-hydroxy-5-methylisoxazole-4-propionic acid
ANOVA	analysis of variance
AP	action potential
ATP	adenosine triphosphate
ATP1α2	Na^+/K^+-ATPase subunit 1-aplha-2
BDNF	brain derived neurotrophic factor
Ca^{2+}	calcium ions
CA	*Cornu Ammonis*
CCCs	chloride cotransporters
CIP1	cation-chloride cotransporter interacting protein 1
CKB	brain creatine kinase
Cl^-	chloride ions
$[Cl^-]_i$	intracellular chloride concentration
CNS	central nervous system
CUB	complement C1r/C1s, Uegf, and Bmp1
DAPI	4',6-diamidino-2-phenylindole
DIV	day *in vitro*
EC	entorhinal cortex
E_{Cl}	reversal potential for chloride
E_{GABA}	reversal potential for GABA
E_i	reversal potential for an ion
EPSC	excitatory postsynaptic current
EPSP	excitatory postsynaptic potential

Erg4	early growth response 4
FBS	fetal bovine serum
FERM	acronym for 4.1 protein, ezrin, radixin and moesin
GABA	gamma-aminobutyric acid
$GABA_AR$	$GABA_A$ receptor
GFP	green fluorescent protein
GLUK1-5	kainate receptor subunits 1-5
GluR1	glutamate receptor 1
GPSC	GABAergic post synaptic current
HA	influenza hemagglutinin
HCO_3^-	bicarbonate ions
HEK293	human embryonic kidney 293 cells
HEPES	4-(2-hydroxyethyl)-1-piperazineethanesulfonic acid
hKCC2	human potassium chloride cotransporter 2
iGluR	ionotropic glutamate receptor
IPSC	inhibitory postsynaptic current
K^+	potassium ions
KAR	kainate receptor
KCC1-4	potassium chloride cotransporter 1-4
K_m	affinity of KCC2 for extracellular potassium
LDLα	low density lipoprotein receptor domain class A
mAChR	muscarinic acetylcholine receptor
mGluR	metabotrophic glutamate receptor
mGluRI	group I metabotrophic glutamate receptor
Na^+	sodium ions

NEM	sulfhydryl agent N-ethylmaleimide
Neto1	neuropilin-1/tolloid-like protein 1
Neto2	neuropilin-1/tolloid-like protein 2
NKCC1	Na^+-K^+-2Cl^- cotransporter 1
NL2	neuroligin-2
NMDA	N-methyl-D-aspartic acid
NMDAR	N-methyl D-aspartate receptor
NRSE	neuronal restrictive silencing element
PAM	protein associated myc
PBS	phosphate buffered saline
PEST	proline/e(glutamate)/serine/threonine
PKC	protein kinase C
PMA	4β-phorbol 12-myristate 13-acetate
PP1	protein phosphatase 1
PSD95	post synaptic density protein 95
RMP	resting membrane potential
S^{940}	serine 940
SCI	spinal cord injury
SLC12	solute carrier family 12
SPAK	ste20-related proline-alanine-rich-kinase
TARP	transmembrane AMPA regulatory protein
TLE	temporal lobe epilepsy
TM	transmembrane
TrkB	tropomyosin receptor kinase B
V_{hold}	membrane holding potential
V_m	membrane potential
WNK	with no lysine kinase

Table of Contents

List of Figures

Chapter 1

Chapter 2

Chapter 3

Chapter 4

Chapter 5

Chapter 6

List of Tables

Chapter 4

Chapter 1. Introduction

1.1 General Objective

Uncovering the cellular basis of memory formation entails understanding the cellular mechanisms underlying both excitatory and inhibitory synaptic plasticity. Much more is known about the cellular and molecular mechanisms of long term potentiation (LTP) at excitatory synapses. LTP is a long term strengthening of transmission between two neurons which results from synchronous activity between them. However, inhibitory synapses also play an important role in the balance of network activity, making inhibitory plasticity an important area of study. GABAergic (gamma-aminobutyric acid releasing) interneurons generate oscillatory activity, regulate and synchronize the activity of pyramidal cells and set time windows for synaptic integration (Pouille & Scanziani 2001). The same mechanisms that underlie changes in synaptic strength involved in learning and memory, particularly the weakening of inhibitory strength at GABAergic synapses, may also underlie the changes that bring about disease states. Neuropathic pain, neuronal injury, stroke, and epileptic seizures all demonstrate impaired synaptic inhibition (Blaesse et al 2009, Coull et al 2005, Huberfeld et al 2007, Kahle et al 2008, Pathak et al 2007, Payne et al 2003, Woo et al 2002).

Throughout my projects, I aimed to add to the current understanding of the characterization of inhibitory synaptic plasticity (Balena & Woodin 2008, Woodin et al 2003) and to determine the mechanism of regulation for the K^+Cl^- cotransporter KCC2, which plays a critical role in determining the inhibitory action of GABA. The **main objective** of my project was to determine how KCC2 is regulated in hippocampal neurons and how KCC2 regulation affects postsynaptic responses. The regulation of KCC2 controls the functional strength of

inhibitory transmission and has recently been shown to also regulate markers of excitatory synaptic formation.

1.2 The Hippocampus

1.2.1 Hippocampal Structure

The hippocampus sits medial to the cerebral cortex and is part of the limbic system of the brain. The limbic system includes the cingulate cortex, olfactory cortex, and amygdala. The hippocampal formation is composed of three parts: the hippocampus proper, the dentate gyrus, and the subiculum. There are two major neuron types within the hippocampus. Pyramidal neurons are the major population of excitatory neurons and inhibitory interneurons provide the synaptic inhibition of the hippocampus (Andersen, et al. 2007). The hippocampus is routinely used as the brain preparation to study inhibitory transmission.

The hippocampus proper appears as a C-shaped structure in cross section resembling a horn which is why it is referred to as cornu ammonis (CA), meaning Ammon's horn (Ammon is an Egyptian deity, who has the head of a ram). Pyramidal neurons, the principle cells of the hippocampus, make up most of the hippocampal proper. The CA is divided into three sub regions along its curved structure: CA1, CA2 and CA3. Each of these regions has nicely organized layers referred to as strata (**Figure 1.2.2.1A**). These six strata are named: the alveus, the stratum oriens, the stratum pyramidale, the lucidum, the stratum radiatum, and the stratum lacunosum/moleculare. The alveus is the deepest layer of the CA region and contains the axons of pyramidal neurons. The stratum oriens contains the basal dendrites of pyramidal neurons and the cell bodies of inhibitory basket cells. The stratum pyramidale contains the cell bodies of

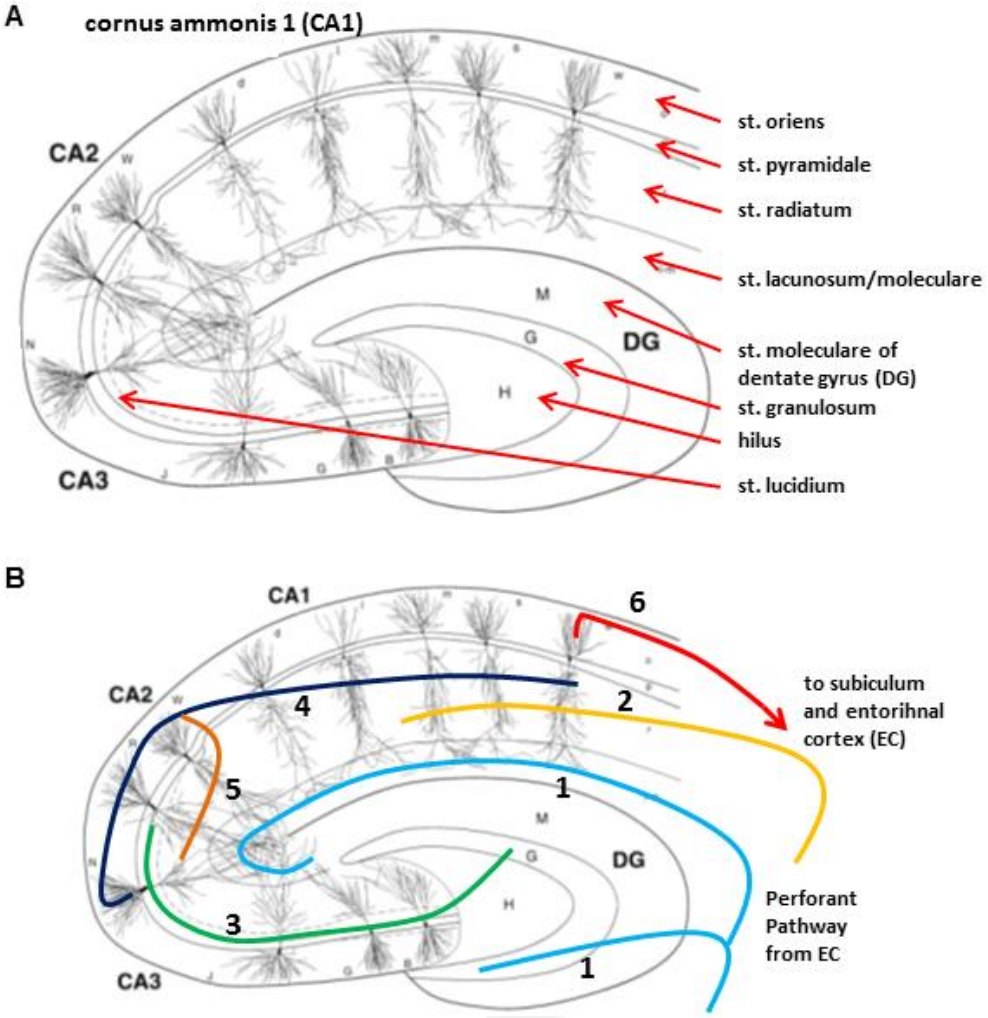

Figure 1.2.2.1 The structure and pathways of the hippocampus. **A**. The structural layers of the hippocampus are labelled (red arrows). **B**. The perforant pathway from the EC projects to the dendrites of DG granule neurons and to the dendrites of CA1 and CA3 pyramidal neurons (**1,2**). Axons from the granule cells in the DG synapse with the proximal dendrites of CA3 pyramidal neurons via mossy fibres (**3**). Axons from CA3 pyramidal neurons synapse with dendrites of CA1 pyramidal neurons via Schaffer collaterals (**4**). CA3 neurons also synapse with themselves through the recurrent commissural pathway (**5**). CA1 pyramidal neurons project their axons to the subiculum and entorhinal cortex (**6**), making up the principal output of the hippocampus (Adapted from Izhizuka et al., 1995).

pyramidal neurons. Only in the CA3 is there the lucidium, the thinnest layer, containing mossy fibers of dentate gyrus cells. The stratum radiatum contains the proximal segments of the pyramidal cell apical dendrites that connect with Schaffer collateral fibers and the axon projections from CA3 pyramidal neurons to the CA1. Lastly, the stratum lacunosum/moleculare contains distal segments of the pyramidal cell apical dendrites that are important for forming a transmission pathway with the perforant path fibers from the entorhinal cortex (Kandel et al. 2000; Paxinos, 2004; Andersen et al. 2007).

1.2.2 Hippocampal Pathways and their Function

The circuitry of the hippocampus is well-defined (**Figure 1.2.2.1B**). In the parahippocampal region of the cortex, information from the visual, auditory and somatic associative cortices collects and transmits through the entorhinal cortex (EC) and into the hippocampus (Kandel et al. 2000; Andersen et al. 2007). In the EC, the information comes in through axons of layers II and III. In layer II, axons project onto granule cells of the dendate gyrus and to the distal dendrites of CA3. This is referred to the perforant pathway because it is here that the axons cross the subiculum to form the input to the hippocampus. The layer II axons form direct synapses with the CA1 pyramidal neurons.

The mossy fiber pathway is made up of the granule cells from the dentate gyrus carrying input from the EC and projecting into the CA3 (Andersen et al. 2007). In the stratum lucidum of the CA3, mossy fibers form large presynaptic terminals onto large spines of the CA3 pyramidal neurons. These axons divide into branches that have two distinct targets: one projecting to additional CA3 neurons through the commissural pathway and one projecting to form synapses with apical dendrites of CA1 neurons via the Schaffer collateral pathway. The principle output of the hippocampus is made up of CA1 neurons sending their axons to the deep

subiculum layers and to the EC, completing the trisynaptic circuit (EC → dentate gyrus → CA3 → CA1)(Amaral & Witter 1989).

In addition to pyramidal neurons and granule cells, the hippocampus has a smaller population of neurons made up of diverse inhibitory interneurons. These interneurons are both morphologically and physiologically diverse (Andersen et al. 2007). Throughout the hippocampus, the interneurons are most involved in local circuitry where a primary role is to balance network activity. GABAergic interneurons generate oscillatory activity, regulate and synchronize the activity of pyramidal cells and set time windows for synaptic integration (Pouille & Scanziani 2001). How the inhibitory response from interneurons onto the postsynaptic neuron is regulated is a major focus of my studies.

One of the reasons that so much research has focused on the inner workings of hippocampal function is because the hippocampus has been deemed the site of long-term memory formation and consolidation in the brain. It was in the mid 1950's that a surgical procedure to remove the medial temporal lobe of a patient named HM, in an attempt to relieve him of debilitating seizures, also left HM devoid of the ability to form new explicit memories with the development of anterograde amnesia (Scoville & Milner 1957). The initial characterization of the unique human model of HM, missing two-thirds of his hippocampal formation, along with additional studies following HM's unique deficits, became the basis for studying the hippocampus as the site of learning and memory formation of the brain (O'Kane et al 2004). Patient HM, now known as Henry Gustav Molaison, died in 2008 and his brain has been sliced for a large-scale anatomical project headed by The Brain Observatory at UC San Diego. Patient HM has perhaps been the most studied patient in the history of medicine (Anand & Dhikav 2012).

1.3 Properties of Chemical Synapses

In the mammalian brain, vast networks of neurons communicate with each other through specialized neuronal structures called the synapse. There are more neuronal synapses in the brain than can be readily imagined; it has been estimated that the 10^{11} neurons in the brain each form anywhere from 1,000 to 10,000 synapses with other neurons (Kandel et al. 2000). The synapse allows information to be passed from one neuron to the next with relative speed but also with spatial precision. This vast network of communicating neurons is responsible for the complex behaviors of mammals.

There are two types of characterized synapses: electrical and chemical. At electrical synapses, gap junctions form membrane channels that allow the flow of ions to pass directly into the next neuron. Each channel formed from adjacent neurons is called a hemi-channel made of connexin proteins. Two hemi-channels form a continuous tunnel for ions to pass between cells, creating the flow of an electrical signal (Connors & Long 2004).

The majority of the synapses in the brain are chemical synapses (Greengard 2001). Chemical synapses lack a continuum between separated neurons and are more complicated, involving a chemical neurotransmitter and both presynaptic releasing mechanisms and postsynaptic receptors. The action potential (AP) arrives in the presynaptic terminal and causes a chemical neurotransmitter to be released, which binds to the postsynaptic receptors to continue the signalling in the postsynaptic neuron and complete the information transfer (Kandel et al. 2000). An AP is a short-lasting electrical event that serves as the method of signal transduction in neurons. The chemical synapse is referred to as excitatory when synaptic activity drives the membrane potential of the postsynaptic neuron above its AP firing threshold or promotes AP

firing. This mode of chemical transmission is most often mediated through neurotransmitters such as glutamate and dopamine. In contrast, chemical synapses are called inhibitory when synaptic activity prevents the postsynaptic neuron's membrane potential from reaching its firing threshold. This mode of chemical transmission is most commonly mediated by neurotransmitters GABA and glycine. So although more complex, chemical synapses have likely evolved because the multi-stage process of transmission allows for more points at which the synapse can be modified, essentially providing more substrates for the modification of synapses which bring about synaptic plasticity.

Both excitatory and inhibitory chemical synapses are composed of a presynaptic neuron and a postsynaptic neuron separated by a 20-40 nm synaptic cleft (Kandel et al. 2000). The presynaptic compartment, called the synaptic bouton, is localized in axon terminals and it contains synaptic vesicles filled with neurotransmitters, with the exception of *en passant* synapses which are synaptic junctions that appear along the axon (Chao et al 2009). A small number of these vesicles are held along the presynaptic plasma membrane at release sites called active zones. Additional vesicles are kept further away from the presynaptic membrane in another pool until needed (Rettig & Neher 2002). Synaptic vesicles are held in the presynaptic active zone by calcium (Ca^{2+}) sensitive vesicle membrane proteins, which bind to various elements of the cytoskeleton. Directly opposite the synaptic bouton is the postsynaptic specialization on the postsynaptic neuron, which contains neurotransmitter receptors, and is most often found on cell bodies or dendrites. The postsynaptic specialization of excitatory synapses is composed of an elaborate complex of interlinked proteins called the postsynaptic density (PSD). The PSD is a specialization of the postsynapse that is dense in protein content. Proteins in the

PSD serve a variety of roles that support neurotransmission, from anchoring neurotransmitter receptors to the membrane to regulating receptor activity (Kennedy 2000, Sheng & Kim 2002).

Synaptic transmission begins when an AP reaches the presynaptic axon terminal and depolarizes the local resting membrane potential. This change results in the opening of a type of voltage-sensing ion channels present on the presynaptic membrane that allow an influx of Ca^{2+} ions into the presynaptic axon terminal, and leads to an increase in the Ca^{2+} concentration in the cytoplasm. This triggers the fusion of synaptic vesicles with the presynaptic plasma membrane. As a result, there is a release of the vesicle neurotransmitter into the synaptic cleft. This marks the conversion of the electrical signal into a chemical signal at the presynaptic terminal (Kandel, Schwartz et al. 2000). Released neurotransmitter diffuses across the synaptic cleft and binds to specific receptors on the postsynaptic membrane. This activates a neurotransmitter receptor resulting in a conformational change and causes channels to open. The subsequent change in conductance alters the membrane potential of the postsynaptic cell. When an ion binds to an ion channel, the receptor is termed ionotropic. The activation of some classes of receptors initiates a metabotropic response that can eventually open an ion receptor. This type of receptor typically involves the activation of secondary messenger systems, and often guanine nucleotide-binding (G) proteins.

If this chemical synapse is excitatory, the ion flux that follows the activation of neurotransmitter receptors leads to a net increase in positively-charged ions within the postsynaptic terminal. This results in a temporary depolarization of the postsynaptic membrane potential referred to as excitatory postsynaptic potential (EPSP), which is a temporary depolarization of the postsynaptic membrane. An EPSP often summates with other EPSPs to drive the neuron's membrane potential toward its AP firing threshold. If it reaches this

threshold, the neuron will fire an AP that will be conducted down the axon and will ultimately result in releasing transmitter on other postsynaptic terminals. In this way, an AP that was converted into a chemical message at the presynaptic axon terminal has been converted back into an electrical signal in the postsynaptic cell. At an inhibitory synapse, receptor activation leads to the production of an inhibitory postsynaptic potential (IPSP) that brings the membrane potential further away from AP firing threshold or shunts excitatory current with a decrease in input resistance.

1.3.1 Neurotransmitters and their Receptors

Neurotransmitters in the central nervous system (CNS) mediate one of two major types of responses: synaptic excitation or synaptic inhibition. Neurotransmitters that are excitatory in action and depolarize the postsynaptic membrane include glutamic acid, acetylcholine, and serotonin. Glutamic acid is also known as glutamate, the most abundant neurotransmitter in the mammalian nervous system and is the transmitter of the vast majority of fast excitatory synapses (Hollmann & Heinemann 1994, McEntee & Crook 1993). At glutamatergic excitatory synapses, there are three classes of ionotropic receptors for glutamate (iGluRs): the *N*-methyl-D-aspartic acid receptors (NMDARs), the α-amino-3-hydroxy-5-methyl-4-isoxazole propionic acid receptors (AMPARs), and the kainate receptors (KARs), named after the synthetic agonists that activate them most effectively (Dingledine et al 1999). Additionally, there are metabotropic glutamate receptors (mGluRs), which have been classified as group I, II, and III mGluRs (Conn & Pin 1997).

Neurotransmitters that are required for inhibitory transmission include primarily GABA and glycine. The main inhibitory neurotransmitter in the CNS is GABA (Bloom & Iversen 1971). At mature synapses, GABA binds to $GABA_AA$ receptors ($GABA_ARs$) and a conformational change in the receptor increases the permeability of the membrane to chloride ions (Cl^-) (Kaila 1994). In addition to the influx of Cl^- through $GABA_ARs$, a small amount of bicarbonate effluxes through the receptor. There are three classes of GABA receptors: $GABA_A$, $GABA_B$ and $GABA_C$. $GABA_A$ and $GABA_C$ receptors are ionotropic and $GABA_B$ receptors are metabotropic. $GABA_BRs$ are G protein-coupled receptors that modulate Ca^{2+} and K^+ channels and elicit relatively slow postsynaptic inhibition (Benarroch 2012). $GABA_BRs$ are broadly expressed in the nervous system and activate a G-protein that ultimately acts to open K^+ channels and hyperpolarize membrane. $GABA_ARs$ are commonly expressed throughout the brain in the postsynaptic membrane of neuronal synapses and are primarily responsible for the fast inhibitory transmission.

In addition to the classic type of phasic inhibition that is rapid, precise and often synchronizes the activity of large populations of cells, there is an alternative type of inhibition. This alternative tonic inhibition is characterized by a consistent activation of $GABA_ARs$ in response to ambient extracellular GABA at a 0.1 -0.4 μM concentration in the synapse (Delgado-Lezama et al 2013, Glykys & Mody 2007, Kuntz et al 2004, Otis et al 1991, Salin & Prince 1996). These receptors are more widespread and are located away from GABA release at the synapses and so have been termed extrasynaptic $GABA_ARs$ (Soltesz et al 1990, Somogyi et al 1989). Generally speaking, extrasynaptic $GABA_ARs$ are δ-subunit containing, but can also be made up of the relatively rare subunits α4, α5 and α6 (Belelli et al 2009, Bianchi et al 2002, Farrant & Nusser 2005, Haas & Macdonald 1999, Saxena & Macdonald 1994). $GABA_ARs$ are

now being targeted to alter the tonic inhibitory current implicated in the disease states of schizophrenia, epilepsy, Parkinson's and chronic pain (Delgado-Lezama et al 2013).

1.3.3 Neurophysiological Membrane Properties

The regulation of neuronal Cl^- in the hippocampus ultimately leads to changes that contribute to the neurophysiological properties of individual neurons and determines the activity of that neuron. These neurophysiological membrane properties include resting membrane potential (RMP), AP threshold and the reversal potential for a specific ions (E_i). RMP is determined by the difference in potential across the cell's membrane when the cell is in its steady-state and not firing an AP. The RMP is mostly determined by the cell membrane's high permeability for potassium ions (K^+) in an outward gradient. RMP is typically close to -65 mV for mature hippocampal neurons (Kandel & Spencer 1961, Segal 1983). Although the RMP is mostly determined by the dominating K^+ current, it is also determined by the sum total of equilibrium potentials for all ions at rest to which a cell is permeable and by the movement of ions by the ATP pumps. In addition to K^+, the neuronal membrane is also slightly permeable to sodium (Na^+) at rest.

E_i is the membrane potential at which there is no net flow of that ion species across the membrane. As described, the RMP of the cell lies close to the equilibrium potential for K^+. When the neuronal membrane becomes highly permeable to another ion, the membrane potential (V_m) shifts towards the E_i for that ion species. This results in a depolarization (becoming more positive) or hyperpolarization (becoming more negative) of V_m. When an ion channel is gated by a neurotransmitter, the equilibrium potential is called the reversal potential.

At an excitatory synapse, the firing of an AP will occur if the V_m depolarizes past the AP threshold. Excitation occurs if the postsynaptic current is sufficient to bring the V_m to AP threshold. For neurons in the hippocampus, the AP threshold is between a membrane potential of -50 to -35 mV (Rushmore et al 1998, Vukicevic & Kellenberger 2004). During the steady resting state, the V_m is far away from the E_{Na+}. The driving force for an ion is the difference between the V_m and E_{Na+} (the E_{Na+} is close to +50 mV). Thus, an increase in permeability of the membrane to E_{Na+} will depolarize V_m past threshold.

If the current hyperpolarizes the V_m or prevents AP firing, then it is described as inhibitory. It is not the $GABA_AR$ that is responsible for rendering the neurotransmitter GABA inhibitory in its functional effect. The opening of the Cl^- permeable $GABA_AR$ results in a conductance that is ultimately determined by the driving force for Cl^-. Therefore, the inhibitory action of GABA is not determined by this neurotransmitter binding to $GABA_ARs$ but is determined by the pre-existing driving force for Cl^- that has been established across the plasma membrane. When GABA binds to the $GABA_AR$, Cl^- flows down its electrochemical gradient according to its driving force. The V_m at which there is no net flux of ions through the $GABA_AR$ is the reversal potential for GABA (E_{GABA}).

Two cation-chloride cotransporters are primarily responsible for establishing the Cl^- gradient in neuronal cells: the Na^+ K^+ $2Cl^-$ cotransporter NKCC1 and the K^+ Cl^- cotransporter KCC2. Both NKCC1 and KCC2 are members of the cation-chloride cotransporter gene family SLC12 (solute carrier family 12) (Mercado et al 2004). NKCC1 brings Cl^- into the cell by secondary active transport that uses the energy from the Na^+ gradient generated by the Na+:K+:ATPase pump (Gamba et al 1993). The ATPase is an enzyme that catalyzes the reaction that converts ATP → ADP to release energy to drive its own transport. KCC2 functions to lower

intracellular levels of Cl^- ($[Cl^-]_i$) by using the energy from the K^+ gradient to transport Cl^- against its electrochemical gradient so that Cl^- is low inside the cell (Payne 1997).

The $GABA_AR$ is not only permeable to Cl^-, but also to bicarbonate (HCO_3^-). However, the permeability ratio of the $GABA_AR$ to $HCO_3^-$and Cl^- is approximately 0.2-0.4 (Kaila 1994), which means that the HCO_3^- current through the receptor plays a much smaller role than Cl^- in creating the postsynaptic response. The reversal potential for HCO_3^- is drastically more depolarized than for Cl^-, sitting around -10mV, resulting in a depolarizing component of the response to $GABA_AR$ channel opening.

Early in development of the nervous system, GABA is an excitatory neurotransmitter. This is because NKCC1 is the dominant transporter in the membrane at this stage of development (Delpire 2000). NKCC1 raises $[Cl^-]_i$, which depolarizes E_{GABA}; thus when GABA binds the $GABA_AR$, it opens to let Cl^- leave the cell. The efflux of Cl^- can depolarize the membrane above the AP threshold, rendering GABA excitatory. During early postnatal life, KCC2 becomes upregulated in neuronal membranes (Rivera et al 2005, Rivera et al 1999). In the rodent hippocampus, KCC2 upregulation occurs between the seventh and tenth postnatal day (Rivera et al 1999). This event corresponds with the shift from excitatory to inhibitory GABAergic transmission. After this developmental threshold, KCC2 is responsible for creating a strong inward electrochemical gradient for Cl^-. This results in the hyperpolarization of E_{GABA} and the mature inhibitory action of GABA (**Figure 1.3.3.1**).

There has been a debate about whether the developmental upregulation of KCC2 is dependent on activity levels or whether is it biologically predetermined. Some studies support the hypothesis that depolarizing GABAergic activity early in development is required for the developmental shift to hyperpolarizing GABAergic transmission and that GABA itself signals

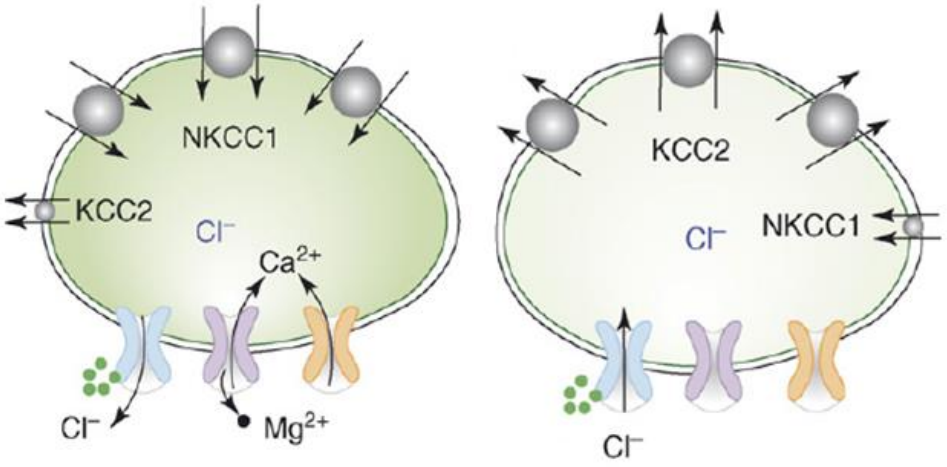

Figure 1.3.3.1. The development of GABAergic transmission in hippocampal neurons. A developmentally immature neuron, with high NKCC1 expression has high $[Cl^-]_i$ (**left**). Subsequent $GABA_AR$ activation results in Cl^- efflux. A developmentally mature neuron (**right**), with KCC2 expression has low $[Cl^-]_i$ as a result of KCC2 expression. $GABA_AR$ activation now results in Cl^- influx. Modified from Fiumellli and Woodin, 2007.

this transition by acting as a self-limiting factor. Several studies have shown *in vivo* and *in vitro* that blocking $GABA_A$Rs both delays the switch in excitation and inhibition and also slows the upregulation of KCC2 (Ganguly et al 2001, Leitch et al 2005, Vu et al 2000). However, two other studies have shown that blocking $GABA_A$R activation had no effect on the time course of KCC2 upregulation (Titz et al 2003) or the developmental hyperpolarization of E_{Cl} (Ludwig et al 2003). These studies propose that mechanisms for blocking GABAergic transmission used in some studies actually mimics neuronal injury, and through this mechanism, prevents KCC2 upregulation. Regardless, the role of activity in the developmental switch still remains elusive.

Recently, it has been proposed that the excitatory action of GABA early in development may be due to an experimental artifact (Bregestovski & Bernard 2012). This suggestion is based on the idea that electrophysiological recordings from standard hippocampal slices are made from neurons that are energy deficient because they are glucose-perfused without endogenous ketone body metabolites (lactate or pyruvate). Perfusing slices with these energy substrates hyperpolarizes E_{GABA} (Holmgren et al 2010, Zilberter et al 2010). Moreover, these same authors also propose that the slicing procedure damages neurons causing $[Cl^-]_i$ to raise (Dzhala et al 2012) and therefore, neurons in slice requires additional high energy substrates (Bregestovski & Bernard 2012).

A recent review article outlines the large body of evidence supporting the validity of the developmental shift in E_{GABA} (Ben-Ari et al 2012b). The developmental shift is not exclusive to slice or even rodents and observations of this shift extend from invertebrates to humans both *in vitro* and *in vivo*. The idea that ketone bodies metabolites are more physiologically relevant and mimic maternal milk is refuted by the fact that the depolarizing shift occurs in non-mammalian species ranging from zebrafish, turtles, chickens to tadpoles (Akerman & Cline 2006, Gonzalez-

Islas et al 2010, Gonzalez-Islas et al 2009, Leitch et al 2005, Reali et al 2011, Sernagor et al 2003, Zhang et al 2010). Several studies looking at KCC2 expression patterns also support the idea that there are changes in KCC2 oligomerization and expression during the second postnatal week which correlates with the hyperpolarization of GABAergic transmission (Blaesse et al 2006, Gulyas et al 2001, Uvarov et al 2009, Watanabe et al 2009). In addition, there are several lines of criticism for the experimental design from Zilberter et al. (2010) including the fact that use of 2-4mM pyruvate in their experiments is 20-40 fold higher than physiological concentrations of pyruvate and this condition drastically changes pH, which directly impacts $[Cl^-]_i$ (Ben-Ari et al 2012b).

1.4 Chloride Regulation

1.4.1 Classification of K^+Cl^- cotransporters

K^+Cl^- cotransporters (KCCs) belong to a superfamily of Cl^- cotransporters that transport Cl^- and cations in the same direction to regulate cell volume, to regulate excretion processes and to provide an electrochemical Cl^- gradient for neuronal signalling (Gamba 2005, Payne 1997). These ion cotransporters exist in many parts of the body throughout many organisms with evolutionarily conserved structure and function (Lauf & Adragna 2004). KCC1, KCC2, KCC3 and KCC4 are the four family members that have been elucidated to date, each differing in properties such as expression pattern and molecular weight. However, all four members are alike in transporting Cl^- along with K^+ in a 1:1 stoichiometric ratio across the membrane, contributing to the K^+ and Cl^- gradients but without altering membrane potential because the net effect of cotransport is electroneutral (Gamba 2005). Transporting K^+ and Cl^- out of the cell is

favoured because of the strong outward K^+ gradient, but these cotransporters are capable of reversing transport direction (Russell 2000). This thermodynamic favourability is what makes these cotransporters ideal for their role in cell volume regulation.

KCC2 is the cotransporter that is the focus of this thesis because it is uniquely brain-specific and its primary role in the brain is to regulate neuronal Cl^- and maintain fast synaptic GABAergic inhibition (Payne et al 1996, Rivera et al 1999). In an initial observation, it was determined that the driving force of Cl^- was completely abolished when KCC2 is knocked down, proposing the role of KCC2 in setting the steep Cl^- gradient that is responsible strong GABAergic inhibition (Claudio Rivera 1999, Rivera et al 1999). More recently, the neuronal restrictive silencing element (NRSE), responsible for KCC2's neuronal-specific expression, was identified in intron 1 in humans and in mice (Karadsheh & Delpire 2001) and its expression during development is tightly correlated with inhibitory responses to GABA (Ben-Ari 2002).

KCC2 expression has been found in nearly every brain structure examined but is not expressed in non-neuronal cells such as glia and astrocytes (Blaesse et al 2009, Hubner et al 2001, Li et al 2002, Williams et al 1999). KCC2 is also expressed in the spinal cord of the CNS (Payne et al 1996). During development, the expression of KCC2 follows a caudal-rostral directional expression corresponding to neuronal maturation patterns (Ikeda et al 2003, Li et al 2002, Stein et al 2004, Wang et al 2002), where KCC2 expression is only detected in differentiated neurons and not in neuronal precursors (Li et al 2002).

It is important to mention that in addition to SLC12A family of proteins and GABARs there have been various Cl^- channels identified in neurons. Additional sources of Cl^- permeability in neurons include the CLC-2 inward rectifying voltage-gated Cl^- channel (Jentsch et al 2002, Staley 1994), the Ca^{2+}-activated chloride channel (CaCC) (Schroeder et al 2008) and

the volume-sensitive outwardly rectifying Cl^- channel (VSOR)(Inoue & Okada 2007). ClC-2 mediates a slow inward rectifying chloride conductance that opens upon hyperpolarization, cell swelling and mild extracellular acidification (Grunder et al 1992, Thiemann et al 1992, Zuniga et al 2004). CaCCs, present in hippocampal neurons, are activated by NMDA-mediated Ca^{2+} influx to reduce EPSPs and increase the threshold of spike generation (Huang et al 2012). VSOR Cl^- channels have also been reported to be activated by NMDA exposure and have been proposed to play a role in mediating an anionic recovery pathway in response to excitotoxicity (Inoue & Okada 2007). It is important to keep in mind the various sources of neuronal Cl^- permeability in under various conditions.

1.4.2 Functional Role of KCC2

The Role of KCC2 in Inhibition

Shortly after KCC2 was proposed to be brain specific, the colocalization of KCC2 and $GABA_AR$ subunits β2/β3 suggested that KCC2 may be involved in GABAergic transmission (Williams et al 1999). As initially suggested, the intracellular Cl^- concentration is determined primarily by two co-transporters, NKCC1 and KCC2 (Gamba 1999, Loscher et al 2013, Mount et al 1998, Mount et al 1999, Rivera et al 2005) where NKCC1 brings K^+ and Cl^- ions into the cell and KCC2 exports these ions. The E_{Cl} of a particular neuron is determined by the expression levels and the regulation of these two transporters. In this way, KCC2 is important for setting the driving force for Cl^- which determines the strength of inhibition by controlling the net flow of Cl^- ions into the cell upon GABA binding the $GABA_AR$ and the subsequent hyperpolarization of

the membrane. Approximately 10 days after birth, the expression of NKCC1 is lowered and KCC2 expression drastically upregulates (Li et al 2002, Wang et al 2002), which is responsible for the reduction in $[Cl^-]_i$ and in rendering the action of GABA inhibitory (Owens et al 1996, Rivera et al 1999). It has been shown that overexpressing human KCC2 in cortical neurons is sufficient to change GABAergic responses from depolarizing to hyperpolarizing (Lee et al 2005b). This developmental shift in the Cl^- electrochemical gradient has been observed in nearly all brain structures and organisms examined, however, there is considerable variation in the developmental time course of KCC2 expression among brain structures both within a species and across species (Ben-Ari 2002). KCC2 is important for maintaining E_{GABA} and determining fast synaptic GABAergic responses in the postsynaptic neuron, but KCC2 also plays several other roles in cellular homeostasis (Gamba 2005).

KCC2 Buffers Extracellular K^+

KCC2 buffers extracellular K^+ and regulates cell volume in neurons, ultimately promoting neuronal survival (A. I. Gulyas 2001, Payne 1997). KCC2 has a low K_m value for K^+ (K_m = 5.2mM), indicating its sensitivity to subtle changes in extracellular K^+ levels. In response to sustained activity in neurons, K^+ levels build up outside the cell. Because KCC2 has a high affinity for $[K^+]_o$, this subtle increase causes KCC2 to reverse transport and buffer K^+. This is a mechanism for neuronal response to depleted $[K^+]_i$ supplements the well characterized mechanisms of K^+ buffering by the Na^+-K^+-ATPase and glial cells (Walz 1989).

KCC2 Regulates Cell Volume

KCC2 and its family members play critical roles in cell volume regulation. All four of the KCCs are swelling-activated, which initially suggested an important role for the KCCs in volume regulation (Lauf & Bauer 1987b). Back in the 1980s, K^+Cl^- cotransport was first defined in red blood cells as a swelling-activated mechanism (Dunham & Ellory 1981, Lauf & Theg 1980). It was then identified that these cells express KCC1 (Su et al 1999), KCC3 (Lauf et al 2001), and KCC4 (Crable et al 2005). The loss of KCC3 provides compelling evidence of the role of the KCCs in cellular volume regulation. Targeted deletion of KCC3 abolishes the volume regulatory decrease in renal proximal tubular cells and prevents hippocampal neurons from being able to sustain volume regulatory decreases (Boettger et al 2003).

Cellular processes such as cell differentiation and apoptosis undergo major changes in cell volume regulation. For example, KCC1, KCC3 and KCC4 are all involved in the volume regulatory changes that are required for proper erythropoiesis (Pan et al 2011). In the brain, KCC2 plays an important role in cell volume regulation. KCC2 has been shown to reduce cell swelling from large influx of ions at dendritic spines resulting from neuronal activity (Gulyas et al 2001). KCC2 is also more sensitive to osmolarity and $[Cl^-]_i$ than other members of its family (Bergeron et al 2006), equipping the cotransporter with the ability to tightly regulate neuronal cell volume. When ions are transported across the plasma membrane, this action moves water molecules through ion channels too. Therefore, KCC2 also plays an additional role in homeostasis by indirectly regulating water movements during ion transport (Gamba 2005). It has been hypothesized that NMDA activation triggers the influx of water through both ionotropic receptors and NKCC1, while delayed response in KCC2 activation is responsible for the efflux of water, all working as a mechanism to regulate the movement of water during synaptic

transmission (Jourdain et al 2011). This role of KCC2 in moving water across the neuronal plasma membrane is especially important because neurons have been shown to lack aquaporins, which are used by other cell types to regulate osmotic stress (Amiry-Moghaddam & Ottersen 2003, Andrew et al 2007).

KCC2 Regulates the Excitatory Synapse

Recently, KCC2 has also been found to play a role at dendritic spines of excitatory synapses (Fiumelli et al 2013, Gauvain et al 2011, Grégory Gauvain 2011 , Li et al 2007). A growing body of evidence supports the notion that KCC2 plays a critical role in the maintaince and formation of excitatory synapses, which is independent of its Cl^- transport ability. When KCC2 expression is suppressed during development, the maturation of dendritic spines does not occur, sustaining dendritic protrusions that have long and motile branches (Li et al 2007). Normally, the C-terminus of KCC2 binds the FERM domain of protein 4.1N to stabilize mature dendritic spines. *In vivo*, premature expression of KCC2 increases spine density and correlates with increased spontaneous excitatory activity (Fiumelli et al 2013). Adding to the understanding of this mechanism, suppression of KCC2 expression decreases the efficacy of excitatory transmission in hippocampal neurons by decreasing the aggregation and increasing lateral diffusion of GluR1-containing AMPA receptors (Gauvain et al 2011). Interestingly, the consensus is that the role KCC2 plays at the excitatory synapse is structural and independent of its Cl^- transport function.

1.4.3 Structure and Properties of KCC2

The family of SLC12A genes encodes the four KCCs, which share a 65-75% identity, a common predicted topology, and a large glycosylated extracellular loop between transmembrane domains 5 and 6 (Mount et al 1999). The differences in these family proteins lie in their ion affinities and sensitivities to transport inhibitors (Mercado et al 2000, Mercado et al 2005, Song et al 2002). However, KCC2 is the only family member that cotransports K^+Cl^- under isotonic conditions in neurons. The SLC12A5 gene, encoding KCC2, is over 30kb in size and contains 24 exons (Sallinen et al 2001). The KCC2 gene has arisen from duplication of genes encoding channel-type protein subunits with fewer transmembrane segments (Saier 2003). In the rat, KCC2 has been found to be made of 1116 amino acids with a molecular weight of approximately 140 kD (Blaesse et al 2006, Uvarov et al 2009).

The KCC2 gene generates two isoforms of the cotransporter, KCC2a and KCC2b (Uvarov et al 2007). KCC2 has a splice variant, KCC2a, consisting of 40 different amino acid residues in the N-terminus but this splice variant only accounts for 10% of the total KCC2 levels in the mature mouse cortex. The isoforms are generated by alternative promoters and the first exon usage. During development, the expression levels of KCC2a remain relatively constant across the cortex and hippocampus, whereas mRNA levels of KCC2b strongly increase. Thus, the reported developmental upregulation of KCC2 is mostly determined by the isoform KCC2b (Uvarov et al 2007, Uvarov et al 2009).

The intracellular N-tail and C-tail of KCC2 are believed to contain regulatory phosphorylation sites for the transporter (Chamma et al 2012, Payne et al 1996, Strange et al 2000) (**Figure 1.4.3.1**). These hydrophobic regions contain putative phosphorylation sites for protein kinase C (PKC) (Thr^{34}, Ser^{728}, Thr^{787}, Ser^{940} and Ser^{1034}) and for tyrosine kinase

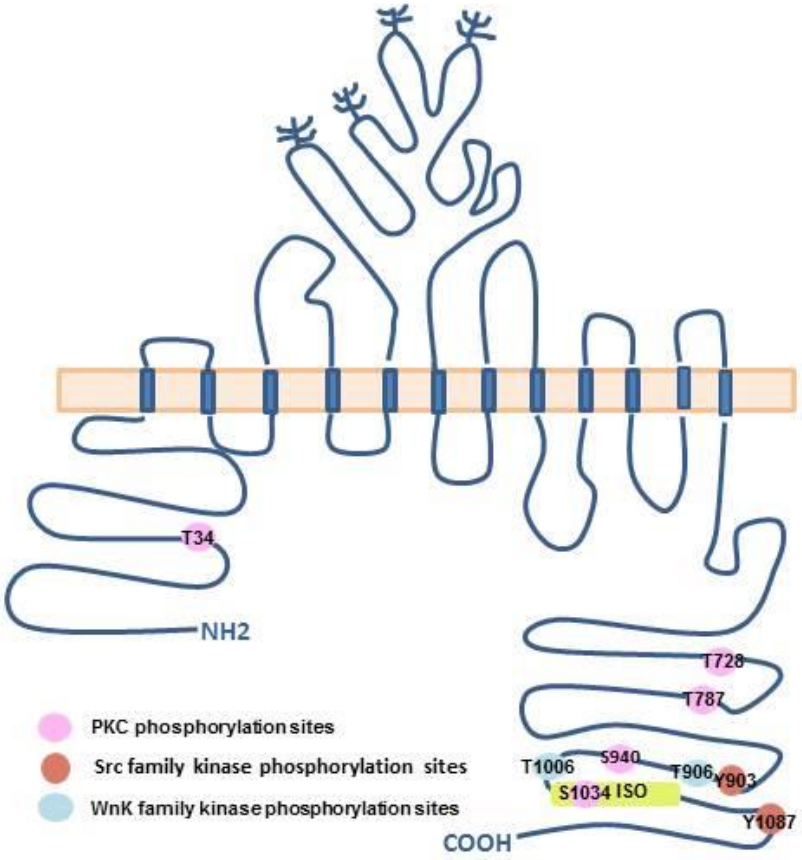

Figure 1.4.3.1. The structure of KCC2. Cartoon of the rat KCC2 K^+Cl^- cotransporter. KCC2 is a ~140kDa protein with a predicted 12 transmembrane topology. It contains several phosphorylation sites on its two large intracellular regions that serve as putative functional regulation sites. Adapted from Chamma et al., 2012.

phosphorylation (Tyr^{1087}). Among the KCCs, Tyr^{1087} is highly conserved while Ser^{940} is unique to KCC2, contained in its extra exon of the SLC12A5 gene (Payne et al 1996). Regions of the C-tail have also been identified as interacting with potential regulatory effectors (Bergeron et al 2006) and cytoskeleton-associated proteins (Li et al 2007). The C-terminal tail has proven to be important for regulating ion transport through kinases and for maintaining structural integrity of neuronal spines (Li et al 2007).

The unique C-terminal region of KCC2 also contains a 15 amino acid domain that is thought to be responsible for a unique function of KCC2 – its ability to constitutively transport K^+Cl^- under isotonic conditions. However, this was demonstrated with chimeric cDNA constructs overexpressed in *Xenopus* oocytes (Mercado et al 2006a). As described in detail in the sections to follow, I have determined that this ISO domain is required for isotonic K^+Cl^- cotransport in hippocampal neurons (Acton et al 2012).

KCC2 contains 12 transmembrane (TM) domains (Williams et al 1999). KCC2 and KCC1 are the most similar in these transmembrane domains with over 90% identity. Across all SLC12A family members, TM2 and TM3 are highly conserved (Payne et al 1996). There is some evidence that these TM domains are involved in determining ion affinity (Russell 2000).

In addition to this emerging structure of KCC2, there is a very large and prominent extracellular loop between TM5 and TM6 which is glycosylated at four positions (Payne et al 1996, Williams et al 1999). The glycosylation increases the molecular weight by approximately 15% and can be reversed by N-glycoside (Williams et al 1999). It is hypothesized that glycosylation is involved in regulating the cotransport of ions, but the exact role of glycosylation between TM5 and TM6 still remains unknown.

KCC2 is sensitive to a variety of pharmacological agents. To activate KCC2, it can be treated with 1mM NEM which is hypothesized to take action through sulfhydryl modification of the protein with the binding site still to be determined (Lauf et al 1985). KCC2 can be inhibited by loop diuretics and is more sensitive to furosemide (20μM) than to bumetanide (55μM) (Payne 1997). It is hypothesized that loop diuretics work via the TM2 and TM3 domains of the KCCs, since these are the most conserved regions and their actions are similar between the family proteins (Gagnon et al 2004). Recently, a KCC2 selective inhibitor was identified, refined and named VU0463271 (Delpire et al 2012). This antagonist has over 100 times more affinity for KCC2 than NKCC1.

The molecular determinants of swelling activation of the KCCs have not been elucidated. One clue to the molecular mechanism of swelling activation of cotransport is that in red blood cells, the function of all four KCCs is completely lost by the inhibition of protein phosphatase-1 with calyculin A (Mercado et al 2000, Mercado et al 2005, Song et al 2002, Starke & Jennings 1993, Strange et al 2000, Su et al 1999). A more recent publication has implicated the WNK4 and SPAK serine-threonine kinases in the volume sensitivity of both KCC2 and NKCC1 cotransport (Gagnon et al 2006).

KCC2 has several characteristics that differentiate it from the other three KCCs. While all K^+Cl^- cotransporters are activated by cell swelling (Lauf and Bauer, 1987; Flatman, 2008), KCC2 is the only family member that is also able to extrude Cl^- in the absence of osmotic stress. The other three KCCs are exclusively swelling-activated, without significant activity under isotonic conditions. KCC2 is, however, also swelling-activated under hypotonic conditions (Strange et al 2000). KCC2 contains a unique domain of ~100 amino acids, rich in prolines, serines, and charged residues, near the end of the cytoplasmic C-terminus. This region

encompasses two predicted Proline/Glutamate/Serine/Threonine (PEST) sequences (Rechsteiner & Rogers 1996). This, in combination with the fact that KCC2 has the most clearly defined physiological role of the four KCCs, suggests that there are molecular determinants of the isotonic transport function of KCC2. The determination of the molecular determinants of constitutive K^+Cl^- cotransport mediated by KCC2 represents a large gap in our fundamental knowledge regarding neuronal Cl^- regulation and inhibitory synaptic transmission. This topic is further explored in Chapter 3 of the Results section.

1.4.4 Protein Interactors of KCC2

Until recently, few proteins had been shown to interact with KCC2. CCC-interacting protein 1 (CIP1) was first identified as a third category of the CCC family because it shares 25% amino acid identity to other CCCs and was shown to inhibit NKCC1 function in a heterologous system (Caron et al 2000). Since then, CIP1 has been shown to directly interact with KCC2 in HEK293 cells and activate the cotransporter, ultimately acting as a reciprocal regulator of KCC2 and NKCC1 (Wenz et al 2009). The expression of CIP1 fits this profile, being ubiquitously expressed both early and later in development, when NKCC1 and KCC2, respectively, play dominating roles in Cl^- transport.

In the brainstem, ATP1α2 plays a critical role during development through its interaction with KCC2, determined by coimmunoprecipitation (Ikeda et al 2004). ATP1α2$^{-/-}$ animals die shortly after birth due to high $[Cl-]_i$ in neurons of the ventrolaterial medulla, detected by gramicidin-perforated patch-clamp recordings. However, the significance of the ATP1α2-KCC2

interaction may be limited to the brainstem, since it has not been demonstrated in any other brain area to date.

CKB has also interacts with KCC2, as first demonstrated by yeast two-hybrid screening *in vitro* (Inoue et al 2004b). These authors later showed that the interaction of KCC2 with brain-type creatine kinase increased the transport activity of KCC2 in heterologous HEK293 cells (Inoue et al 2006a). In addition, the protein associated with Myc (PAM) is a KCC2 interactor, where a study utilizing Rb^+ flux assays determined that PAM-KCC2 interaction increases KCC2-mediated flux (Garbarini & Delpire 2008). These studies are limited by solely exploring the role of these interacting proteins in expression systems and have not demonstrated the physiological significance of these interactions in neurons.

Recently, it has been shown that neuroligin-2 (NL2), a protein that plays a role in cell adhesion regulating GABAergic synaptogenesis, also regulates the expression of KCC2 (Sun et al 2013). When NL2 is knocked down, KCC2 expression levels are decreased and E_{GABA} depolarizes. In development, the knocking down of NL2 results in a delay of the GABAergic developmental switch. In the heterologous expression system, there was no evidence of direct interaction.

KCC2 plays an important role in maintaining dendritic spines at excitatory synapses where it binds to the spectrin-actin binding scaffolding protein 4.1N (Li et al 2007). Interestingly, 4.1N has recently been identified as an interactor of the GluK1 and GluK2 subunits of KARs (Copits & Swanson 2013). The C-terminal interaction of these KAR receptor subunits to 4.1N has is important for the cell surface expression and endocytosis of GluK1 and GluK2. PKC also regulates the interaction of KARs with 4.1N.

1.4.5 Transcriptional and Post-Translational Regulation of KCC2

KCC2 plays a critical role in CNS function, therefore, understanding the regulation of KCC2 in neurons is essential. To date, the regulation of KCC2 is still not well understood. In the past few years, many studies have turned their focus to the transcriptional regulation and the post-translational modification of KCC2.

KCC2 is uniquely regulated at the transcriptional level to ensure it is only expressed in neurons. An NRSE within intron 1 of the KCC2 gene silences reporter gene activity in non-neuronal cells (Karadsheh & Delpire 2001). Within this 21-base pair promoter region, the early growth factor 4 (Egr4) binds Egr4 proteins (Uvarov et al 2006). This factor has been proposed to play an important role in the developmental up-regulation of KCC2, because the expression of KCC2 can be reduced by antisense knockdown of Egr4 or from the addition of a dominant-negative form of Egr4. However, many details are left to be elucidated regarding the transcriptional regulation of KCC2. What other regulatory proteins contribute to the RNA polymerase complex?

To date, the kinases identified to be involved in the post-translational phosphoregulation of KCC2 are CKB, with no lysine kinases (WNKs), protein kinase C (PKC), and tyrosine kinase. CKB is an ATP-generated enzyme that interacts directly with KCC2 and activates KCC2 when they are coexpressed in HEK293 cells (Inoue et al 2004a, Inoue et al 2006b, Mahajan et al 2000). Tyrosine phosphorylation reduces the cell surface stability and activity of KCC2 during neuronal stress (Wake et al 2007a). WNK3 from the family of WNK serine/threonine kinases, is responsible for down-regulating KCC2 (Kahle et al 2010). Also, proteins commonly regulated

by PKC activation are involved in regulating regions of the C-terminus of KCC2 (Bergeron et al 2006).

CKB interacts, as described above, with KCC2 (Inoue et al 2004a). It was determined that amino acids 1048-1114 are critical for this interaction. Although, it is not clear what the exact role of CKB is in regulating KCC2, it is known that CKB primarily regenerates ATP sources and that CKB can exist both as a cytosolic protein and as a membrane bound protein (Crawford et al 2002, Mahajan et al 2000, Wyss & Kaddurah-Daouk 2000). CKB was shown to shift the reversal potential of glycine and GABA when gramicidin perforated patch recordings were made in HEK293 cells and in cortical cultured neurons (Inoue et al 2006a). Both of these studies indicate that CKB may indirectly activate KCC2 by changing the K^+ gradient through the generation of ATP or CKB may be present for the use of other KCC2 regulatory kinases. Another study shows that CKB also interacts with C-terminus of KCC3 when screened using a yeast two-hybrid approach, but the function of this interaction has not been elucidated (Salin-Cantegrel et al 2008).

PKC plays a critical role in directly regulating KCC2 function (Lee et al 2011, Lee et al 2007). Using both coexpression in HEK293 cells and a *Escherichia* coli expression with in vitro kinase assay, PKC was shown to directly phosphorylate S^{940} located within the C-terminal cytoplasmic tail of KCC2. By measuring the rate of internalization, S^{940} phosphorylation has been shown to increase cell membrane stability. Furthermore, this phosphorylation site also results in an increase in ion transport as measured by Rb^+ flux assay. Together, this work identifies PKC and S^{940} as an important regulatory pathway in KCC2 function. These results stand in contrast to two initial studies focusing on the role of PKC-mediated actions in the

downregulation of KCC2 cotransport function (Bergeron et al 2006, Fiumelli et al 2005). However, these studies did not address the direct role of PKC in phosphorylating S^{940}.

S^{940} is also involved in a mechanism underlying pathophysiological glutamate release that is observed in several disease states (Lee et al 2011). These authors determined that NMDA receptor activity and Ca^{2+} influx caused the dephosphorylation of S^{940} leading to a loss of KCC2 function. Protein phosphatase 1 (PP1) mediated the dephosphorylation events of S^{940} that coincided with a deficit in hyperpolarizing GABAergic inhibition due to the loss of KCC2 activity. This study points to the significance of targeting the post-translational states of KCC2 in treating diseases that are characterized by hyperexcitability and the loss of inhibition. Another study links the dephosphorylation of S^{940} to the reduction in KCC2 cotransport function in response to stress (Sarkar et al 2011). Interestlingly, group I metabotropic glutamate receptors (mGluR1s) have been shown to rapidly increase KCC2 transport function through a PKC-mediated mechanism (Banke & Gegelashvili 2008).

Tyrosine phosphorylation of the C-terminal of KCC2 also plays a role in membrane surface stability of the protein (Lee et al 2010). Using HEK293 cells, this group identified the major phosphorylated tyrosine residues to be Y^{903} and Y^{1087} and determined that when these sites are phosphorylated, KCC2 remains less stable in the membrane and experiences an increase in lysosomal degredation. Further, this lysosomal degredation can be triggered indirectly by activation of mAChRs in hippocampal culture with pilocarpine that enhance tyrosine phosphorylation. Interestingly, pilocarpine has previously been used to induce seizures. Thus, tyrosine phosphorylation may underlie the pathological mechanism for the loss of functional KCC2, such as in epilepsy.

Another tyrosine phosphorylation site, Y^{1087}, regulates the oligomerized form of KCC2 and its association with lipid rafts (Watanabe et al 2009). When Y^{1087} is mutated, E_{GABA} depolarizes and the characteristic punctae staining of KCC2 becomes more diffuse. In addition, this same study found that when tyrosine phosphorylation was inhibited, an increased population of KCC2 became associated with lipid rafts and KCC2 of the oligomerized form decreased. It has previously been shown that throughout postnatal development, the ratio of KCC2 oligomers to monomers increases, correlating with the upregulation of active KCC2 (Blaesse et al 2006). Thus, the oligomeric form of KCC2 is the mature, active form of the cotransporter. Disrupting membrane rafts strongly activates KCC2 (Hartmann et al 2009). This data provides evidence that membrane rafts inactivate KCC2 but activate NKCC1 and that this form of regulation can also serve as a means by which to reciprocally alter the transport function of these cotransporters to achieve fast Cl^- regulation.

Members of the serine-threonine kinases, WNK3 and WNK4, have also been implicated in the regulation of KCC2. Kinase-active WNK3 is a potent activator of NKCC1 and inactivator of both KCC1 and KCC2 (Kahle et al 2005). Interestingly, when WKN3 is inactivated by a point mutation, the effects are reversed and KCC2 is activated. This study proposed that WNK3 is not directly responsible for the phosphorylating KCC2, but that SPAK is the direct mediator of phosphorylation. Although it is not known how WNK3 itself is regulated, WNK1 is responsive to changes in hypotonic and hypertonic stress, indicating that the WNK proteins may be signalled by changes in cell volume and $[Cl^-]_i$ (Kahle et al 2005, Lenertz et al 2005, Xu et al 2000). In this way, WNK has the potential to act as a molecular switch to coordinate the regulation of reciprocal cotransporters NKCC1 and KCC2.

WNK1 and SPAK play a role in the developmental regulation of chloride homeostasis (Inoue et al 2012). Exogenous taurine added to neurons *in vitro* activates WNK1 and downstream SPAK, but that this effect could be nullified with Thr^{906} and Thr^{1007} substitutions of KCC2. *In vivo*, it was shown that embryonic brains have consistently higher levels of SPAK than neonatal brains suggesting that taurine and the WNK1/SPAK pathway may be involved in regulating Cl^- homeostasis during development.

WNK4 can inhibit KCC2 when heterologously expressed in *Xenopous* oocytes under hypotonic, cell-swelling conditions when KCC2 is maximally active (Garzon-Muvdi et al 2007). WNK2 has been elucidated as a brain specific serine-threonine kinase present in the cortex, the thalamus and the cerebellum of mammals (Rinehart et al 2009). Like the other WNKs, WNK2 reciprocally activates NKCC1 and inhibits KCC2 and forms a complex with SPAK in neurons. Together, the regulation of KCC2 by the WNKs point to a model of reciprocal Cl^- regulation for NKCC1 and KCC2. More work is required to elucidate the exact signals that induce this regulation *in vivo*.

The Ca^{2+}-activated protease calpain can regulate KCC2 by cleaving the cotranporter and reducing its active pool (Puskarjov et al 2012). Calpain is activated by the $[Ca^{2+}]_i$ and Brain Derived Neurotrophic Factor (BDNF) binding to its receptor TrkB (Zadran et al 2010). The Ca^{2+-}dependent downregulation of KCC2 and reduced Cl^- extrusion has been observed under various plasticity-induction protocols (Fiumelli & Woodin 2007, Lee et al 2011, Loscher et al 2013) and involves the BDNF/TrkB signalling pathway (Rivera et al 2004). When neurons are exposed to excitotoxicity, calpain-mediated downregulation of KCC2 results, which suggests that calpain may be an important regulator of GABAergic transmission (Puskarjov et al 2012).

For the last decade, it has been known that BDNF regulates KCC2 expression. The action of BDNF is directional and depends on whether it is released during development or released in response to excessive activity during a pathological condition. During the early postnatal period, BDNF upregulates KCC2 (Aguado et al 2003). In the embryonic hippocampus, increasing BDNF expression increases spontaneous network activity and increases KCC2 expression (Aguado et al 2003). Conversely, when neonatal mice lack the BDNF TrkB receptor, their intrinsic rate of activity and KCC2 expression is decreased (Carmona et al 2006). BDNF, as well as neutotrophic factor neurturin, induces extracellular signal-regulated kinase ½ (ERK1/2) dependent Erg4 expression of the KCC2b promoter (Ludwig et al 2011a, Ludwig et al 2011b). Together, this suggests that BDNF plays a role in the developmental upregulation of KCC2.

In the mature brain, exposing hippocampal neurons to BDNF acting through the TrkB pathway causes a rapid, on the order of minutes, down-regulation of KCC2 mRNA and KCC2 protein (Rivera et al 2002, Rivera et al 2004). Acute application of BDNF to hippocampal cultures has been shown to correlate with depolarized E_{GABA} and a decrease in KCC2 expression (Wardle & Poo 2003). The downregulation of KCC2 by BDNF following injury plays a role in resetting these neurons to their immature state that may function to promote the formation of new neuronal connections post-injury (Shulga et al 2009). As discussed in the next section, neuropathic pain which involves the downregulation of KCC2 also correlates with the release of BDNF (Coull et al 2005).

1.4.6 KCC2 dysfunction and neurological disorders

The impairment of KCC2 expression and/or function has been implicated in several disease states. These disease states include epilepsy, spinal cord spasticity, schizophrenia and neuropathic pain. In these conditions, a rise in $[Cl^-]_i$ results from a decreased KCC2 expression level in a population of neurons.

Epilepsy is characterized by over excitability of neuronal circuits and compromised GABAergic synaptic transmission (Treiman 1990). When glutamatergic signalling increases and when GABAergic signalling decreases, neuronal circuits can become hyperactive (Kahle et al 2008). When even just a small population of electrical firing becomes synchronized, larger networks get recruited and this is how a seizure begins. In neonatal seizures, temporal lobe epilepsy (TLE), and in seizures that occur as a result of ischemic-hypoxic insult, the Cl^- gradient shifts to resemble an immature state where Cl^- is building up inside the neurons (Kahle et al 2008).

Neonatal seizures are defined by epileptic episodes occurring within the first 28 days of life (Kahle et al 2008, Scher & Painter 1989). NKCC1 expression is relatively high early in development, so pharmaceutical targets to treat neonatal epilepsy have focused on targeting NKCC1. By blocking these cotransporters in infants, the Cl^- channels opened by GABA would only result in shunting or short-circuiting excitatory inputs and depolarizing currents (Jean-Xavier et al 2007). Bumetanide has been shown to reduce seizures in rats without any adverse effects in electrolyte balance or in hemodynamics (Dzhala et al 2005, Sullivan et al 1996). Currently, human neonatal trials are underway to determine whether or not infants suffering from neonatal seizures show reduced symptoms, with minimal side effects, to bumetanide treatment (Kahle et al 2008).

In TLE, excitatory GABAergic signalling results from perturbed neuronal Cl^- transport (Cohen et al 2002). In other organisms, the loss of KCC2 produces a similar phenotype. A KCC2 knockout in *Drosophila melanogaster* results in flies with decreased GABAergic signalling an increased susceptibility to seizures (Hekmat-Scafe et al 2006). When mice have a knockdown of the major isoform of KCC2, they exhibit seizures and then died shortly after birth (Hubner et al 2001, Woo et al 2002). Currently, bumetanide treatment is considered the most likely potential treatment for TLE in adults because of the observation that KCC2 is downregulated and NKCC1 is increased in function during TLE (Kahle et al 2008). However, what still remains elusive is whether or not the downregulation of KCC2 causes TLE or is the result of hyperexcitability.

Following ischemic injury and hypoxia in mammals, seizures occur during a period defined as reperfusion (Kahle et al 2008). During reoxygenation, neurons suffer from a rise in $[Cl^-]_i$ due to an expression of NKCC1 (Galeffi et al 2004, Inglefield & Schwartz-Bloom 1998). Serine threonine phosphorylation is responsible for this pathological increase in NKCC1 (Schomberg et al 2001, Su et al 2002). However, whether this mechanism reciprocally regulates KCC2 during hypoxic-ischemic insult is still unknown.

After spinal cord injury (SCI), it is common to observe both a reduction in inhibitory transmission and spasticity. KCC2 is downregulated by SCI via a BDNF-mediated mechanism (Boulenguez et al 2010). Interestingly, after SCI BDNF is also required for the upregulation of KCC2. Serotonin, acting on the 5-hydroxytryptamine type 2A receptor, hyperpolarizes IPSPs in spinal neurons and upregulates KCC2 (Bos et al 2013). Serotonin was effective in these experiments for reducing spasticity following SCI, but more work is needed to develop a more specifically targeted agonist.

KCC2 also plays a role in neuropathic pain mediated by the spinal cord. Local blockade of KCC2 or knockdown of KCC2 reduces the nociceptive threshold in rats (Coull et al 2003). One of the most common chronic pain pathways, the trigeminal neuropathic pain pathway, has also shown a decrease in KCC2 to correlate with pain (Wei et al 2013). Following nerve injury, there is an increase in calpain activity causing cleavage of KCC2 at the C-terminus and that by inhibiting calpain, normal levels of inhibition are restored (Zhou et al 2012). In diabetic neuropathic pain, the expression of KCC2 is reduced and GABA expression is elevated in the dorsal horn lamina correlated with neuronal hyperexcitability and spontaneous hyperactivity (Morgado et al 2008). Like in the case of epilepsy, more work needs to be done to elucidate the direct or indirect role of KCC2 in neuropathic pain (Hasbargen et al 2010, Price et al 2009).

Finally, altered function of the CCCs in the prefrontal coretex is involved in schizophrenia. Schizophrenia is a neurological condition with several genetic implications and risk factors. It has been proposed that seizures, implicating the downregulation of KCC2, contribute to schizophrenia by inappropriately accelerating the neuronal differentiation process (Ben-Ari et al 2012a, Hyde et al 2011, Kalkman 2011) Truncated transcripts of KCC2 have also been shown to correlate with schizophrenia and related disorders (Tao et al 2012).

1.5 KCC2 Regulatory Proteins

1.5.1. General Properties of Neto Proteins

Neto (neuropilin-1/tolloid-like) proteins are type I transmembrane proteins named for their sequence similarity with the known axon guidance protein neuropilin (He & Tessier-Lavigne 1997) and the dorsoventral patterning protein tolloid (Shimell et al 1991). To date, two

Neto proteins have been elucidated and named Neto1 and Neto2. The *Neto1* and *Neto2* genes encode two evolutionarily conserved neuronal proteins with the C-terminus facing the cytoplasm and N-terminus facing the extracellular space at the neuronal membrane. These proteins contain two extracellular CUB domains (for Complement C1r/C1s, Uegf, and Bmp 1), one LDLa motif (low-density lipoprotein receptor domain class A), a single pass transmembrane domain, and a cytoplasmic tail (Michishita et al 2003, Michishita et al 2004, Stohr et al 2002).

Expression of Neto1 and Neto2 is high in the cerebral cortex, olfactory bulb, olfactory tubercle, pons and hippocampus. However, in the cerebellum, Neto1 is only expressed in Purkinje cells while Neto2 is expressed in both the Purkinje and granule cell layers. In the hippocampus, Neto2 is uniformly expressed in the pyramidal cells and weakly expressed in the granule cells while Neto1 mRNA is seen throughout the pyramidal and granule cell layer with strong expression in CA3 pyramidal cells (Man Tang 2012, Ng et al 2009, Zhang et al 2009).

Functionally, Neto1 and Neto2 play differential roles in regulating glutamatergic transmission. Neto1 physically interacts, via its ectodomain, with the NR2A and NR2B subunits of the NMDAR (Ng et al 2009). In addition, Neto1 interacts with PSD95 through its PDZ ligand, in both hippocampal fractions and in transfected HEK293 cells. The functional significance of the disruption of these interactions in Neto1-null mice was found to be a reduction in LTP at Schaffer collateral CA1 synapses and a reduction in spatial learning performance in the Morris water maze. This solidified the role for Neto1 in synaptic plasticity and learning. Neto2 directly interacts with the KAR subunit GluR6 in rat cerebellar lysates and modulates properties of the glutamate-evoked current (Zhang, et al. 2009). Over the course of my studies, as I will describe in detail in Chapter 4 of this thesis, I have found that Neto2 is a

novel interactor of KCC2 and is involved in maintaining physiological levels of GABAergic inhibition in mature mouse hippocampal neurons (Ivakine et al 2013).

1.5.2 General Properties of Kainate Receptors

KARs are one of the three subtypes of ionotropic receptors that are gated for the binding of the excitatory neurotransmitter glutamate (Dingledine et al 1999). KARs have been shown to be implicated in human diseases that include epilepsy, migraines and neuropathic pain and targeting KARs pharmacologically is effective in modulating neuronal activity (Contractor et al 2011).

KARs are tetrameric receptors comprised of five potential subunits: GLUK1-5 (formerly termed GLUR5-7, KA1-2) (Castillo PE 1997, Chittajallu R 1996, Hollmann & Heinemann 1994, Wisden et al 1993). The first KAR subunit gene (GluK1) was cloned in 1990 (Bettler et al 1990), but since then, KARs have remained the least well-understood receptors of the glutamate-gated ion channel family. The tetrameric co-assemblies that make up functional KARs in neurons are composed of GluK1, GluK2, GluK3, GluK4 and GluK5. The GluK1, GluK2 and GluK3 subunits are capable of assembling into homo- and heteromeric KARs. The GluK4 and GluK5 are only capable of forming heteromers with GluK1, GluK2 or GluK3. These diverse combinations of KARs, along with their distinct subcellular targeting to the dendrite and soma in neurons, at distinct synapses are thought to all be factors in contributing towards the diversity in KAR function (Contractor et al 2011).

KARs play multiple roles in modulating both excitatory and inhibitory synaptic transmission (Contractor et al 2011, Swanson & Sakai 2009). Perhaps the most functionally distinct property of KARs is that their time-course is an order of magnitude longer than other

glutamate receptor types (Castillo et al. 1997). An important functional aspect of KARs, is that there are two possible downstream outcomes resulting from glutamate-binding. First, KARs permit an ionic influx of cations when glutamate binds. This is commonly referred to as a rapid ionotropic transmission (Perrais et al 2010). Secondly, KARs can act as metabotropic receptors, resulting in the activation of second messenger signaling cascade (Rodriguez-Moreno & Sihra 2007). In these two ways, KARs are potentially involved in a diverse set of functions. KARs at presynaptic terminals can regulate neurotransmitter release for both glutamatergic and GABAergic synapses, regulating neuronal excitability (Lerma 2006).

KARs demonstrate a very selective distribution in each brain area. Various KAR subunits have selected distribution throughout each brain region, including selective expression in the pre and postsynapses (Castillo et al 1997, Copits & Swanson 2012). This differential expression pattern contributes to the elusive comprehensive understanding of multiple functions of KARs.

1.5.3 Neto Proteins as Auxiliary Subunits of Kainate Receptors

Since Zhang et al.(2009) first showed that Neto2 modulates the functional properties of KARs, a new concept has developed in the KAR field that focuses on the role of transmembrane accessory subunits of the receptors. Zhang et al. (2009) identified Neto2 as a KAR interactor. Neto2 modulates the channel properties of recombinant and native KARs while also modulating KAR-mediated EPSCs. Recombinantly expressed KARs have currents that are over an order of magnitude faster than native KARs (Copits & Swanson 2012), which led to the hypothesis that native KARs may be regulated by modulatory proteins. Native AMPA receptors, another

ionotropic glutamate receptor type, also require transmembrane auxiliary subunits (TARPs) (Nicoll et al 2006). Auxiliary subunits are defined as (1) as a non-pore-forming subunit, (2) a direct and stable interaction with a pore-forming subunit, (3) modulation of channel properties and/or trafficking in heterologous cells, (4) a necessity *in vivo* (Yan & Tomita 2012). Neto2 was shown to slow the deactivation and desensitization of GluK2 homomeric KARs in heterologous systems and to accelerate recovery from desensitization (Zhang et al 2009), essentially mimicking native KAR currents. Neto2 did not affect the cell surface expression of KARs. In cerebellar granule neurons, cotransfection of Neto2 with a GluK2 mutant that reduces KAR desensitization significantly increased the frequency of recorded miniature EPSCs. Neto2 coexpression also slowed the decay kinetics of these KAR-mediated mEPSCs. A more recent study showed that Neto2 can slow the desensitization and modulate most KARs when Gluk1, Gluk1/5 or GluK2/5 are co-expressed with Neto2 (Straub & Tomita 2012). Thus, Neto2 is a novel KAR-associated protein that modulates KAR channel properties. Whether Neto2 acts as an auxiliary protein for synaptic KARs in its native form in the brain has yet to be shown.

Neto1 is also a KAR auxiliary subunit (Tang et al 2011). Neto1-null mice show a 50% reduction in the abundance of GluK2 KARs in hippocampal postsynaptic density. In these Neto1-null mice, there is a reduction in the KAR-mediated EPSC amplitude and the EPSCs decay is more rapid than in wildytpe mice. Tang et al. (2011) did not see any additional structural or functional deficits in the Neto1/2 double mutant, which led to the conclusion that the Neto1 protein is also required for synaptic function of KARs. Since their group had already determined that Neto1 plays a critical role in regulating subunit composition of and synaptic plasticity mediated by NMDARs, Neto1 seems to be an important regulator of two classes of ionotropic glutamate receptors.

This same group continued to establish the distinct roles of Neto1 and Neto2 as auxiliary proteins regulating post-synaptic KARs (Tang et al 2012). Neto1 plays a more important role in regulating hippocampal KARs where Neto2 regulates KARs in the cerebellum, where it was initially discovered. Neto2 has been suggested to play a critical role in stabilizing KARs by promoting the interaction of GluK2 KARs with the scaffolding protein GRIP through the PDZ-domain. These results propose that Neto1 and Neto2 play differential roles at various synapses by regulating the surface stability of KARs.

1.6 Objectives and Aims

The **main objective** of the present study is to examine the mechanisms that regulate KCC2 function in hippocampal neurons. Specifically, I had **three objectives** that have allowed me to address my main objective. First, I assayed KCC2's transport function under isotonic conditions; specifically, I have determined the molecular domain of the cotransporter required for constitutive Cl^- transport (Acton et al 2012). Secondly, I have investigated a novel KCC2-interacting protein named Neto2 and its critical effect on the postsynaptic action of GABA (Ivakine et al 2013). My last finding further explores Neto2 as a KAR auxiliary protein and the effect of this interaction on the expression pattern and membrane stability of KCC2.

To accomplish this, I had **3 specific aims**:

Aim I: Determine the molecular constituents of KCC2 isotonic cotransport function in neurons.

Aim II: Determine the role of the Neto2:KCC2 interaction on the physiological regulation of KCC2.

Aim III: Determine the role of the Neto2:KCC2:GluK2 interaction on the expression pattern and membrane stability of KCC2.

Chapter 2. Materials and Methods

2.1 Cell Culture Preparation

Low-density cultures of dissociated postnatal mouse hippocampal neurons were prepared [as similarly described for rodents (Balena et al 2008)] from postnatal day 0–1 mice from C57Bl/6 (wildtype), Neto2$^{-/-}$ and GluK1/2$^{-/-}$ mice (Ivakine et al 2013). All experiments were performed in accordance with guidelines from the University of Toronto Animal Care Committee and the Canadian Council on Animal Care. Rat hippocampal cultures were made, similarly, from E18 embryonic rats by anesthetizing pregnant rats with CO_2 gas, and sacrificed via cervical dislocation Embryos were removed from the mother and placed in cold dissection medium. In short, hippocampi were removed and treated with trypsin for 15 min at 37 °C, followed by gentle trituration. The dissociated cells were plated at a density of ∼50,000 cells per mL on poly-D-lysine–coated 25mm glass coverslips in Neurobasal medium (Invitrogen), supplemented with 2% B-27 (Invitrogen) and 10% FBS (Sigma). Twenty-four hours after plating, one-third of the medium was replaced with original plating medium, and then changed again every 3 days. Recordings were made after 9–13 days in culture (DIV).

Neto2 knockout cultures were made from Neto2$^{-/-}$ congenic mice. Neto2$^{-/-}$ mice on mixed 129/C57BL/6 background were backcrossed to C57BL/6 mice for 10 generations, and the resulting Neto2$^{+/-}$ heterozygous mice were intercrossed to generate Neto2-null mice. The resulting Neto2$^{+/-}$ heterozygous mice were intercrossed to generate Neto2-null mice. Congenic Neto2$^{-/-}$ mice were born at a normal Mendelian ratio. They displayed normal reproductive behavior and their life span was undistinguishable from their wild types (Ivakine et al 2013).

2.2 Patch Clamp Electrophysiology

Recordings were performed with a MultiClamp 700B (Molecular Devices) patch-clamp amplifier, and filtered at 5 kHz. Data were acquired and analyzed using Clampfit 9 (Molecular Devices). Neurons were continuously perfused (at ~1 mL/min) with standard extracellular recording solution containing the following (in mM): 150 NaCl, 3 KCl, 3 CaCl·2H2O, 2 MgCl2·6H2O, 10 Hepes, 5 glucose (pH 7.4, 301–315 mOsm). Recordings started when the series resistance dropped below 50 MΩ. Current–voltage measurements were made by 30s step depolarizations from very hyperpolarized voltages (-100mV to -80mV) all the way to depolarized values (about -30 mV) in voltage-clamp mode, during which a 10 μM GABA puffed onto the soma. A linear regression of the GABAergic postsynaptic current (GPSC) amplitude measurements was used to calculate the voltage dependence of GPSCs and the intercept of this line with the abscissa was taken as E_{Cl}. Basic membrane properties (AP threshold, AP amplitude, input resistance, and RMP) of these neurons were measured in current clamp by recording the cells' response to small 10-pA step injections (starting at -50 pA; see **Figure 2.3.3.1**). When bumetanide (10 μM; Sigma) was required, it was applied to the cells through the bath perfusion. The KCC2-specific antagonist VU0240551 (25 μM; Sigma-Aldrich) was applied acutely to the cell culture recording dish and the perfusion was terminated.

2.2.1 Perforated Patch Clamp

Patch clamp electrophysiology was first established by Neher and Sakmann in the 1970's and has since formed the basis of the technique in neurophysiology (Neher et al 1978). A glass

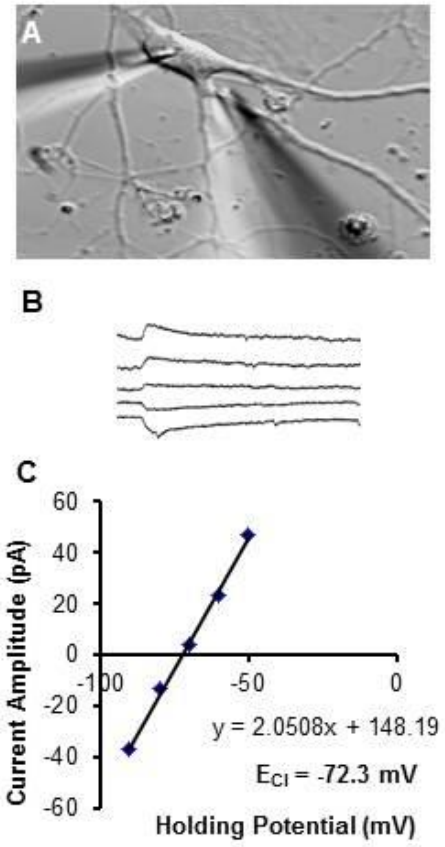

Figure 2.3.3.1. Schematic of how E_{Cl} is determined experimentally. **A**. Bright field image showing a patch onto the hippocampal neuron and the puffing pipette releasing 10µM GABA from a picospritzer (© Balena 2011) **B**. A sample image of the Cl^- current traces recorded in voltage clamp when GABA binds $GABA_A$Rs on the soma of the neuron. **C**. A linear regression of the current-voltage relationship where the x-intercept is taken as $E_{Cl.}$

pipette is used to form a gigaohm (GΩ) seal with the neuronal membrane. The pipette holds a chlorided silver wire immersed in intracellular solution and can detect changes in electrical activities. This electrical signal is relayed to an amplifier for the scientist's analysis. A commonly used version of the original patch clamp technique is called the perforated patch method (Lindau & Fernandez 1986). What distinguishes perforated patch from other types of electrophysiology is that the intracellular solution contains a perforating agent, which is typically an antibiotic such as amphotericin-B or gramicidin. When a GΩ seal is made between the pipette tip and the neuronal membrane, the perforating agent begins to work on the neuronal membrane by forms channels in the area of the membrane inside the tip. This provides electrical access to the intracellular space of the neuron while still maintaining the majority of the endogenous content of the cytoplasm. Both amphotericin-B and gramicidin form channels which are permeable to monovalent cations and small uncharged molecules, but amphotericin-B is considered partially permeable to Cl^- while gramicidin is considered to form perforations in the membrane that are not permeable to Cl^- (Kyrozis & Reichling 1995, Owens et al 1996). My supervisor has shown that both perforating agents produce identical results in several experiments (Woodin et al 2003), but gramicidin is considered the preferable perforating agent for experiments where Cl^- gradients must remain undisturbed, such as in my present experiments measuring E_{Cl}. For this reason, only gramicidin (18 mM; Sigma-Aldrich, Oakville, ON) was utilized in the present experiments. The pipettes were filled with an intracellular solution containing 150 mM KCl, 10 mM HEPES, and 18nM gramicidin, pH 7.4, osmolarity = 300 mOsmol.

During perforated patch clamp experiments, once a GΩ seal is obtained, the neuron's activity is observed in either voltage clamp mode or current clamp mode. Voltage clamp

involves setting a holding potential (V_{hold}; the voltage one wishes the neuron to remain at, which is usually close to the RMP). This is achieved by injecting current through the pipette to hold or clamp the neuronal membrane at the desired potential, through a negative feedback system. In this mode, one can observe any currents across the membrane of the neuron during the experiment. Conversely, in current clamp mode the experimenter chooses how much current, if any, to inject into the neuron at rest and allows the experimenter to observe changes in the potential difference across the membrane.

During the present experiments, recordings started after the series resistance had dropped below 50 MΩ, where no adjustment was made for the voltage drop across gramicidin recordings. For experiments described in the results section, the extracellular solution was bicarbonate-free and buffered with HEPES. This makes the HCO_3^- current through the $GABA_AR$ negligible and for this reason, I report E_{Cl} instead of E_{GABA} in the results section.

2.2.2 Whole Cell Patch Clamp

During a whole cell recording, the experimenter "pops" the GΩ seal to make the intracellular solution continuous with the cytoplasm of the neuron. In the present experiments, I used the whole-cell technique to expose the neuron to a Cl^- load from the intracellular solution. By doing so, experimenters can assess and quantify the Cl^- extrusion efficacy. A method of Cl^- loading via the recording pipette was introduced by Jarolimek and co-authors who used this method in cell culture (Jarolimek et al 1999). For Cl^- loading experiments, pipettes (5–7 MΩ) were filled with an internal solution containing the following (in mM): 90 K^+-gluconate, 50 KCl, 10 HEPES, 0.2 EGTA, 4 ATP, 0.3 GTP, and 10 phosphocreatine (pH 7.4, 300 mOsm). Neurons were perfused (1 ml/min) with either isotonic or hypotonic extracellular solution [isotonic

(inmM): 150 NaCl, 3 KCl, 3 CaCl2·2H2O, 2 MgCl2·6H2O, 10 HEPES, 5 glucose at pH 7.4, 301–315 mOsm; hypotonic: (in mM) 75 NaCl, 1.5 KCl, 1.5 CaCl2·2H2O, 2 MgCl2·6H2O, 5 HEPES, 2.5 glucose at pH 7.4, 180–185 (mOsm)].

2.3 Recording the Reversal Potential for Chloride

2.3.2 Picospritizing GABA

Current–voltage measurements were made by 30s steps depolarizations from very hyperpolarized voltages (-100mV to -80mV) all the way to depolarized values (about -30 mV) mVs in voltageclamp mode, during which a 10 µM GABA puff was applied to the soma using a picospritzer. GABA (10µM) was made up in extracellular solution and back-loaded in a long, 5-7MΩ resistance glass pipette and attached to the end of a picospritzer. The pipette was lowered to be within 10µM of the soma of the neuron of interest.

2.3.3 Electrophysiological Recording Analysis

A linear regression of the IPSC amplitude was used to calculate the voltage dependence of IPSCs; the intercept of this line with the abscissa was taken as E_{Cl} (experiments were performed in bicarbonate-free solution buffered with HEPES, the GABA current was solely mediated by Cl^-, and thus I report E_{Cl} and not E_{GABA}).

E_{Cl} values were obtained from current/voltage curves (IV curves) run in voltage clamp mode. The V_{hold} of the postsynaptic neuron was varied by 10 mV increments (as described above). While the postsynaptic neuron was held at each of these values for 100 ms, 10µM GABA pipette was “puffed” by the picospritzer releasing a small amount of pressure to cause

GABA to bind to the postsynaptic receptors. Using Clampfit, two cursors were placed on the resulting recording trace (one just before the current, and the other at the peak of the current) and the peak amplitude was exported to a spreadsheet in Microsoft Excel (Microsoft, Redmond, WA) and graph against V_{hold}. A best-fit line was constructed, and the intercept of this line with the abscissa was taken to be E_{Cl} (**Figure 2.3.3.1**). Electrophysiological values have not been corrected for the liquid junction potential of -7 mV. The expected $[Cl^-]_i$ was calculated using the Nernst equation.

2.4 Transfecting Hippocampal Cultured Neurons

Lipofectamine 2000 was used to transfect cDNA constructs into cultured hippocampal neurons, according to a modified version of the manufacturer's instructions (Invitrogen). Transfection was performed in Neurobasal media (Invitrogen). First, two eppendorf tubes were filled with 20µL of Neurobasal media. To one, 6µg DNA construct of interest was added and to the other, 6µL of Lipofectamine2000 was added. Each solution was left to incubate in separate eppendorfs for 5 minutes. After 5 minutes, the 26µL of media in the eppendorf with the Lipofectamine 2000 solution was added, entirely, to the eppendorf containing the DNA. After the two solutions incubated for 30 minutes, it was then added to neuronal culture that contained only 750µL of suspended media in it. Cultures were left in a 37°C, 5% CO_2 incubator for 18-24 hours before experiments were performed to allow for protein expression of the DNA of interest.

2.5 Immunohistochemistry

A modified immunohistochemistry protocol was used in the present experiments where the incubations were reduced in time and occurred at 37°C to prevent the neurons from washing off the coverslips. Coverslips containing the cultured neurons were chilled for 5 minutes on ice and washed with standard 1x phosphate-buffered saline (PBS), prior to fixation with 4% paraformaldehyde (PFA)/4% sucrose in PBS. Cells were permeabilized with 0.1% Triton in PBS, washed in PBS, and then blocked with 10% goat serum in PBS for 45 minutes at room temperature. The coverslips were incubated in a primary antibody (for example, rabbit polyclonal anti-KCC2 antibody (1:1000 dilution; Sigma)) at 37 °C for one hour. The coverslips were brought to room temperature and washed with PBS. Cells were then incubation with the secondary antibody conjugated to a flourophore for 1 hour in the dark at room temperature (1:250 dilution in 1x PBS + 10% serum). The coverslips were washed prior to a 5 minute incubation with DAPI. Finally, the coverslips were mounted on glass slides with ProLong Gold Antifade (Invitrogen).

The specific details of each individual immunohistochemical experiment and the details of how immunofluorescence images were captured on a confocal microscope and the details of the analysis for each set of experiments are outlined in each specific results section.

2.6 Statistical Analysis

All data is presented as mean ± SEM. One-way ANOVA was used in Chapter 4 to compare E_{Cl} values obtained from rat hippocampal neurons under different conditions and expressing different constructs and in an immunohistochemistry experiment comparing total levels of KCC2 expression between neurons expressing cDNA constructs and in Chapter 5 to

compare E_{Cl} values for knockdown and rescue condition experiments. A standard t-test was used in Chapter 4 to compare immunohistochemistry staining patterns between neurons expressing HA-tagged versions of cDNA constructs, in Chapter 5 to compare E_{Cl} between hippocampal neurons from different mouse genetic backgrounds and for morphological analysis, and in Chapter 6 to compare immunohistochemical staining patterns between mice of different genetic backgrounds. Statistical analysis was performed using SigmaStat (SPSS Inc., San Rafael, CA) for Windows PC. Sigma Stat determined that the use of parametric statistical tests was appropriate based on normal distributions of each of the data sets.

Chapter 3. The KCC2 ISO Domain is Required for Cl^- Transport

3.1 Statement of Authorship

The results from this chapter were published in the Journal of Neuroscience in June 2012:

Acton, B.A., Mahadevan, V., Mercado, A., Uvarov, P., Ding, Y., Pressey, J., Airaksinen M.S., Mount, D.B., and Woodin, M.A. (2012). Hyperpolarizing GABAergic Transmission Requires the KCC2 C-terminal ISO Domain. J Neurosci 32(25):8746-51.

My contributions to this manuscript include: generating the hypothesis and experimental design, performed all of the experimental data collection and data analysis for this project and co-writing the manuscript. Professor David B. Mount (*Renal Division, Veterans Affairs Boston Healthcare System, Harvard Medical School, West Roxbury, Massachusetts USA)* provided the majority of the cDNA constructs used in these experiments (Mercado et al 2006a). Dr. Pavel Uvarov (*Neuroscience Center and Institute of Biomedicine, University of Helsinki, Helsinki, Finland)* generated a critical HA-tagged KCC2 construct requested by the reviewers of the manuscript. Vivek Mahadevan (*Department of Cell & Systems Biology, University of Toronto, Toronto, Ontario, Canada)* assisted with the confocal microscopy. All data presented in this thesis are from experiments that I have performed.

3.2 Introduction, Objectives and Hypothesis

While all K^+Cl^- cotransporters are activated by cell swelling (Flatman 2008, Lauf & Bauer 1987b), KCC2 is the only family member that is also able to extrude Cl^- in the absence of osmotic stress. KCC2 extrudes Cl^- under isotonic conditions by deriving energy from the K^+ gradient established by the Na^+-K^+-ATPase (Payne et al., 1996). As a result, KCC2 maintains a

low concentration of intracellular Cl^- ($[Cl^-]_i$), which upon $GABA_AR$ activation allows Cl^- influx down its electrochemical gradient. The failure thus far to define the molecular determinant(s) of constitutive K^+Cl^- cotransport mediated by KCC2 represents a large gap in our fundamental knowledge regarding neuronal Cl^- regulation and inhibitory synaptic transmission. My **objective** in the present study was to identify the molecular determinants of KCC2 K^+Cl^- cotransport under isotonic conditions. Based on the previous work of our collaborators using a Rb^+-uptake assay, they demonstrated that a C-terminal domain renders KCC2 constitutively active in *Xenopus* oocytes (Mercado et al 2006a), I **hypothesized** that this same domain also confers KCC2 with the ability to extrude Cl^- from neurons under physiologically normal isotonic conditions. The following chapter describes the experimental details, the results and the conclusions from those experiments.

3.3 Materials and Methods (Specific to Chapter 3)

3.3.1 cDNA Constructs

Most of the cDNA constructs used in the present experiments were designed by our collaborator, Professor David B. Mount (*Renal Division, Veterans Affairs Boston Healthcare System, Harvard Medical School, West Roxbury, Massachusetts USA).* In brief, the KCC2ΔISO construct was generated by serial mutagenesis of hKCC2 (QuikChangeII, Stratagene), replacing residues 1022-1037 with the equivalent region of KCC4; the entire open reading frame was sequenced to verify the successful final sequence and exclude PCR-generated errors. The other cDNA constructs were the same as those we generated previously (Mercado et al 2006b). Briefly, all of the constructs are composed of the cDNA of the gene of interest in the bicistronic pMES vector (gift of Karl Kandler; (Lee et al 2005a)), which contains a cytomegalovirus

enhancer, a β-actin promoter, internal ribosome entry site (IRES), and an EGFP reporter. Two additional cDNA constructs were generated by Dr. Pavel Uvarov (*Neuroscience Center and Institute of Biomedicine, University of Helsinki, Helsinki, Finland).* He created extracellular-tagged KCC2-HA and KCC2ΔISO-HA constructs ideally suited for quantifying their membrane expression. A triple tandem copy of the influenza virus HA peptide (YPYDVPDYA) was inserted into the second extracellular loop of KCC2.

3.3.2 Live Immunostaining

Coverslips containing the cultured neurons were washed for 5 min at 37°C in isotonic extracellular solution. The coverslips were incubated in mouse monoclonal anti-HA antibody (Roche) at 37°C for 1 h. Cells were washed once for 5 min in isotonic XCS and then incubated with the secondary Alexa Fluor 555 goat anti-mouse antibody (Invitrogen) for 1 h in the dark at 37°C. The coverslips were imaged while being perfused with isotonic XCS at room temperature to mimic electrophysiological recording conditions. Immunofluorescent images were acquired on a Wave FX spinning disc confocal system (Quorum Technologies) with Zeiss Observer Z1 inverted microscope, using a 60x 1.4-NA oilimmersion objective. Z-stacks were acquired at a pixel resolution of 1024xy with a *z*-step of 0.2 µm. Samples were acquired sequentially using line-lambda mode at excitation wavelengths of 488 nm (for GFP) and 568 nm (for Cy3). Images were acquired and analyzed using Volocity 3D Image Analysis software (PerkinElmer). A minimum of 12 cells were imaged and analyzed from four coverslips in each condition. We measured anti-HA (Cy3) immunofluorescence cluster intensity in the *z* plane, under constant illumination. The soma and the first 50µM of the most prominent primary dendrite of GFP-positive neurons were selected as the area of interest (AOI). Clusters were defined as regions within the AOI whose fluorescence intensity was significantly greater than that of the average

fluorescence intensity within the field of view. The anti-HA intensity for KCC2ΔISO was calculated as a percentage of anti-HA intensity of KCC2-HA after background subtraction.

Immunofluorescent images were acquired on a Wave FX spinning disc confocal system (Quorum Technologies) with Zeiss Observer Z1 inverted microscope, using a 60x 1.4-NA oil immersion objective. Normally, z-stacks were acquired at a pixel resolution of 1024xy with a z-step of 0.1 µm. Samples were acquired sequentially using line-lambda mode at excitation wavelengths of 488nm (for GFP) and 568nm (for Cy3). Images were acquired and analyze using Nikon EZ-C1 software.

3.4 Results: Characterization of KCC2-KCC4 Chimeric Proteins in Hippocampal Neurons

To determine the region of KCC2 that is required for isotonic K^+Cl^- cotransport, I transfected cultured hippocampal neurons with cDNA constructs and used electrophysiology to assay their ability to regulate neuronal Cl^-. Experiments were designed to be performed on neurons expressing the constructs of interest compared to neurons overexpressing human KCC2 (hKCC2) as the positive control, and compared to neurons overexpressing the vector alone as the negative control. All cDNA constructs contain an IRES promoter that independently drove the expression of enhanced green fluorescent protein (GFP). The expression of GFP was used exclusively to identify the neurons expressing the construct of interest for electrophysiological recordings (**Figure 3.4.1.1**).

3.4.1 Characterization of Hippocampal Cultured Neurons Expressing hKCC2

I first transfected cultured hippocampal neurons with full length hKCC2. Transfected neurons were identified by GFP fluorescence and patched with a pipette containing the antibiotic gramacidin in order to make Cl^- impermeable perforated patch recordings. To obtain E_{Cl}, 10μM GABA was pico spritzed at the soma of the neuron while simultaneously recording the membrane potential. As would be predicted, increased KCC2 expression increased Cl^- extrusion, which significantly hyperpolarized E_{Cl} (-97.56 mV ± 4.49 mV, n = 9, $p < 0.001$; **Figure 3.4.2.1B**) compared to both vector alone (-61.46 ± 4.15 mV, n = 6; **Figure 3.4.2.1B**) and untransfected neurons in the same culture dish (-58.44 ± 2.95 mV, n = 8). This data also demonstrates that in 10-13 DIV hippocampal neurons, endogenous KCC2 expression is not maximal. At this point, E_{Cl} still has a range over which it can hyperpolarize.

3.4.2 Characterization of Hippocampal Cultured Neurons Expressing KCC2ΔISO

Based on our collaborators' previous demonstration using a Rb^+ influx assay that a C-terminal amino acid sequence (amino acids 1022-1037; ISO domain) is required for isotonic constitutive activity of KCC2 in *Xenopus* oocytes (Mercado et al 2006b), I hypothesized that this same C-terminal domain may confer KCC2 with the ability to cotransport K^+ and Cl^- in neurons under isotonic conditions. To test this hypothesis, I transfected neurons with a chimeric construct that was generated by replacing the C-terminal amino acids in the ISO domain (aa1022-1037) with the corresponding amino acids from the KCC2 paralog KCC4 (KCC2ΔISO); KCC4 is the family member most similar to KCC2, but is not expressed in hippocampal neurons (Karadsheh et al 2004). In contrast to KCC2 overexpression, neurons transfected with KCC2ΔISO did not have significantly hyperpolarized E_{Cl} values (-59.19 ± 11.33 mV, n = 11; **Figure 3.4.2.1B**);

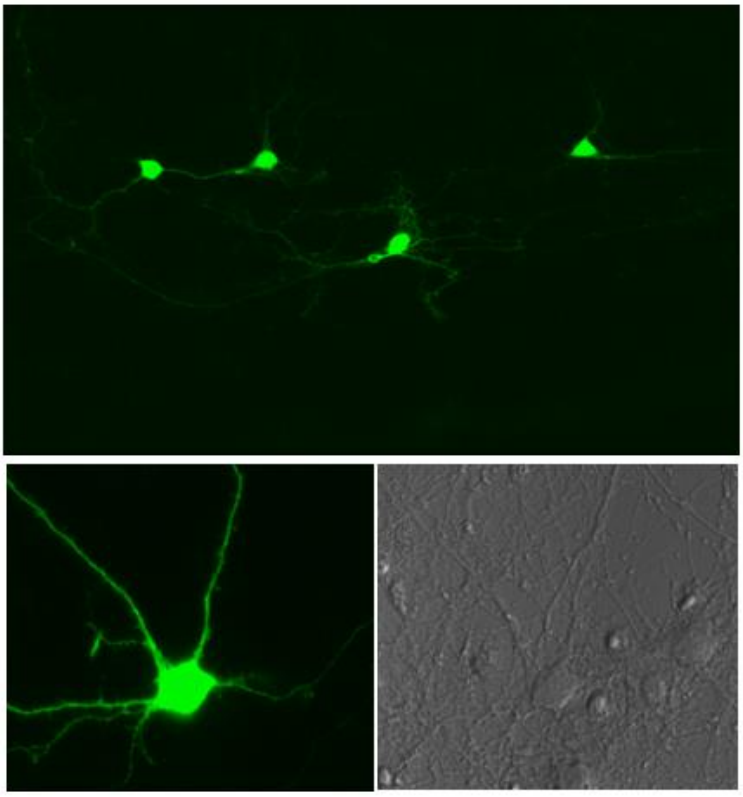

Figure 3.4.1.1. Fluorescent images of hippocampal neurons overexpressing KCC2ΔISO. Expression of the chimeric construct KCC2ΔISO is indicated by the reporter expression of GFP when neurons are exposed to 488nm illumination. Bottom right is a bright field image of the GFP positive cell from the bottom left.

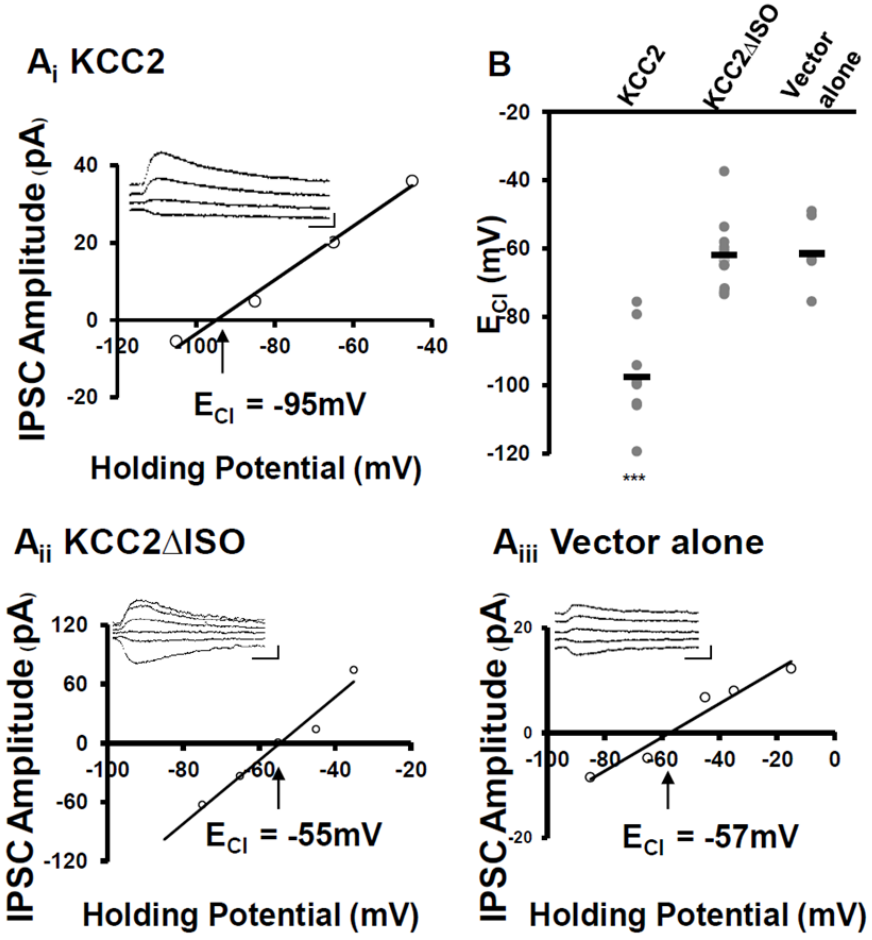

Figure 3.4.2.1. KCC2ΔISO does not transport Cl^- under isotonic conditions A. Examples of gramicidin perforated patch-clamp recordings obtained from neurons overexpressing KCC2 (**Ai**), KCC2ΔISO (**Aii**), and vector alone (**Aiii**). The IPSC amplitude was plotted against the holding potential, and the intercept of this curve with the *x*-axis was taken as E_{Cl} (arrows). Insets, Traces of IPSCs for the examples shown. Scale bars: 60 pA, 150 ms. **B**. Summary of all experiments similar to ***A*** shown as a distribution plot. ****p* <0.001.

infact, the E_{Cl} of neurons expressing this KCC2ΔISO construct was not significantly different from neurons expressing the vector alone ($p > 0.05$). Thus, chimeric KCC2 that lacks the ISO domain is unable to extrude Cl^- from neurons under isotonic conditions.

3.4.3 Characterization of KCC2ΔISO Membrane Trafficking

The lack of KCC2-mediated Cl^- extrusion by KCC2ΔISO could have resulted from an inability of this chimeric protein to be expressed in the same levels as wildtype KCC2. To test if this was the case, I first performed immunohistochemistry on neurons transfected with KCC2ΔISO or KCC2, and compared the intensity of anti-KCC2 staining in transfected neurons to untransfected neurons in the same field of view (**Figure 3.4.3.1 and 3.4.3.2**). I found that in neurons transfected with KCC2ΔISO, anti-KCC2 immunostaining was 461% higher than untransfected cells expressing endogenous levels of KCC2 (**Figure 3.4.3.2B**; $p < 0.001$). Similarly, overexpressing full-length KCC2 resulted in a 549% increase in anti-KCC2 immunostaining compared to untransfected neurons (**Figure 3.4.3.2B**; $p < 0.001$). There was no significant difference in anti-KCC2 immunostaining between neurons overexpressing KCC2ΔISO and KCC2 ($p > 0.05$). Importantly, anti-KCC2 fluorescence in untransfected neurons was not significantly different for neurons expressing the vector alone ($p > 0.05$).

Although expression levels are the same in hippocampal neurons overexpressing KCC2ΔISO or KCC2, I performed an additional live imaging experiment to confirm that the chimeric proteins are actually inserted into the membrane as functionally active KCC2 would be. To test this, my collaborator generated extracellular-tagged KCC2-HA and KCC2ΔISO-HA

constructs ideally suited for quantifying their membrane expression. A triple tandem copy of the influenza virus HA peptide (YPYDVPDYA) was inserted into the second extracellular loop of KCC2. I detected the tagged, membrane-expressed KCC2 by live immunostaining using an anti-HA antibody. I compared the cluster intensity of anti-HA staining in KCC2ΔISO-HA transfected neurons to KCC2-HA neurons. I found that in neurons transfected with KCC2ΔISO-HA, the normalized cluster intensity was the same as in neurons transfected with KCC2-HA (**Figure 3.4.3.3B$_i$**; p= 0.5). Both untransfected and transfected neurons incubated with the secondary antibody alone showed no significant Cy3 fluorescence. I also performed gramicidin perforated-patch recordings of the HA-tagged constructs under isotonic conditions to confirm the HA-tagged constructs are functionally equivalent to the original chimeric constructs used in the initial electrophysiological experiments. I found that E_{Cl} of KCC2-HA was significantly hyperpolarized (-78.71 ± 5.39 mV, n = 10, $p < 0.05$; **Figure 3.4.3.3B$_{ii}$**), when compared with KCC2ΔISO-HA alone (-53.79 ± 8.56 mV, n=5; **Figure 3.4.3.3B$_{ii}$**). When these immunofluorescence results are taken together with my electrophysiological measurements of E_{Cl}, I am able to conclude that the C-terminal 15 amino acid ISO domain is the critical region required for KCC2-mediated isotonic Cl^- transport in neurons.

3.4.4 Characterization of Hypotonic Shock on Chimeric Proteins

In addition to being active under isotonic conditions, KCC2 can also be activated by hypotonic shock, which induces cell swelling (Lauf & Bauer 1987a). Several other members of the CCC family are swelling or shrinkage-activated and function in ion regulation and cell

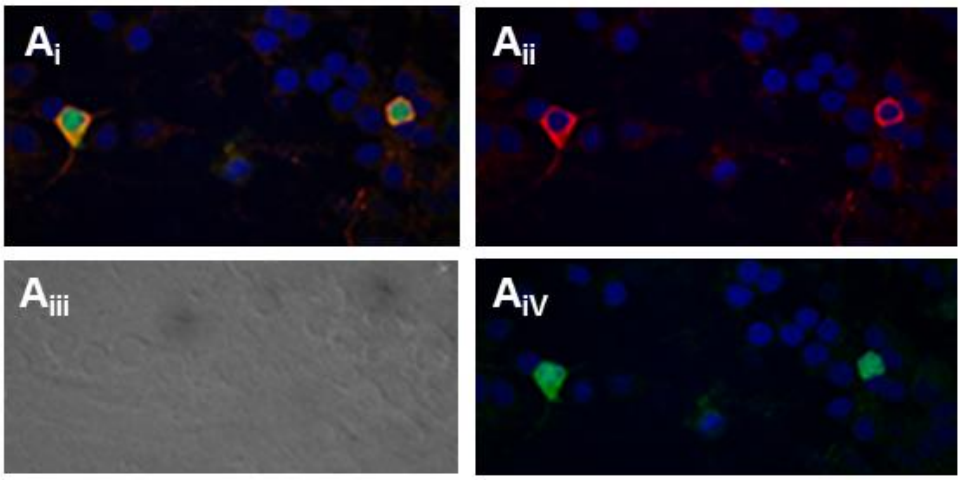

Figure 3.4.3.1. KCC2-backboned construct expression is confirmed by immunohistochemistry. Confocal microscopic immunoflourescence images of cultured hippocampal neurons from untransfected wildtype and KCC2ΔISO expressing neurons (GFP-positive). Neurons are stained for anti-GFP (green) anti-KCC2 (Cy3, red) and DAPI (blue). **Ai.** Overlay of GFP, anti-KCC2 and DAPI in a transfected neuron and untransfected neurons in the same field of view. **Aii.** GFP-positive cell reporting the expression of KCC2ΔISO. **Aiii**. Bright field image of the same field of view. **Aiv.** Anti-KCC2 staining (Cy3, red) at the level of DAPI. Staining pattern is consistent with overexpression of the KCC2ΔISO protein.

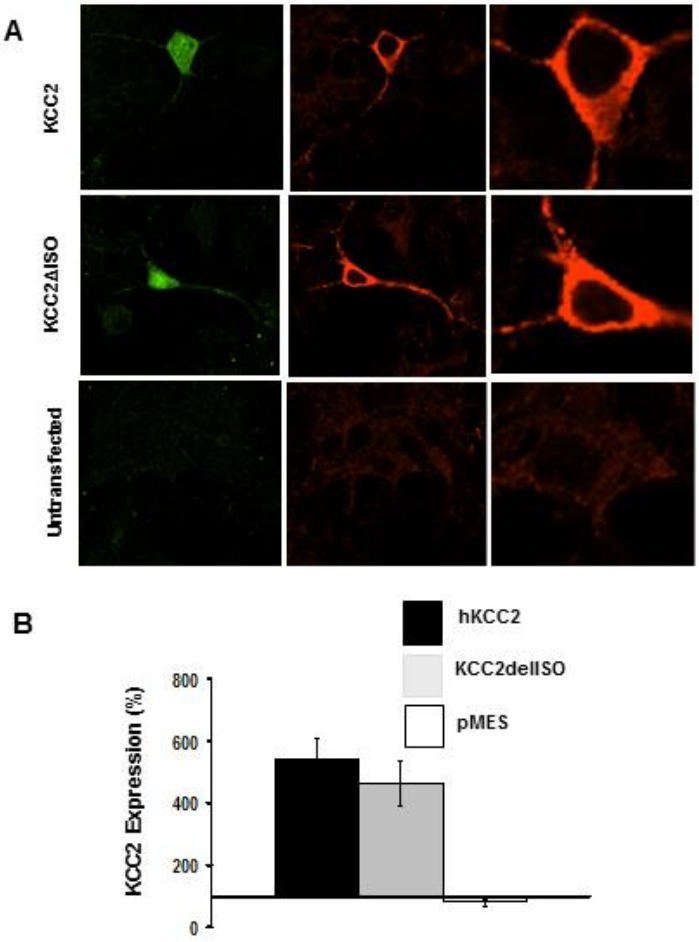

Figure 3.4.3.2. KCC2-backboned constructs are expressed at the same levels in hippocampal neurons. **A.** Confocal microscopic immunoflourescence images of cultured hippocampal neurons from untransfected wildtype and KCC2ΔISO expressing neurons (GFP-positive) and untransfected neurons. Neurons are stained for anti-GFP (green) anti-KCC2 (Cy3, red) **B.** Anti-KCC2 expression quantified for percentage of Cy3 staining compared to untransfected cells, includes all experiments similar to A.

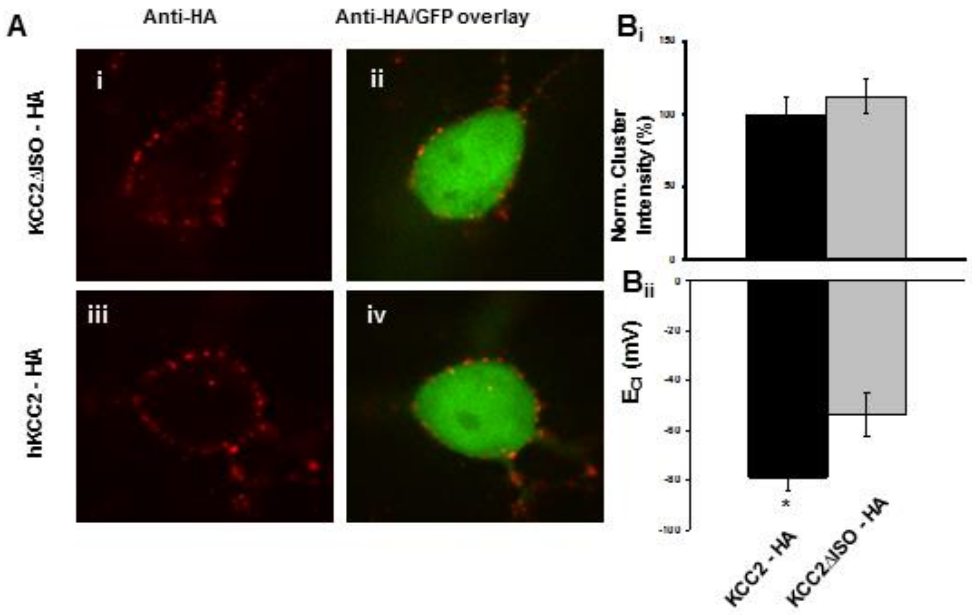

Figure 3.4.3.3. Membrane expression of KCC2-KCC4 chimeric proteins in hippocampal neurons. ***A***. Confocal microscopic immunofluorescent images from single optical sections of anti-HA and GFP in cultured hippocampal neurons. Neurons were stained for anti-HA (Cy3, red). **i**, **ii**, KCC2ISO-HA. **iii**, **iv,** KCC2-HA. Scale bar, 20m. ***B***, Summary of anti-HA normalized cluster intensity for all GFP-positive neurons (KCC2ISO-HA: *n*=13; KCC2-HA: *n*=12; *p* = 0.5). Neurons expressing the KCC2-HA construct show hyperpolarized values of E_{Cl} while KCC2ΔISO-HA is devoid of Cl^- transport (**Bii**). **p* < 0.05.

volume maintenance (Flatman 2008, Lauf & Bauer 1987a). To determine whether the ISO domain is also required for swelling-induced activation of KCC2, I again performed gramicidin perforated patch recordings and measured E_{Cl} from neurons expressing the constructs of interest; I induced cell-swelling by exposing neurons to hypotonic conditions (180 mOsM extracellular solution). When I recorded from neurons transfected with KCC2ΔISO I found that hypotonic shock induced a significant hyperpolarization of E_{Cl} compared to isotonic conditions (ΔE_{Cl} = -31.08 mV ± 4.09 mV (from -57.53 mV to -88.61 mV), n = 6, $p < 0.01$; **Figure 3.4.4.1**). Hypotonic shock produced no significant change in E_{Cl} from neurons overexpressing KCC2 (from -97.56 mV to -95,44 mV), because neuronal Cl^- was already at a very low concentration (4.04 mM, as predicted from the Nernst equation). This result is supported by my finding that both untransfected neurons and neurons transfected with an empty vector, were significantly hyperpolarized by hypotonic extracellular solution (untransfected: ΔE_{Cl} = -21.05 mV ± 1.80 mV (from -58.44 mV to -79.5 mV), n = 9, $p < 0.01$; transfected: ΔE_{Cl} = -15.97 mV ± 3.89 mV (from -61.45 mV to -77.42 mV), n = 9, $p < 0.01$; **Figure 3.4.4.1B**). I next compared the swelling-induced activation of KCC2ΔISO to that of a related family member, Δ, which is exclusively swelling-activated and not endogenously found in hippocampal neurons (Karadsheh et al 2004, Lauf & Bauer 1987a). Recordings from KCC4-transfected neurons revealed that hypotonic shock induced a similar hyperpolarization of E_{Cl} (ΔE_{Cl} = 27.22 mV ± 4.04 mV (from -52.31 mV to -79.53 mV), n = 11, $p < 0.01$; **Figure 3.4.4.1B**), when compared to KCC2ΔISO. Thus by removing the ISO domain, but maintaining its swelling-activated transport, I have voided KCC2 of its primary neuron-specific function, which demonstrates that there are exclusive molecular determinants of isotonic and swelling-induced K^+Cl^- cotransport.

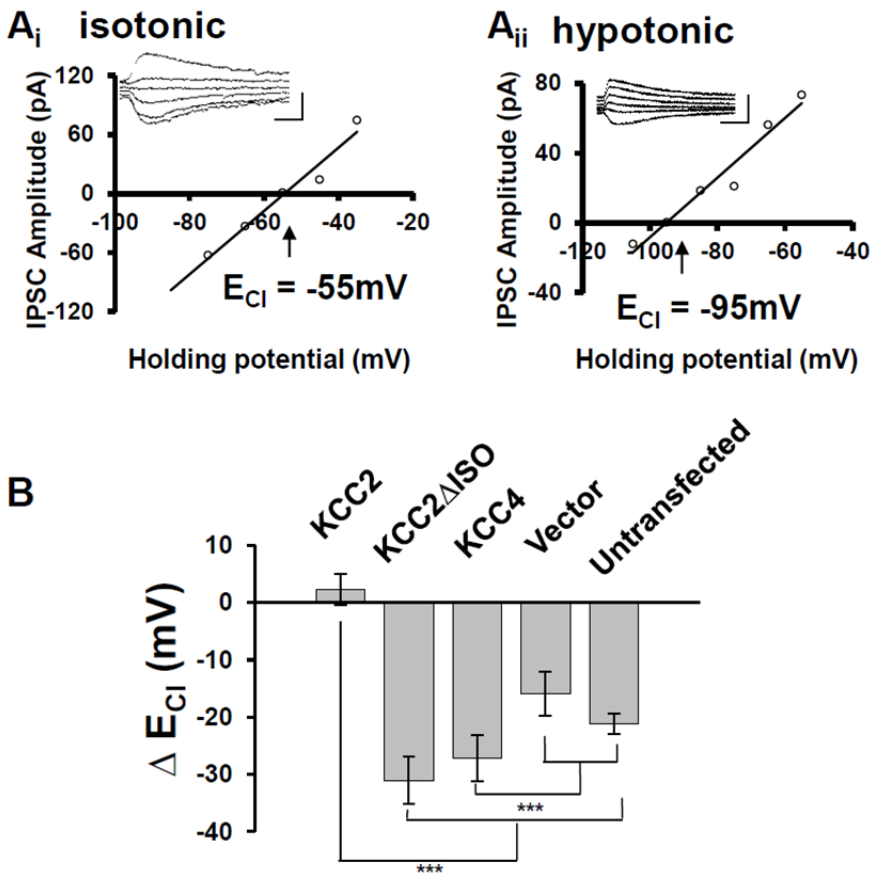

Figure 3.4.4.1. Hypotonic shock recovers K^+Cl^- transport function in KCC2ΔISO. **A**. Examples of gramicidin perforated patch-clamp recordings obtained from neurons in hippocampal culture overexpressing KCC2ΔISO in isotonic (300 mOsM) (**i**) and hypotonic (180 mOsM) (**ii**) extracellular solution. The IPSC amplitude was plotted against the holding potential, and the intercept of this curve with the *x*-axis was taken as E_{Cl} (arrows). Insets, Traces of IPSCs for the examples shown. Scale bars: 100 pA, 150 ms. **B**. Summary of the change in E_{Cl} from isotonic to hypotonic conditions for both untransfected and transfected cultured hippocampal neurons. Transfected neurons overexpressed KCC2, KCC2ΔISO, KCC4, or an empty vector. Data were not paired, but were obtained from separate populations of neurons (in either isotonic or hypotonic conditions). ***$p < 0.001$.

3.4.5. Characterization of Chimeric Proteins under a Cl^- Load

In *Xenopus* oocytes the KCC2 ISO domain is both required and sufficient for constitutive transport activity, as demonstrated using a Rb^+ influx assay (Mercado et al 2006b). I next asked whether the ISO domain was also sufficient for constitutive function, by attempting to confer KCC4 with the ability to extrude Cl^- from neurons under isotonic conditions. I transfected cultured hippocampal neurons with a KCC2-KCC4 chimeric construct, where I introduced the KCC2 ISO domain into KCC4 (KCC4-ISO). When I made gramicidin perforated patch clamp recordings from neurons transfected with KCC4-ISO, I found that isotonic Cl^- transport was not conferred (E_{Cl} = -61.92 ± 2.83 mV, n = 12; **Figure 3.4.5.1A**), compared to neurons transfected with KCC2 (n = 12; $p > 0.05$; **Figure 3.4.5.1A**). However, it is known that K^+Cl^- cotransporter activity (including KCC4) is increased at higher levels of intracellular Cl^- (Bergeron et al 2009, Bergeron et al 2006, Gillen & Forbush 1999), thus we asked whether increased levels of neuronal Cl^- were required to reveal whether the addition of the ISO domain to KCC4 could confer this cotransporter with constitutive isotonic activity. I performed this experiment by loading neurons with 50mM $[Cl^-]_i$ and found that the ISO domain could in fact confer KCC4 with constitutive isotonic activity. Under these conditions of elevated neuronal Cl^-, I found that KCC4 containing the ISO domain (KCC4-ISO) significantly hyperpolarized, when compared to full length KCC4 (KCC4-ISO E_{Cl} = -23.08 ± 3.96 mV, n = 14; KCC4 E_{Cl} = 13.04 ± 2.49 mV, n = 11; $p < 0.05$; **Figure 3.4.5.1B**). Moreover, the E_{Cl} of neurons overexpression KCC4-ISO was not significantly different from neurons overexpressing KCC2 (KCC2 E_{Cl} = -34.17 ± 4.93 mV, n= 16; $p > 0.05$; **Figure 3.4.5.1 B**), indicating that the addition of the KCC2 ISO domain to KCC4 can confer KCC4 with constitutive isotonic transport when neuronal Cl^- levels have been

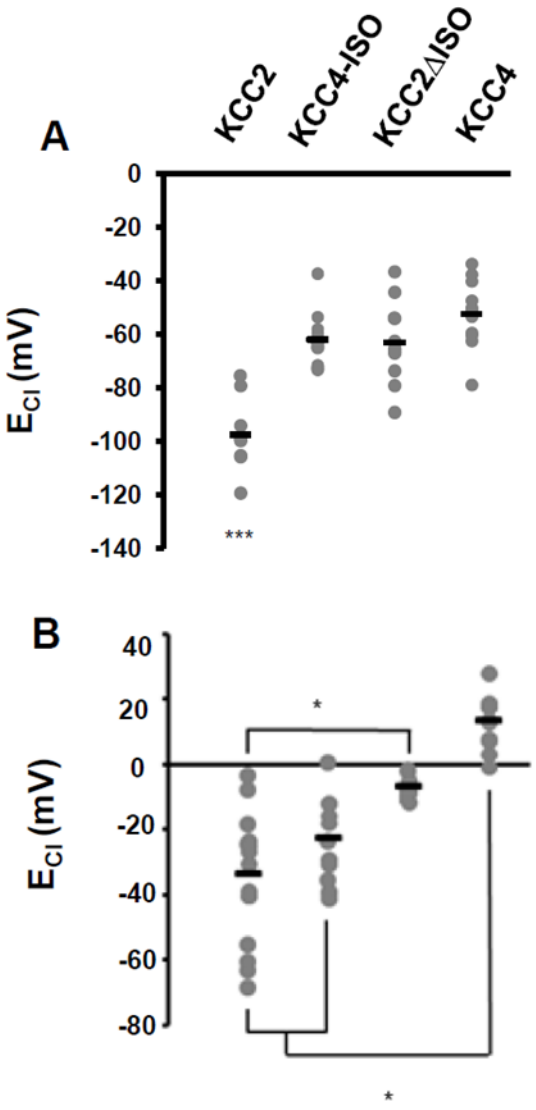

Figure 3.4.5.1. The KCC4-ISO rescue of isotonic transport depends on neuronal Cl^-. ***A***. Summary figure plotting the distribution of E_{Cl} in neurons overexpressing KCC2-KCC4 chimeric proteins under isotonic extracellular conditions. ***B***. Summary figure plotting the distribution of E_{Cl} in neurons overexpressing KCC2-KCC4 chimeric proteins and loaded with 50mM intracellular Cl^- under isotonic extracellular conditions. *$p < 0.05$, ***$p < 0.001$.

elevated to promote KCC4 function.

3.5 Conclusion

To determine what confers KCC2 with this unique ability to transport Cl^- isotonically, I took a gene modification approach and assayed neuronal Cl^- regulation. My hypothesis that these 15 amino acids on the C-terminus of KCC2 are responsible for KCC2 cotransport under isotonic conditions in neurons was based on our collaborator's work using a Rb^+-uptake assay that demonstrated that a C-terminal domain renders KCC2 constitutively active in *Xenopus* oocytes (Mercado et al 2006a). My objective was to determine whether this same domain also confers KCC2 with the ability to extrude Cl^- from neurons under physiologically relevant isotonic conditions in neurons. My findings provide the first demonstration of a KCC2-specific C-terminal domain responsible for conferring constitutively active isotonic transport in neurons (Acton et al 2012). Moreover, I discovered that this KCC2-unique domain is not required for the cell swelling-induced activation of KCC2 in neurons, demonstrating that separate molecular mechanisms determine KCC2 function during physiological and presumably pathophysiological states. The implications of this discovery are discussed in Chapter 6.

Chapter 4. The Neto2:KCC2 Interaction is Required for Synaptic Inhibition

4.1 Statement of Authorship

The results from this chapter were published in February 2013 in the Proceedings of the National Academy of Science:

Ivakine, E.A.*, **Acton, B.,A**.*, Mahadevan, V*., Ormond, J., Tang, M., Pressey, J.C., Huang, M.Y., Ng, D., Deplire, E., Salter, M.W., Woodin, M.A., McInnes, R.R. (2013). Neto2 is a KCC2 Interacting Protein Required for Neuronal Cl^- Regulation in Hippocampal Neurons: Proc atl Acad Sci USA 26:110(9): 3561-6.

*denotes joint first-authorship

This collaboration began in the McInnes Lab at Sick Kids where post-doctoral fellow Evgueni Ivakine *(Program in Developmental and Stem Cell Biology, and eNeurosciences and Mental Health, Hospital for Sick Children Research Institute, Toronto, ON,Canada M5G 1X8*) identified Neto2 as a potential interactor of KCC2. I completed all of the electrophysiological recordings as well as the calcium imaging and morphological analysis in the manuscript. Vivek Mahadevan *(Department of Cell and Systems Biology, University of Toronto, Toronto, ON, Canada M5S 3G5)* and Evgueni Ivakine performed all of the biochemical experiments. I also played a primary role in data interpretation and writing of the manuscript. All data presented in this thesis are from experiments that I have performed.

4.2 Introduction, Objectives and Hypothesis

Neto2 is a CUB domain-containing transmembrane protein abundantly expressed in neurons (Michishita et al 2003), which is important for proper neurological function (Finelli et al 2012). CUB domains are evolutionarily conserved protein domains (Bork & Beckmann 1993) that participate in protein–protein interactions (Tu et al 2008, Zheng et al 2004). KCC2

interacting proteins required for KCC2 transport and function in the mature CNS have not been identified, which represents a large gap in our fundamental knowledge regarding neuronal Cl^- regulation and inhibitory synaptic transmission. Neto proteins were previously identified as auxiliary subunits of ionotropic glutamate receptors, including KAR and NMDA receptors (Ng et al 2009, Straub et al 2011, Tang et al 2012, Tang et al 2011, Zhang et al 2009), and this study further extends the role of the Neto proteins to inhibitory synapses. An initial unbiased proteomic screen and immunoprecipitation experiments determined that Neto2 interacts with KCC2 *in vivo*.

In the present study, my **objective** was to define the role of Neto2 as a KCC2 interacting protein *in vivo* and here, I aimed to determine if this interaction is required for normal levels of neuronal Cl^- homeostasis. I designed the present experiments to elucidated the role of this association and to characterize the importance of the Neto2:KCC2 interaction in the normal neurophysiological function of KCC2. I **hypothesized** that the Neto2:KCC2 interaction is required for normal levels of GABAergic inhibition in hippocampal neurons. In this chapter, I describe my experimental design and results that support the role of Neto2 in maintaining KCC2 cotransport function and consequently, strong GABAergic inhibition in hippocampal neurons (Ivakine et al 2013).

4.3 Materials and Methods (Specific to Chapter 4)

4.3.1 Ca^{2+} Imaging

Hippocampal neurons were loaded with the membrane permeable fluorescent Ca^{2+} indicator Fluo 4-AM (Invitrogen) for 30 min at 37 °C, 5% CO_2. Fluo 4 was dissolved in dimethyl sulfoxide (DMSO) and 20% pluronic acid to a stock concentration of 1 mM and then diluted to 1

μM in our XCS. Following dye loading, the cells were thoroughly washed with XCS. Neurons were placed into the chamber of an inverted microscope (Olympus IX71) equipped with an Olympus 0.6 N.A., 40× objective. Fluo 4 was excited at 488 nm through a monochromator (Photon Technology International), controlled by the ImageMaster software (Photon Technology International). Fluorescence emission of labeled cells at 510 nm was detected with a 16-bit CCD camera (Cascade 650; Photometrics, Roper Scientific). Images of 653 × 492 pixels were accumulated at 500- to 1,000-ms intervals. A neuron that change by 2,000 fluorescent units over a 5s interval was considered to be active. This was based on previous demonstration in the Woodin Lab that an elecited AP caused a change in 2,000 flourescent units on average in a single neuron.

4.3.2 DNA Expression Constructs

Full length mouse Neto2 cDNA (encoding 1–525 aa) and deletion mutants: Neto2-Δecto-HA were generated by PCR and subcloned into a variant of pcDNA3.1mycHisA(+) (Invitrogen) containing two copies of the HA epitope tag, and sequence verified. pMES-KCC2 plasmid containing full-length human KCC2 cDNA was a kind gift from Dr. David Mount (Harvard MedicalSchool, Cambridge, MA). pMES-Neto2 construct was generated by subcloning a full-length Neto2 cDNA into a pMES vector. The deletion construct Neto2-Δecto-HA, containing the cytoplasmic tail used in **Figure 4.4.4.2,** was transfected into cultured hippocampal neurons and it was cotransfected with pMES-GFP to serve as the reporter.

4.3.3 Silencing Agents

KCC2 siRNA was used which is a small interfering RNA plasmid targeted toward KCC2 (KCC2 siRNA; catalog #sc-42607), and a nonsilencing control plasmid (catalog #sc-108060), were both purchased from Santa Cruz Biotechnology. The KCC2 siRNA (m) is a pool of three different siRNA duplexes (all sequences are provided in 5′ → 3′ orientation) as follows: sc-42607A (sense, CCCUAUGUCUUCAG UGAUAtt; antisense, UAUCACUGAAGACAUAGGGtt); sc-42607B (sense, CUACGAGAA GACAUUAGUAtt; antisense, UACUAAUGUCUUCUCGUAGtt); sc-42607C (sense, CAAGU CACCUCUAUAAUCAtt; antisense, UGAUUAUAGAGGUGACUUGtt). **In Figures 4.4.3.1 and 4.4.6.1**, the change in E_{Cl} was calculated by subtracting E_{Cl} in siRNA silenced neurons from neurons transfected with a nonsilencing control plasmid. When KCC2 siRNA or the nonsilencing control plasmid were transfected into cultured hippocampal neurons, they were cotransfected with pMES-GFP.

4.3.4 Antagonists

For the experiments that required a KCC2 antagonist, VU0240551 (25 μM; Sigma-Aldrich, Oakville, ON) was added to the XCS in which the cell culture incubated for 15 minutes prior to the beginning of each electrophysiological experiment. The same concentration of the pharmacological agent was also present for the entire duration of the experiment. Bumetanide, which antagonizes NKCC1, was used at 10μM (Sigma-Aldrich, Oakville, ON) in the same manner.

4.3.5 Scholl Analysis

Neurons were transfected with pMES-GFP construct and images of GFP-positive neurons were taken using a 10×, 1.4 N.A. objective. Z-steps were taken at 0.2 μm. Morphological

analysis was performed on these z-stacks using Velocity 3D Image Analysis Software (PerkinElmer) by implementing Scholl analysis to analyze the amount of dendritic branching. The number of branches, at intervals of 20 μm from the centroid of the soma, were counted. An average measure of the cell diameter was also taken.

4.3.6 Cell Death Assay

Cell death was assayed in wild-type and Neto2$^{-/-}$ by incubating cultures in 1× PBS with 14 μM propidium iodide (PI) for 20 min at 37 °C. Confocal images were taken using a 10×, 1.4 N.A. objective under bright-field and Cy3 settings. The number of neurons in the field of view (FOV) was counted under bright-field illumination. PI-positive neurons were counted (indicated by Cy3 staining) and presented as a proportion of the number of neurons in the FOV.

4.4 **Results**: Identification and Characterization of Neto2-null Hippocampal Cultured Neurons

4.4.1. Characterization of E_{Cl} in Neto2-null mice

Having established that Neto2 interacts with KCC2, I asked whether Neto2 regulates KCC2 function. Based on the critical role of KCC2 in extruding neuronal Cl^-, I examined KCC2 function by recording E_{Cl}, which is principally determined by $[Cl^-]_i$. Using the gramicidin perforated patch clamp technique to record E_{Cl} without altering $[Cl^-]_i$, I found that hippocampal neurons cultured from Neto2-null mice had significantly depolarized E_{Cl}, in comparison with wild type (**Figure 4.4.1.1**; wild type: −75.2 ± 2.1 mV, n = 14; Neto2$^{-/-}$: −53.7 ± 2.4 mV, n = 11; $p < 0.001$).

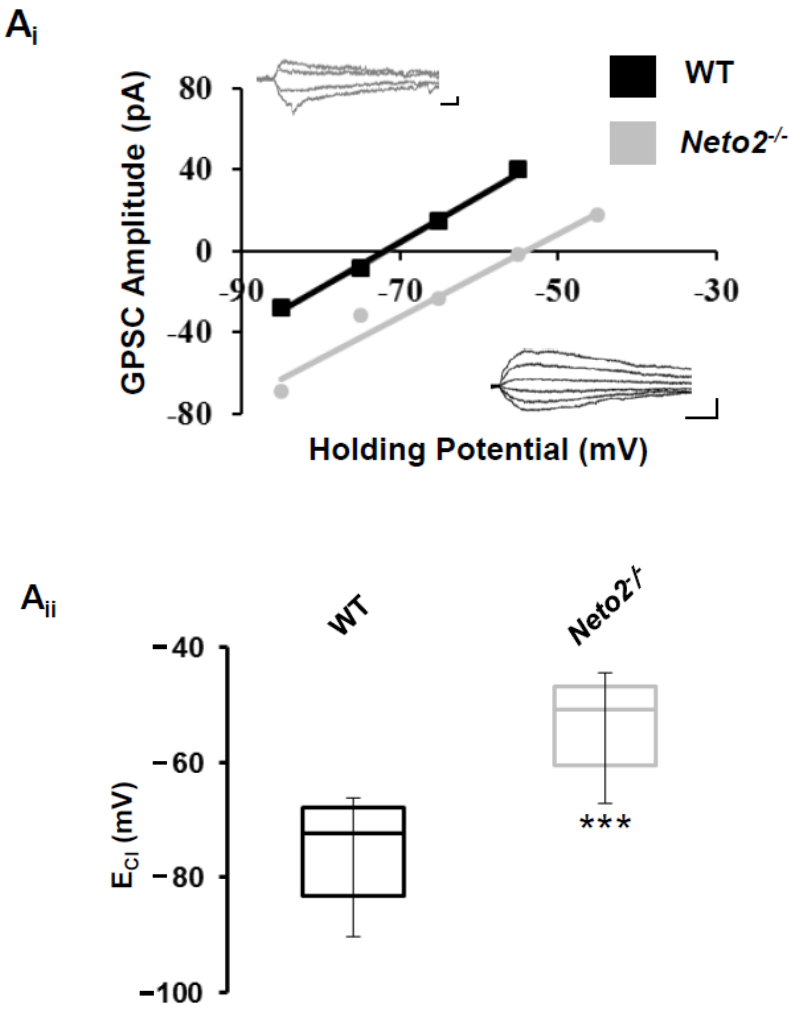

Figure 4.4.1.1. Neto2-null mice have depolarized E_{Cl} compared with wildtype neurons. **Ai**. Example of gramicidin perforated patch clamp recordings obtained from neurons in dissociated culture prepared from the hippocampus of Neto2-null mice (gray) and wildtype mice (black). The GABAergic postsynaptic current (GPSC) amplitude was plotted against the holding (membrane) potential of the postsynaptic membrane, and the intercept of this curve with the x-axis was taken as E_{Cl}. (Insets) Traces of GPSCs for the examples shown. (Scale bars: 20 pA, 50 ms.) **Aii**. Summary of all experiments similar to Ai. *** p <0.001

4.4.2 Electrophysiological Properties and Activity Levels of Neto2-null Neurons

Remarkably, in some neurons, the depolarization of E_{Cl} reached levels above the threshold for action potentials, thus rendering GABA excitatory (2 of 11 neurons). The depolarization of E_{Cl} in Neto2$^{-/-}$ neurons, relative to wild-type neurons, was not accompanied by significant changes in any other neuronal properties that I examined electrophysiologically, including resting membrane potential, input resistance (IR), AP amplitude, or AP threshold (**Table 1**) except AP frequency (**Table 2**). To examine the activity levels at different age points in culture, wildtype and Neto2$^{-/-}$ neuronal cultures were loaded with Fluo4-AM Ca^{2+} imaging dye and the number of action potentials fired per 5 second interval was recorded. The results (shown in **Figure 4.4.2.1**) show no difference in the activity of cultured neurons at any time point before the neurons were used for experiments. Taken together, these results indicate that the loss of Neto2 is specific to depolarizing E_{Cl} relative to wildtype neurons.

4.4.3 Depolarization of E_{Cl} in Neto2-null Neurons is Due to KCC2

If the depolarization of E_{Cl} in Neto2-null mice, relative to wildtype mice, is due to the dysfunction of KCC2 resulting from the loss of the Neto2:KCC2 interaction, then suppressing KCC2 function should produce a significantly smaller depolarization of E_{Cl} in Neto2-null mice compared with wildtype mice. To test this prediction, I compared the change in E_{Cl} between wildtype and Neto2$^{-/-}$ neurons, in response to both the specific KCC2 antagonist VU0240551 (25 μM) and siRNA-mediated silencing of KCC2. As hypothesized, pharmacological inhibition of KCC2 with VU0240551 produced a significantly larger change in E_{Cl} in wildtype neurons

	RMP (mV)				IR (mΩ)				AP Threshold (mV)				AP Amplitude (mV)			
	MEAN	SE	n	p	MEAN	SE	n	p	MEAN	SE	n	p	MEAN	SE	n	p
Culture WT	-69.71	2.56	14	0.80	608.61	64.00	14	0.64	-46.44	2.23	13	0.58	30.72	2.75	16	0.35
Culture Neto2-/-	-68.73	2.75	16		657.90	45.26	16		-44.89	2.33	6		27.56	2.06	13	

Table 4.4.1.1. Neurons from Neto2-null mice have normal electrophysiological properties. Average values for the electrophysiological properties of wildtype and Neto2$^{-/-}$ neurons. Values were taken from the same electrophysiological recordings made when E_{Cl} was recorded. The p value is greater than 0.5 for each the resting membrane potential (RMP), the input resistance (IR), the action potential threshold (AP) and the action potential amplitude (AP) indicating that neurons from Neto2$^{-/-}$ mice have normal electrophysiological properties.

	AP frequency (Hz)			
Preparation	mean	SE	n	p
culture WT	5.45	1.49	10	
culture Neto2$^{-/-}$	16.22	4.04	9	0.018

Table 4.4.1.2. Neto2-null mice are more excitable than wildtype.
Electrophysiological recordings were made at the same time as E_{Cl} was recorded to observe the excitability of neurons by injecting current through the patch pipette. Neurons from Neto2$^{-/-}$ cultures fire more action potentials per second than wildtype neurons ($p < 0.018$).

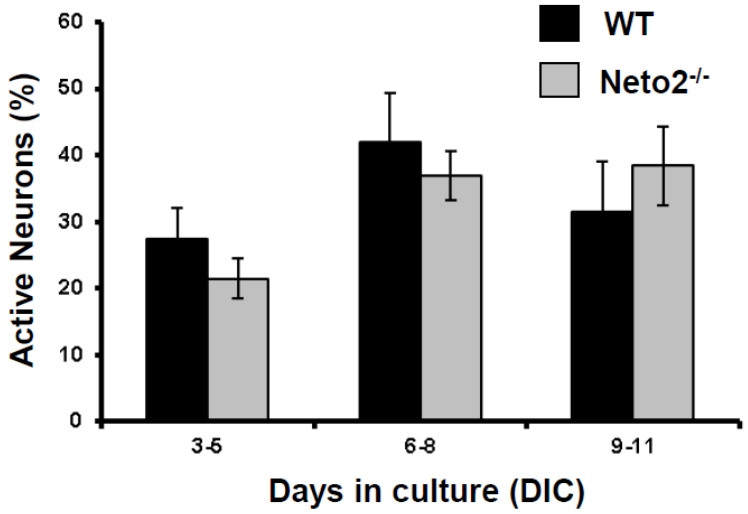

Figure 4.4.2.1. Neto2-null mice have normal levels of neuronal activity. Neuronal activity was assayed using Ca^{2+} imaging at three different time points (DIV 3–4, 6–8,9–11). Active neurons were defined as those with an increase of 2,000 fluorescent units within a 5s interval (which we determined corresponds with the fluorescence increase during an action potential). There were no significant differences in the percentage of active neurons between cultures prepared from either wild-type or Neto2-null mice

compared with Neto2$^{-/-}$ neurons (**Figure 4.4.3.1A$_i$**; $p < 0.001$). siRNA-mediated silencing of KCC2 also produced a significantly larger change in E_{Cl} in wild-type neurons compared with Neto2$^{-/-}$ neurons (**Figure 4.4.3.1A$_{ii}$**; $p < 0.05$). Importantly, transfecting wild-type and Neto2$^{-/-}$ neurons with a non-silencing control plasmid produced no significant change in E_{Cl} ($p > 0.05$). Taken together, suppressing KCC2 function, both pharmacologically and by using a siRNA interference approach, revealed a significantly smaller effect on E_{Cl} in Neto2-null mice, suggesting that the absence of the Neto2:KCC2 interaction occluded the depolarizing effect of KCC2 suppression on E_{Cl} that occurred in wildtype neurons. The other major CCC in neurons that functions under isotonic conditions in neurons of the hippocampus is NKCC1. Although NKCC1 is expressed only at low levels in mature neurons, it was conceivable that the loss of Neto2 altered E_{Cl} through a regulation of NKCC1. To test this possibility, I inhibited NKCC1 with 10 μM bumetanide, and again compared the change in E_{Cl} between wildtype and Neto2$^{-/-}$ neurons. There was no significant difference in the amount of E_{Cl} hyperpolarization produced by NKCC1 inhibition (**Figure 4.4.3.1**; $p = 0.113$); however, the hyperpolarization in both conditions reflects the presence of some functional NKCC1 in both wild-type and Neto2$^{-/-}$ cultures. Taken together, these experiments demonstrate that the decrease in neuronal Cl^- regulation and subsequent depolarization of E_{Cl} in neurons from Neto2$^{-/-}$ mice, compared with wild types, is dependent on KCC2. This result is consistent with the lack of interaction between Neto2 and NKCC1 (Ivakine et al 2013).

4.4.4 Characterization of the Neto2-null Phenotype Rescue

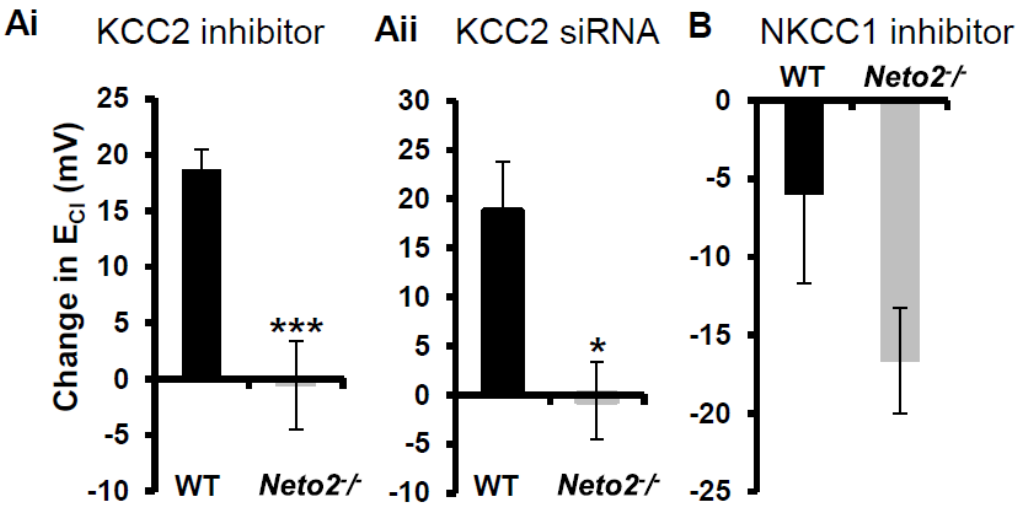

Figure 4.4.3.1. Neto2-null neurons do not show further depolarization in E_{Cl} when KCC2 is inhibited. **Ai.** Bar graph illustrating the change in E_{Cl} in response to 25μM VU0240551 obtained from wild-type and Neto2$^{-/-}$ neurons. **Aii.** Bar graph illustrating the change in E_{Cl} in response to siRNA-targeted to KCC2 obtained from wildtype and Neto2$^{-/-}$ neurons. **B.** Bar graph illustrating the change in E_{Cl} in response to 10μM bumetanide obtained from wildtype and Neto2$^{-/-}$ neurons. * $p < 0.05$, *** $p < 0.001$.

If the depolarized E_{Cl} in Neto2-null mice was directly due to the loss of Neto2, then transfecting cultured Neto2$^{-/-}$ hippocampal neurons with a DNA construct containing full-length Neto2 (FL-Neto2) should hyperpolarize E_{Cl}. When FL-Neto2 was introduced into these neuronsE_{Cl} significantly hyperpolarized in comparison with Neto2$^{-/-}$ neurons (**Figure 4.4.4.1A$_{ii}$**; Neto2$^{-/-}$: -55.8 ± 3.9 mV, n = 9; FL-Neto2 rescue: -73.2 ± 3.1 mV, n = 9; $p < 0.001$). Transfecting Neto2-null neurons with a control vector produced no significant change in E_{Cl} compared with Neto2$^{-/-}$ neurons (**Figure 4.4.4.1A$_{ii}$**; -58.6 ± 2.3 mV, n = 5; $p = 0.503$). These results indicate that the depolarization of E_{Cl} observed in Neto2-null mice can be rescued by reintroducing the protein, which confirms that the alterations in E_{Cl} observed in the Neto2-null mice is due to the loss of the Neto2 protein.

In the initial screen, KCC2 was shown to interact with Neto2 using the Neto2 cytoplasmic tail as bait (Ivakine et al 2013). I next asked whether this domain was capable of rescuing the depolarization of E_{Cl} in Neto2$^{-/-}$ neurons. When I transfected Neto2$^{-/-}$ neurons with the construct containing the cytoplasmic tail of Neto2, I observed a significant change in E_{Cl} compared with Neto2$^{-/-}$ neurons recorded from untransfected neurons in the same culture dishes (**Figure 4.4.4.2A$_{ii}$**; Neto2$^{-/-}$: -53.1 ± 3.3 mV, n = 8; cyto-Neto2 rescue: -68.2 ± 3.1 mV, n = 7; $p = 0.005$). Because the construct containing the cytoplasmic tail did not contain a fluorescent reporter, I visualized transfection by cotransfecting with a GFP-containing construct. As a positive control, I also cotransfected this GFP construct and FL-Neto2, and as I observed previously in **Figure 4.4.4.1**, FL-Neto2 could rescue E_{Cl} (Neto2$^{-/-}$: -53.1 ±3.3 mV, n = 8; FL-Neto2 rescue: -70.3 ± 2.2 mV, n = 6; $p = 0.002$). These results demonstrate that the depolarization of E_{Cl} recorded in Neto2$^{-/-}$ neurons can be rescued by reintroducing Neto2 protein

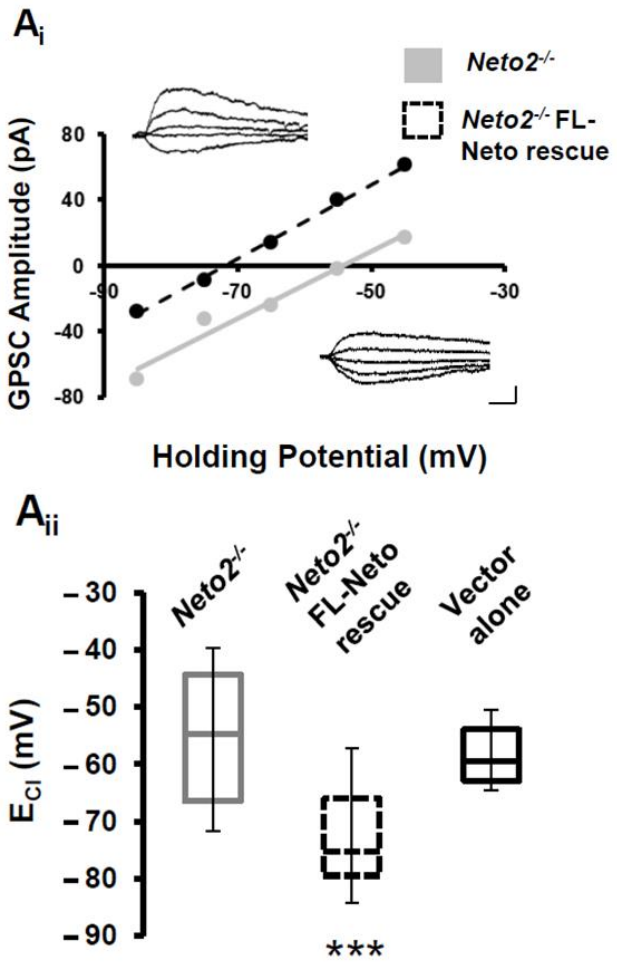

Figure 4.4.4.1. Reintroduction of Neto2 in Neto2$^{-/-}$ neurons rescues E_{Cl}. Ai. Example of gramicidin perforated patch-clamp recordings of E_{Cl} obtained from Neto2$^{-/-}$ neurons (gray) and Neto2$^{-/-}$ neurons transfected with full length Neto2 (Neto 2$^{-/-}$ FL-Neto rescue; dashed line). (Insets) Traces of GPSCs for the examples shown. (Scale bar: 40 pA, 100 ms.) **Aii.** Summary of all experiments similar to Ai. **p < 0.01,

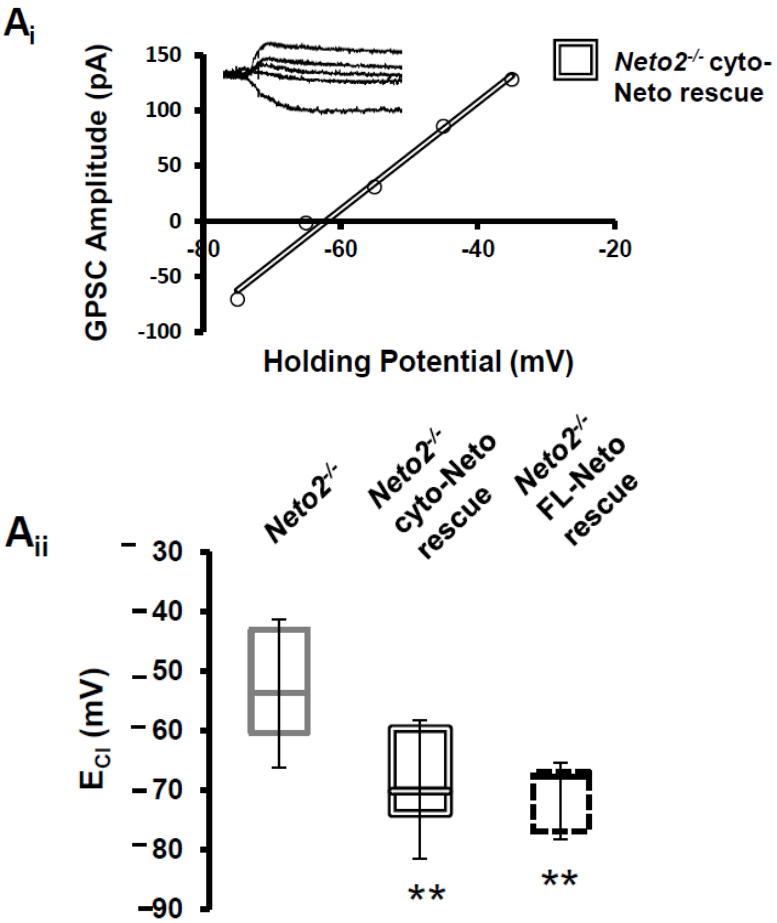

Figure 4.4.4.2. Cytoplasmic tail of Neto2 rescues E_{Cl}.
Ai. Example of E_{Cl} recordings obtained from Neto2$^{-/-}$ neurons transfected with the cytoplasmic tail of Neto2$^{-/-}$ (Neto2$^{-/-}$ cyto-Neto rescue; double line). (Scale bars: 30 pA, 50 ms.) **Aii**. Summary of all experiments similar to Ai. ** $p < 0.01$.

devoid of the ectodomain. This observation is important because the cytoplasmic tail of Neto2 was critical for the interaction of Neto2 and KCC2 in heterologous cells.

4.4.5 Neto2 Is Required to Maintain Efficient KCC2-Mediated Cl^- Extrusion

I have shown that the loss of Neto2 produces a decrease in KCC2-mediated Cl^- extrusion, but is Neto2 required on an on-going basis to maintain efficient Cl^- regulation? To address this question, we used a Neto2-specific silencing shRNA. If the sole function of Neto2 is to initially up-regulate KCC2, I would not expect that silencing of Neto2 in neurons already expressing KCC2 would alter E_{Cl}. When mature hippocampal cultured wild-type neurons were transfected with the silencing Neto2 shRNA construct, E_{Cl} depolarized relative to untransfected neurons (wild type: -66 ± 3.1 mV, n = 8; Neto2 silenced: -54.4 ± 2.2 mV, n = 8; p = 0.016; **Figure 4.4.5.1Aii**). Transfecting neurons with a scrambled shRNA as a gene silencing control produced no significant change in E_{Cl} (-64.7 ± 2.9 mV, n = 5; **Figure 4.4.5.1Aii**) compared with wildtype neurons (p = 0.936). Thus, Neto2 is required on an ongoing basis to maintain efficient KCC2-mediated Cl^- extrusion.

4.4.6 Neto2 Regulated Chloride Extrusion Efficacy

There is KCC2 present in the membrane of $Neto2^{-/-}$ neurons, so I next asked whether or not this residual protein was still capable of extruding Cl^-. Functional changes in the Cl^- extrusion capacity of KCC2 can be examined in the presence of an ionic load (Khirug et al 2005, Payne et al 2003, Zhu et al 2005). I examined the function of KCC2 in Neto2-null mice by

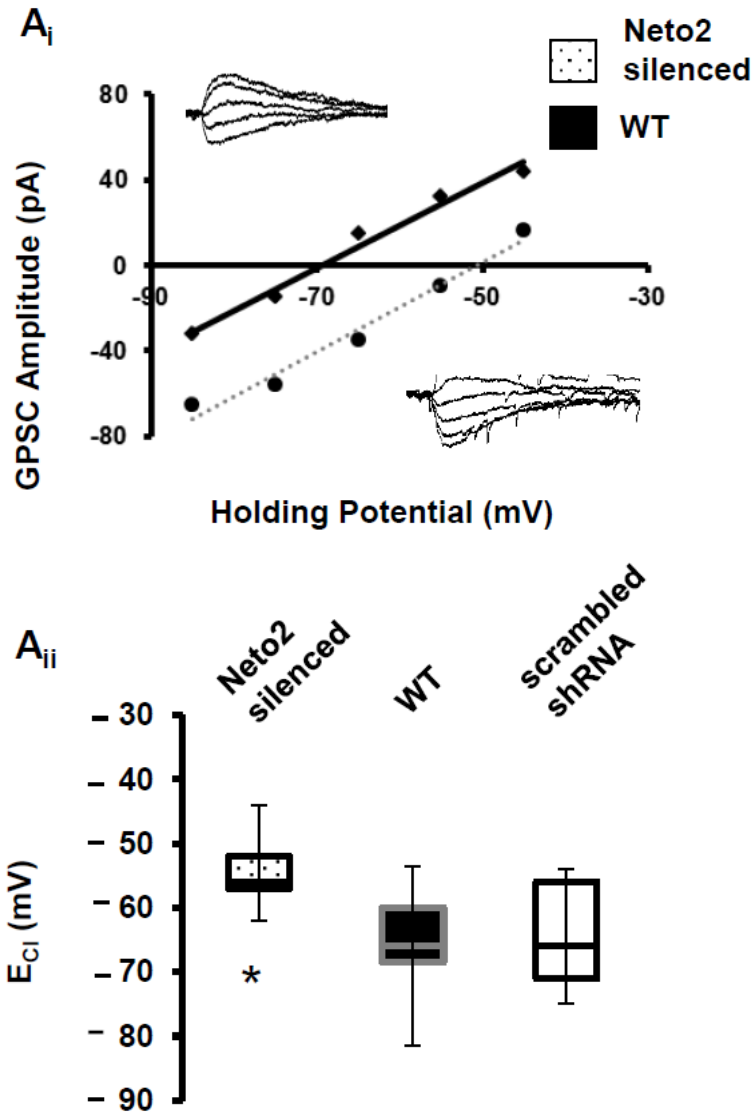

Figure 4.4.5.1. E_{Cl} depolarizes when Neto2 is silenced in the wildtype neurons. **Ai**. Example of E_{Cl} recordings obtained from wildtype neurons (black) and neurons transfected with a Neto2 shRNA (Neto2 silenced; stippled). (Scale bars: 30 pA, 50 ms.) **Aii.** Summary of all experiments similar to Ai. *p < 0.05.

loading the neuronal soma with 50 mM Cl^- through the patch pipette. Neurons from wild-type mice loaded with Cl^- had a measured E_{Cl} of −30.8 ± 4.6 mV (n = 7), whereas Neto2$^{-/-}$ neurons showed a depolarized E_{Cl} of -0.18 ± 7.9 mV (n = 9). When KCC2 was pharmacologically inhibited with VU02450551 (25 μM) under the Cl^- loading condition, I found a significant difference in the change in E_{Cl} between wild-type and Neto2$^{-/-}$ neurons (wildtype: 23.2 ± 5 mV, n = 10; Neto2$^{-/-}$: −4.9 ± 4.9 mV, n = 14; p = 0.001; **Figure 4.4.6.1A$_i$**). Next, I verified the effect of pharmacological inhibition of KCC2 on E_{Cl} using KCC2 siRNA, and found a significant difference in the change in E_{Cl} between wild-type and Neto2$^{-/-}$ neurons (wildtype: 19.7 ± 4.6 mV, n = 8; Neto2$^{-/-}$: -4.4 ± 2.7 mV, n = 7; p < 0.001; **Figure 4.4.6.1A$_{ii}$**). The suppression of KCC2 by both pharmacological inhibition and siRNA interference each produced a significantly smaller change in E_{Cl} in Neto2$^{-/-}$ neurons compared with wildtype neurons, consistent with a lack of functional KCC2 in the membrane of Neto2$^{-/-}$ neurons. The E_{Cl} values recorded in the presence of the KCC2 antagonist are more depolarized than the Nernst equation would predict (∼28 mV). However, the predicted value does not take into consideration transporter activity. When the Cl^- loading experiments were performed in the presence of the NKCC1 antagonist bumetanide (10 μM), the significant difference in the change in E_{Cl} between wildtype and Neto2$^{-/-}$ neurons was still present (wildtype bumetanide: -6.5 ± 1.6 mV, n = 6; Neto2$^{-/-}$ bumetanide: -23.7 ± 3.5 mV, n = 7; p = 0.002; **Figure 4.4.6.1B**). These experiments demonstrate that loss of Neto2 leads to a reduction in the Cl^- extrusion efficacy of the remaining KCC2 in Neto2$^{-/-}$ neurons.

4.4.7 Morphological Characterization of Neto2-null Hippocampal Cultured Neurons

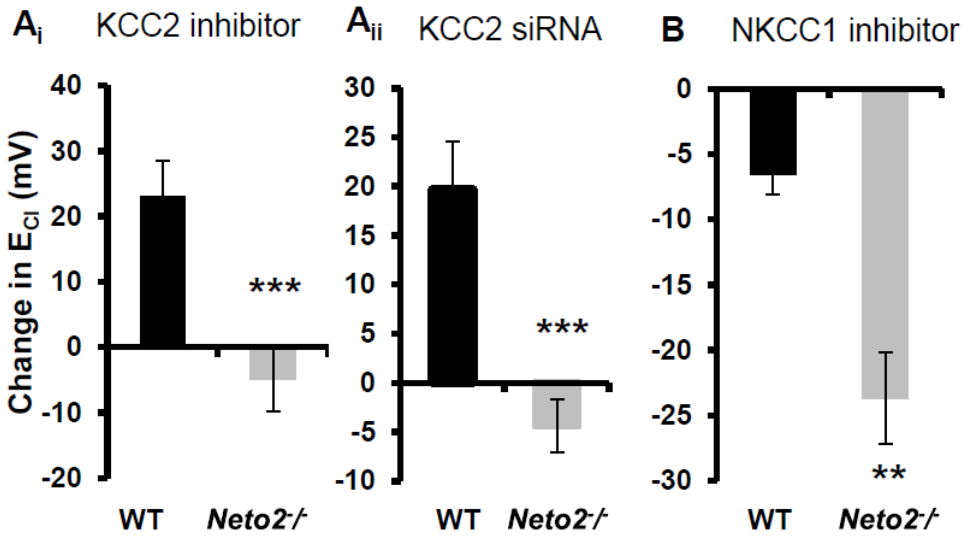

Figure 4.4.6.1. KCC2 inhibitor and KCC2 knockdown do not further depolarize E_{Cl} in Neto2$^{-/-}$ neurons. **A**. Summary of all whole cell recordings obtained from neurons loaded at the soma with 50 mM Cl^-. Recordings were made from wild-type neurons (black), and Neto2$^{-/-}$ neurons (gray) in the presence of (**Ai**) 25 µM VU0240551, (**Aiii**) transfected with siRNA KCC2, and (**B**) 10 µM bumetanide.

My results demonstrate that the functional significance of the Neto2:KCC2 interaction is to promote proper KCC2-mediated Cl^- extrusion in hippocampal neurons. However, KCC2 also plays an additional role in regulating neuronal morphology (Blaesse et al 2009, Li et al 2007). I tested the possibility that disrupting the Neto2:KCC2 interaction also affects neuronal morphology by performing a Scholl analysis on cultured wildtype and Neto2$^{-/-}$ hippocampal neurons. Scholl analysis is commonly used in to characterize the morphological characteristics of an imaged neuron. I found no significant difference between the number of dendritic intersections between wildytpe and Neto2$^{-/-}$ neurons (**Figure 4.4.7.1A$_{iii}$**; P = 0.6). In addition, I also examined soma size, neuronal density, and cell death (using propidium iodide). I found no significant differences in any of these parameters between wild-type and Neto2$^{-/-}$ neurons (soma size: **Figure 4.4.7.1A$_{iv}$**, p = 0.315; neuronal density: **Figure 4.4.7.2A$_{ii}$**, p = 0.96; cell death: **Figure 4.4.7.2A$_{iii}$**, p = 0.07). In summary, disruption of the Neto2:KCC2 interaction produced no significant differences in neuronal survival or morphology, leaving the main functional significance of the Neto2: KCC2 interaction is for the maintenance of proper KCC2-mediated Cl^- extrusion.

4.5 Conclusions

In summary, I have identified Neto2 as a regulator of KCC2 transporter activity. I obtained compelling lines of converging evidence in support of decreased Cl^- extrusion in Neto2-null mice. I demonstrated, using electrophysiology, that Neto2-null neurons were unable to extrude a Cl^- load, indicating that the function of the remaining neuronal KCC2 in Neto2-null is severely compromised. Remarkably, the decrease in KCC2 function in Neto2-null neurons can be such that intracellular Cl^- levels rise to the point where GABAergic transmission becomes

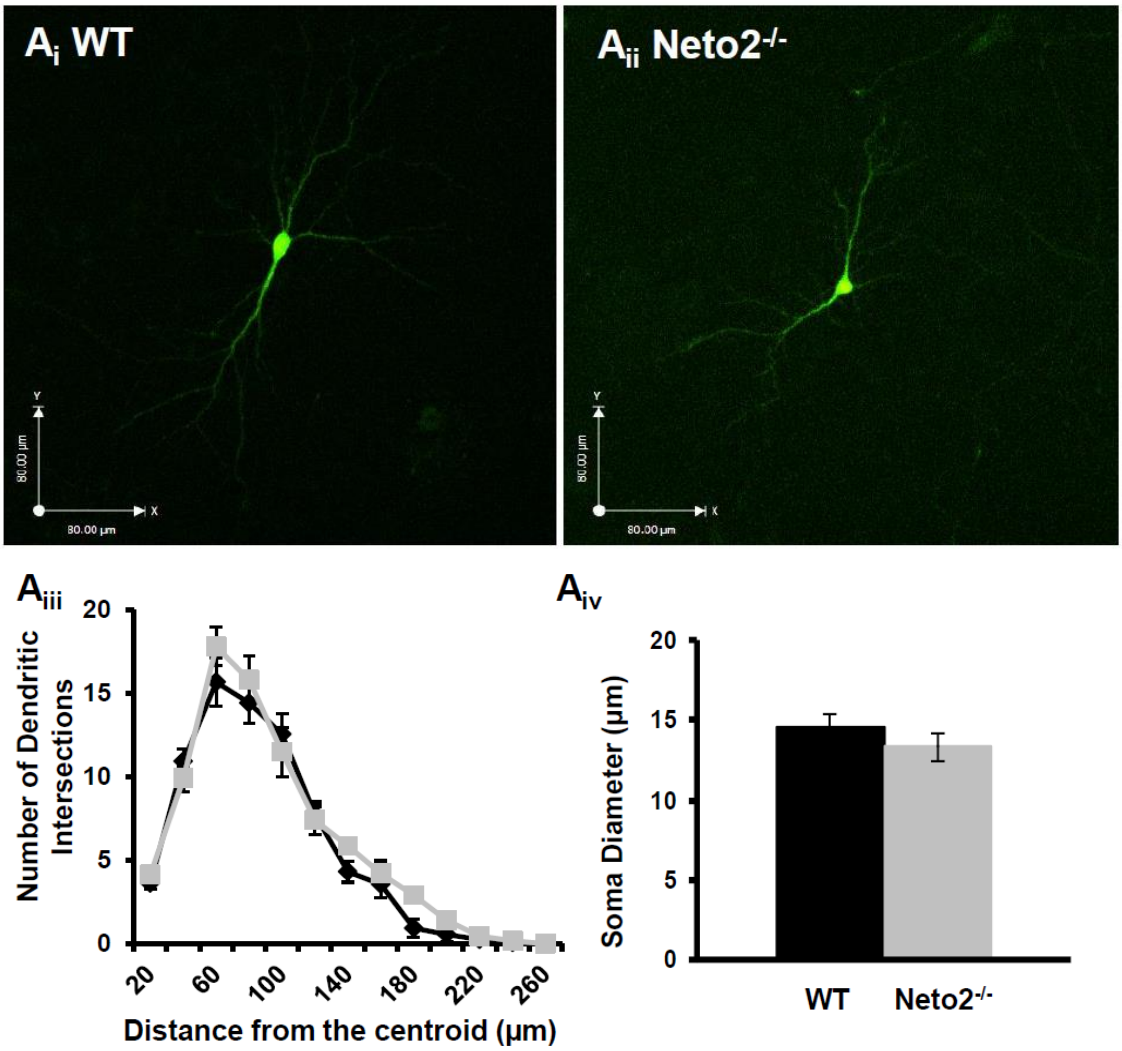

Figure 4.4.7.1. Neuronal morphology is not affected in Neto2-null mice. Example fluorescent images of a wildtype (**Ai**) and a Neto2$^{-/-}$ (**Aii**) neurons used for performing the Scholl analysis. (**Aiii**) Summary of Scholl analysis performed on wild-type (n = 16) and a Neto2$^{-/-}$ (n = 22) neurons. (**Aiv**) Quantification of the soma size diameter of wildtype and Neto2$^{-/-}$ neurons, obtained from the same neurons analyzed in Aiii.

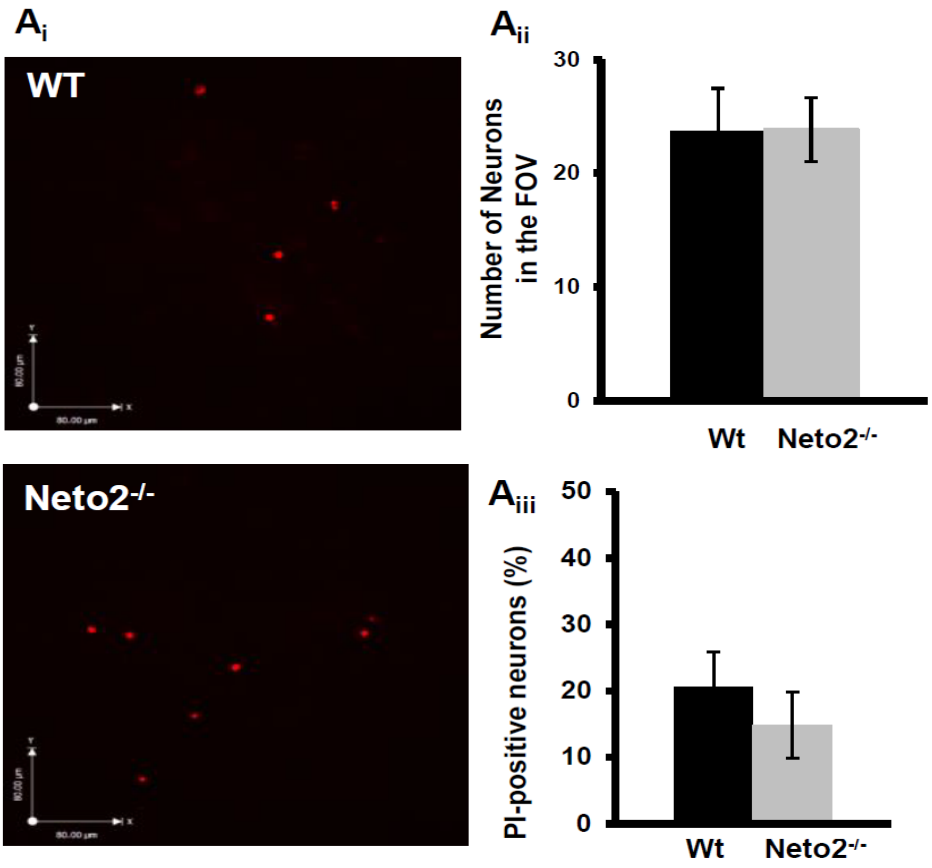

Figure 4.4.7.2. Neuronal cell death is not affected in Neto2-null mice. **Ai**. Example fluorescent images of wild-type and a Neto2$^{-/-}$ neurons stained with propidium iodide (PI). **Aii**. Average number of neurons in thefield of view (FOV) (counted under bright-field illumination; wild type, n = 12; Neto2$^{-/-}$, n = 12). **Aiii.** Percentage of neurons positive for PI, determined in relation to the total number of neurons in the FOV.

excitatory. The functional Neto2:KCC2 interaction is fundamental because the loss of Neto2 causes the neuronal Cl^- gradient to collapse. Thus, I have discovered that Neto2 interacts with the key protein that regulates the strength of inhibitory synaptic transmission in the CNS. Neto2 also binds to KARs (Zhang et al 2009). This work demonstrates that Neto2 is a multifunctional protein that can modulate the activity of both ion channels and transporters. By regulating proteins involved in both excitatory (KARs) and inhibitory (KCC2) neurotransmission, Neto2 is uniquely positioned to fine-tune synaptic activity on both neuronal and network levels. This finding raises the possibility that other CUB domain-containing proteins may function in a similar manner to regulate more than one class of membrane proteins.

The Neto2:KCC2 interaction was initially identified using the Neto2 cytoplasmic tail, but then later demonstrated that it is the CUB domains and not the cytoplasmic tail that is required for the interaction in heterologous HEK293 cells, suggesting that in our initial screen we likely pulled out KCC2 in a multiprotein complex. This possibility was strengthened by our finding that we could rescue the depolarization in E_{Cl} in Neto2-null neurons using the cytoplasmic tail alone. The identification of the additional protein(s) in this Neto2:KCC2 multiprotein complex is an important direction of future research, given the importance of this complex in regulating inhibitory synaptic transmission. The implications of this discovery are discussed in Chapter 6.

Chapter 5. The GluK1/2:KCC2 Interaction Positively Regulates KCC2

5.1 Statement of Authorship

The results from this chapter have not yet been published. Some of the work of this chapter is included in a manuscript submitted recently to Cell Reports:

Mahadevan, V., Pressey, J.C., **Acton, B.A**., Huang, M.Y., Puchalski, A., Ivakine, E.A., Delpire, E., McInness, R.R., Woodin, M.A. Native KCC2 is in a multimeric complex with kainate receptors and the auxiliary subunit Neto2. Cell Reports (Submission #418).

All work presented in this Chapter are results from experiments I performed. I designed the experiments presented here, collected the data, analyzed and interpreted the data. The remaining data that did not go into the Cell Reports manuscript is currently being put together with additional work from Jessica C. Pressey *(Department of Cell & Systems Biology, University of Toronto, Toronto, Ontario, M5S 3G5, Canada)* for a second manuscript outlining the mechanism for the Neto2:KCC2:GluK2 interaction.

5.2 Introduction, Objectives and Hypothesis

In the previous chapter, I identified that Neto2 is a KCC2-interacting protein that is essential for maintaining normal KCC2-mediated Cl^- homeostasis (Ivakine et al 2013). Neto2 interacts with both GluK2 and KCC2 through its extracellular CUB domains (Ivakine et al 2013, Tang et al 2011). This suggests that either there are two separate populations of Neto2 that bind GluK2 and KCC2, or that these three proteins are in the same macromolecular complex. Neto2 is a transmembrane protein that is both an auxiliary subunit for the KAR subunit GluK2, and a K^+Cl^- cotransporter (KCC2) interacting protein. Vivek Mahadevan (graduate student, Woodin Lab) found that these three proteins coexist in a macromolecular complex (unpublished data,

Woodin Lab) and are colocalized in hippocampal and cortical neurons (Pressey, unpublished data). Inhibiting GluK2 depolarized the reversal potential for GABA, suggesting that kainate-receptor signaling maintains KCC2 function and thus the strength of synaptic inhibition (Mahadevan and Pressey, unpublished data).

The **objective** of this chapter of my thesis was to determine the role of a primary KAR subunit, GluK2, in the expression pattern, distribution and neuronal surface stability of KCC2. I define cell-surface stability as a relative measure of how long KCC2 is visible in the membrane before being endocytosed. Since it has been determined that the Neto2:GluK2:KCC2 interaction is required for normal levels of synaptic inhibition (Pressey, unpublished data), I **hypothesized** that a primary function of this interaction is to maintain the cell-surface stability and membrane expression patterns of KCC2. The experiments to follow were designed to examine the expression patterns of KCC2 in GluK1/2$^{-/-}$ hippocampal neurons compared to wildtype hippocampal neurons in both fixed and live preparations.

5.3 Materials and Methods (Specific to Chapter 5)

5.3.1 Live Immunostaining Analysis

Live immunostaining was performed as described before (Acton et al 2012). Briefly, cultured neurons were washed in standard XCS, prior to incubating them with mouse monoclonal anti-HA antibody at 37 °C for 15 minutes. Following incubation with the primary antibody, cells were again washed in XCS prior to a 15 minutes dark incubation in secondary Alexa Fluor 555 goat anti-mouse antibody. Images were acquired after 15 minutes of incubation in the secondary antibody. Neurons were imaged on a Wave FX spinning disc confocal system

(Quorum Technologies) with a Zeiss Observer Z1 inverted microscope using a 60x 1.4NA oil immersion objective. Images were acquired and analyzed using Volocity 3D Image Analysis software (Perkin Elmer). z-stacks were acquired at a pixel resolution of 1024xy with a z-step of 0.2 µm. Samples were acquired sequentially using line-lambda mode at excitation wavelengths of 488 nm and 568 nm. Anti-HA (Cy3) immunofluorescence cluster intensity was measured under constant illumination. Puncta were identified using the object identification tool is Volocity software. The percentage of puncta on the surface was determined by determining the location of the puncta relative to the surface of the cell. To do this I first used the analysis program to identify the centroid of the cell (based on volume). I then randomly selected a z-stack in the mid-region of the cell and drew a vector from the centroid to edge of the GFP fluorescence through the puncta. If the puncta were at the end of the vector they were classified as being on the surface; any puncta that were part-way along the vector were considered internalized and calculated as a percentage of the total length of the vector (see **Figure 5.4.3.1**).

5.3.2 Inhibitors

Prior to incubation with the phosphospecific anti-S^{940} KCC2 Ab (Phosphosolutions, Colorado) neurons were incubated in a blocking solution of 10% goat serum. Added to the blocking solution was 2µM Na_3VO_4 which is a phosphatase inhibitor. In addition, 4µM NaF was also added to help preserve the fixated tissue.

5.3.3 Chemicals

Glutamate and 4β-phorbol 12-myristate 13-acetate (PMA) were used in the following experiments. Glutamate was used at a final concentration of 20µM diluted in extracellular

solution. PMA was used at 1µM and diluted in the extracellular solution. PMA is a putative protein kinase C activator. For these conditions, neurons were perfused with extracellular solution containing these drugs.

5.4 **Results**: Characterization of KCC2 Distribution in GluK1/2$^{-/-}$ Neurons

5.4.1 Differential KCC2 Staining in wildtype versus GluK1/2$^{-/-}$ Neurons

GluK2 is required for Neto2 expression and stability in the neuronal membrane (Zhang et al 2009). Since the loss of Neto2 results in decreased immunoreactivity of anti-KCC2 at the neuronal membrane of Neto2$^{-/-}$ neurons (Ivakine et al 2013), I tested the hypothesis that KCC2 expression is altered in GluK1/2$^{-/-}$ neurons. I performed standard immunohistochemical experiments with an anti-KCC2 antibody (Sigma Aldrich, Oakville) to observe the immunoreactivity patterns in both wildtype and GluK1/2$^{-/-}$ neurons. Hippocampal neurons from GluK1/2$^{-/-}$ cultures show a distinct staining pattern: KCC2 immunoreactivity was highest inside the soma and is more intense than staining visible in wildtype soma (wildytpe: 23526 ± 1189 FIUs, n = 47; GluK1/2 $^{-/-}$: 44075 ± 1313 FIUs, n = 49; p <0.001; **Figure 5.4.1.1A$_{i}$, A$_{ii}$**). However, wildtype neurons showed more intense anti-KCC2 staining across the first 50µM of the major dendritic process (wildytpe: 14008 ± 884 FIUs, n = 47; GluK1/2$^{-/-}$: 9671 ± 816 131 FIUs, n = 49; p <0.001; **Figure 5.4.1.1A$_{i}$, A$_{iii}$**). Together, these results provide evidence that GluK1/2$^{-/-}$ regulates the distribution pattern of KCC2 expression or that GluK1/2 in turn regulates KCC2 through its interaction with Neto2.

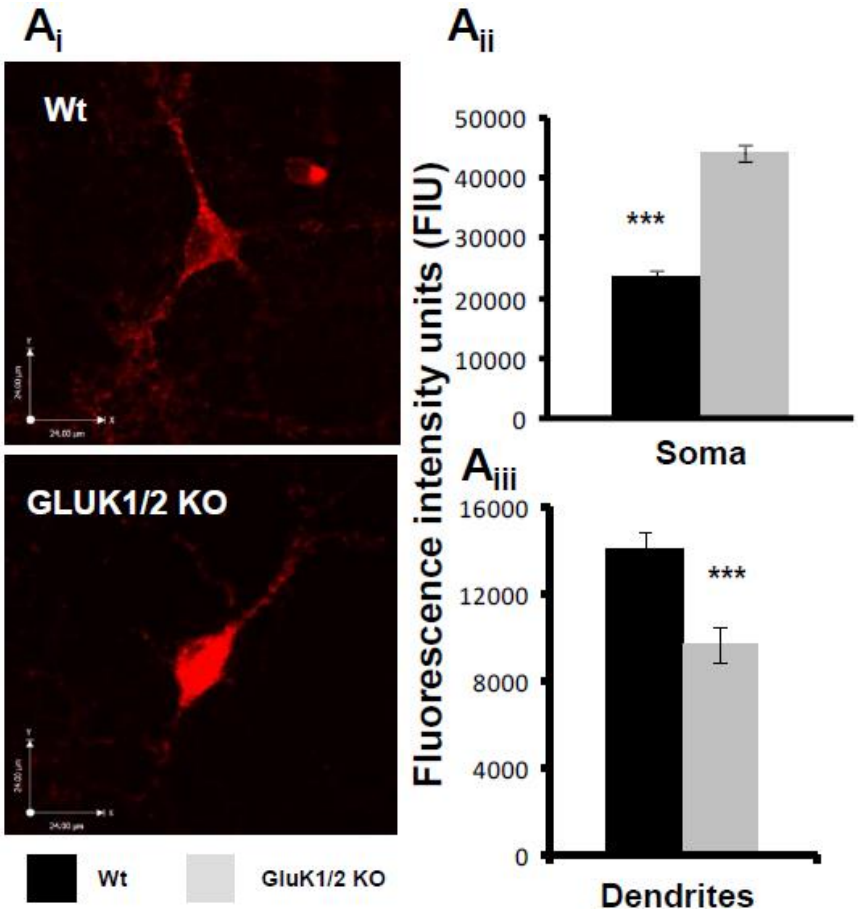

Figure 5.4.1.1. KCC2 is localized to the soma in GluK1/2$^{-/-}$ hippocampal neurons. **Ai.** Confocal micropscopy images of wildytpe and GluK1/2$^{-/-}$ neurons stained with anti-KCC2 (Cy3). **Aii.** Flourescence intensity quantification of average wildtype (n= 47) and GluK1/2$^{-/-}$ (n= 49) intensity measurements taken from a 10µM diameter circle placed over the soma. **Aiii.** Average flourescence intensity quantification from the first 20µM of the largest process from wildtype (n= 47) and GluK1/2$^{-/-}$ (n=49), similar to images takes in Ai.

5.4.2 Differential Phospho-specific anti-KCC2 Staining in GluK1/2 $^{-/-}$ Neurons

The Woodin Lab has preliminary biochemical evidence to suggest that GluK1/2$^{-/-}$ neurons have reduced KCC2 phosphorylation at the S^{940} phosphorylation site (Vivek Mahadevan, unpublished data). S^{940} has been shown to be necessary for KCC2 transport function as well as for the membrane stabilization of the cotransporter (Lee et al 2007). Based on my observation above that GluK1/2$^{-/-}$ neurons show altered KCC2 expression I hypothesized that GluK1/2$^{-/-}$ neurons may also have altered levels of KCC2 S^{940} phosphorylation. To test whether or not GluK1/2$^{-/-}$ neurons show altered immunoreactivity of the S^{940} phosphorylation site, I used a KCC2 S^{940}-targeted antibody and performed immunohistochemistry on neurons from wildtype and GluK1/2$^{-/-}$ neurons. Neurons from GluK1/2$^{-/-}$ cultures showed decreased S^{940} phospho-specific KCC2 immunoreactivity compared to wildtype (GluK1/2 $^{-/-}$: 12878 ± 921 FIUs, n = 12; wildytpe: 22663 ± 3232 FIUs, n = 12; $p < 0.05$; **Figure 5.4.2.1A,B**). These results indicate that neurons lacking GluK1/2 show reduced levels of the functional pool of the S^{940} phosphorylated KCC2.

In this subset of experiments described above for **Figure 5.4.2.1**, I used neurons from the same sets of cultures and ran parallel experiments, similar to **Figure 5.4.1.1**, staining some coverslips with anti-KCC2 and some with anti-S^{940} KCC2. Results from these experiments were consistent with findings in **Figure 5.4.1.1**, showing that although anti-KCC2 immunoflourescence in GluK1/2$^{-/-}$ somas is more pronounced than wildtype, anti-S^{940} KCC2 immunoflourescence was greatly reduced compared to wildtype (**Figure 5.4.2.1B**).

5.4.3 Differential Cell Surface Expression of Overexpressed KCC2

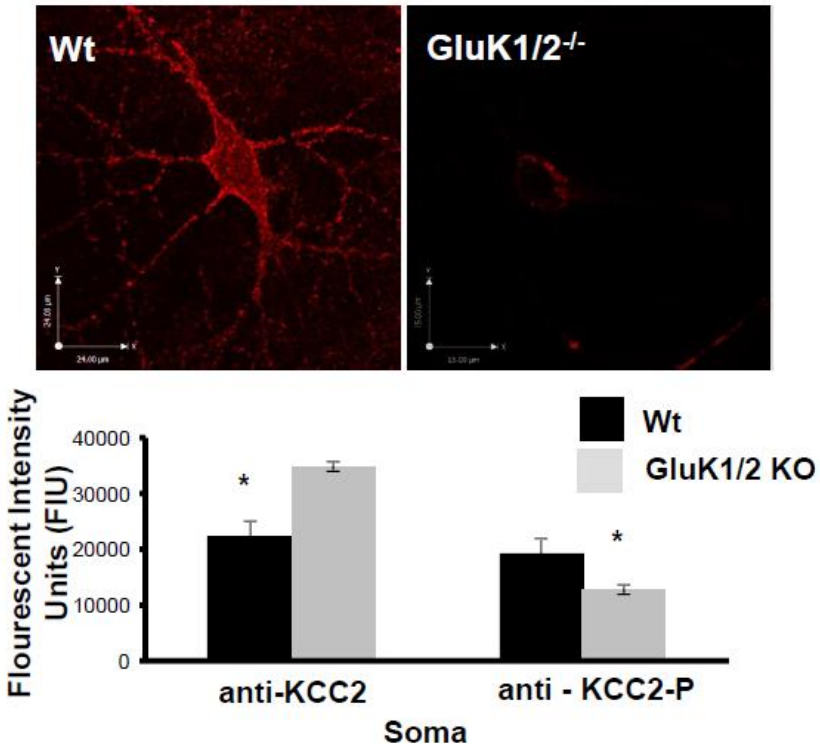

Figure 5.4.2.1. GluK1/2$^{-/-}$ neurons show reduced anti-phosphospecific KCC2 staining. A. Confocal micropscopy images of wildytpe (**Ai**) and GLUK1/2$^{-/-}$ neurons (**Aii**) stained with anti-S^{940} KCC2 Ab (Cy3). B. Flourescence intensity quantification of average wildtype (n=12) and GLUK1/2$^{-/-}$ (n=12) measurements taken from a 10µM diameter circle placed over the soma, from images similar to Ai. Neurons from the same culturing conditions were stained with both anti-KCC2 and anti-S^{940} KCC2.

The findings I presented above demonstrate that GluK1/2 is important for regulating the expression pattern of KCC2 in fixed neurons. However, there is no commercially available antibody targeted for the extracellular domain of KCC2. In addition, those experiments were performed on fixed neurons, and there is some concern that fixation and permeabilization can alter immunoreactivity. I designed a live imaging protocol to image live KCC2 in the membrane of wildtype and GluK1/2$^{-/-}$ neurons. I overexpressed an extracellular-tagged HA-KCC2 DNA construct with a GFP reporter used in my previous experiments (Acton et al 2012) and I probed for surface level KCC2 with an anti-HA antibody. After acquiring z-stacks using a laser confocal within 15 minutes of washing-out the secondary anitbody, I analyzed the amount of surface and internalized anti-HA punctae. I found that GluK1/2$^{-/-}$ neurons showed reduced surface expression of anti-HA expression on the cell surface compared to wildtype neurons (GluK1/2$^{-/-}$: 75.6 ± 3.6%, n = 24; wildtype: 93.8% ± 3.8, n=30; $p < 0.01$; **Figure 5.4.3.1A,B**). In addition, I observed the there was a reduction in the number of punctae on the surface of the soma in GluK1/2$^{-/-}$ compared to wildtype (GluK1/2$^{-/-}$: 19.9 ± 1.1, n = 24; wildtype: 25.6 ± 31.4, n=30; $p < 0.01$; **Figure 5.4.3.1C**). These results indicate that exogenously overexpressed KCC2 has reduced capacity to maintain surface stability in GluK1/2$^{-/-}$ neurons.

In order to assess the expression level of HA-KCC2 in both wildtype and GluK1/2$^{-/-}$ neurons, I transfected neurons with the same HA-KCC2 construct and performed a double immunostaining protocol to stain for the surface and internalized pools of HA-KCC2 separately. **Figure 5.4.3.2** shows example images of a transfected wildtype neuron labelled with anti-HA (Cy3 secondary) before fixing and permeabilization and then labelled with anti-HA post-fixation and permeabilization (350 secondary). Importantly, there is no difference in the immunofluorescence signal for the internalized pool of overexpressed HA-KCC2 between

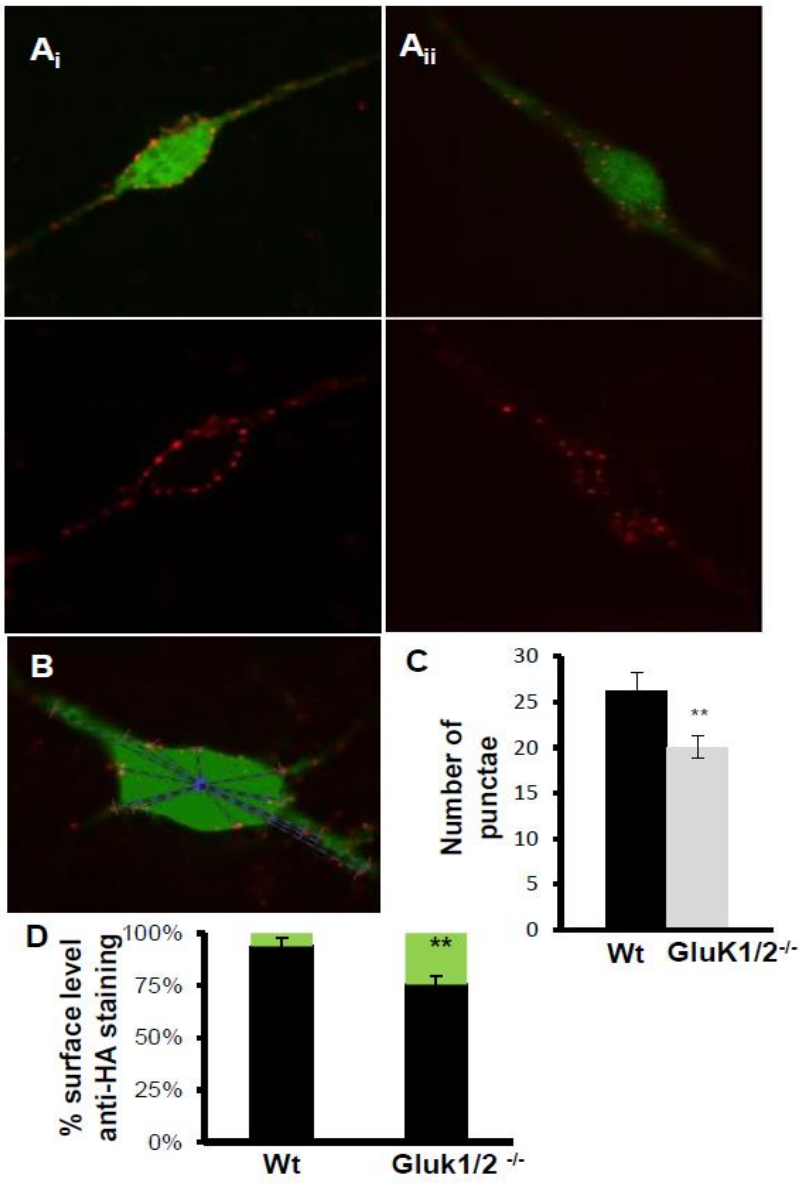

Figure 5.4.3.1. GluK1/2$^{-/-}$ neurons show reduced levels of membrane HA-KCC2. **A**. Example images of wildtype (**Ai**) and GluK1/2$^{-/-}$(**Aii**) expressing GFP (indicating expression of HA-KCC2) and Cy3 (anti-HA membrane labelling of HA-KCC2). **B**. Example image of the centroid and vectors used in membrane-staining analysis (see methods). **C**. Average number of anti-HA punctae from immunostained wildtype (25.6 ± 1.4, n =30) and GluK1/2$^{-/-}$ (19.9 ± 1.1, n = 24). **p < 0.01**D**. Summary figure for all neurons similar to A, quantifying the amount of membrane staining compared to internalized HA-KCC2 for wildtype (93.8% ± 3.8, n = 30) and GluK1/2$^{-/-}$ (75.6% ±3.6, n = 24).

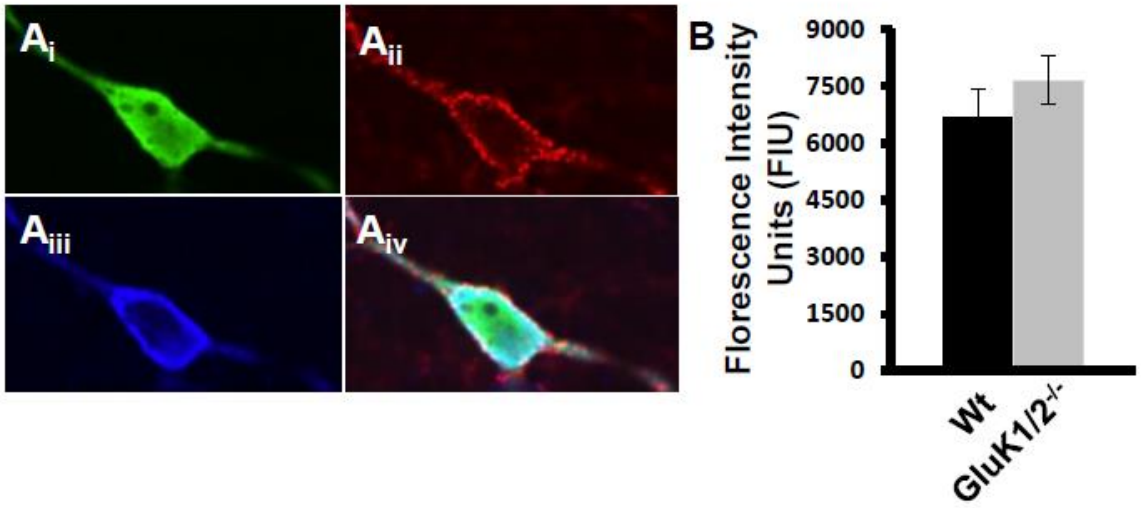

Figure 5.4.3.2. HA-KCC2 is expressed at the same levels in wildtype and GluK1/2$^{-/-}$ neurons. **A**. Example image of a wildtype neuron expressing HA-KCC2 indicated by GFP (**Ai**), tagged on the extracellular portion with anti-HA (Cy3, **Aii**). Post-fixation and permeabilization, neurons were stained for anti-HA (blue, **Aiii**) and flourescent images were overlayed (**Aiv**). **B**. Levels of anti-KCC2 were analyzed and compared between from wildtype (n = 10) and GluK1/2$^{-/-}$ (n = 10) averaging all examples similar to A.

GluK1/2$^{-/-}$ and wildtype neurons (350 secondary) (GluK1/2$^{-/-}$: 7654 ± 1627, n = 10; wildtype: 6688 ± 721, n=10; p <0.01; **Figure 5.4.3.2B**). This result suggests that there is not a difference in the ability of GluK1/2$^{-/-}$ to transcribe or translate the overexpressed HA-KCC2 but that a difference in surface stability underlies the difference in the immunoreactivity expression pattern seen in **Figure 5.4.3.1**.

GluK1/2$^{-/-}$ neurons display a reduced pattern of surface level immunolabelled KCC2. Next, I asked whether the anti-HA surface expression phenotype can be dynamically altered by chemical treatment, as endogenous KCC2 levels are. It has been showed that 20μM glutamate can quickly reduce the surface levels of KCC2 within minutes (Lee et al 2011). After a baseline, I added 20μM glutamate for 10 minutes and then re-imaged the immunolabelled neurons. After a 10 minute treatment of 20μM glutamate, the total number of anti-HA punctae at a randomized z-stack decreased in wildytpe neurons (wildtype baseline: 26.1 ± 2.3; wildtype 20μM glutamate treatment 16.9 ± 1.7, n=10; p <0.001). Under the same treatment, the number of punctae in GluK1/2$^{-/-}$ neurons also decreased (GluK1/2$^{-/-}$ baseline: 22.3 ± 2.2; GluK1/2$^{-/-}$ 20μM glutamate treatment 15.5 ± 1.5; n= 6; p <0.01). There is no difference between the amount of change observed in punctae level reduction between wildtype and GluK1/2$^{-/-}$ neurons exposed to 10 minutes of 20μM glutamate (**Figure 5.4.3.3A**). Of the punctae still present in the z-stack after the 20μM glutamate condition, there was no change in the amount of surface level anti-HA immunolabelling in GluK1/2$^{-/-}$ neurons, however, there was a reduction in the amount of surface level anti-HA immunolabelling in wildtype neurons (**Figure 5.4.3.3B**). These results are especially important because they indicate that the levels of immunoreactivity in these anti-HA live imaging experiments represent a pool of KCC2 that can be actively regulated.

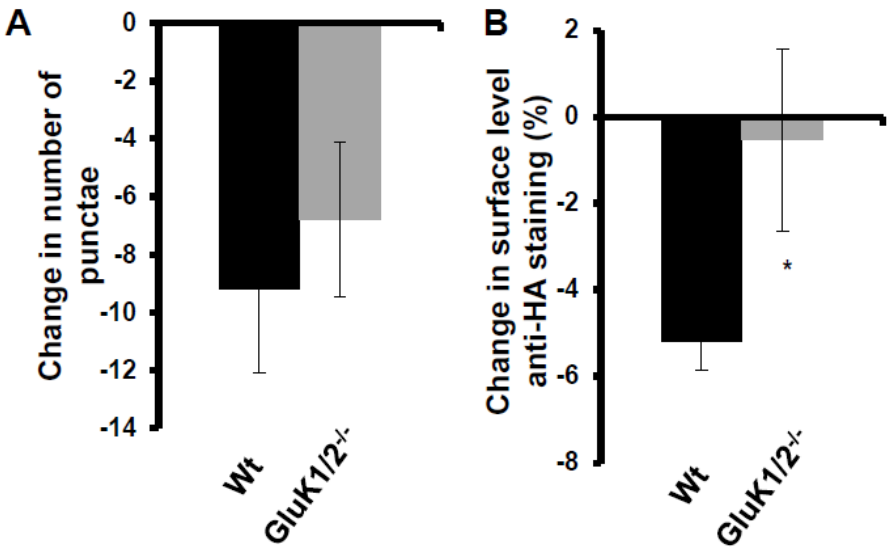

Figure 5.4.3.3. Glutamate treatment downregulates HA-KCC2 membrane expression. **A**. When both wildtype and GluK1/2$^{-/-}$ hippocampal neurons are treated with 20μM glutamate, the number of anti-HA punctae decreased from baseline. **B**. Upon treatment of 20μM glutamate, wildtype neurons show a decrease in the number of surface anti-HA punctae as GluK1/2$^{-/-}$ levels, initially lower than wildtype, remain unchanged.

Since the levels of immunolabelled HA-KCC2 can be down-regulated in the live imaging experiment, I asked whether the levels of HA-KCC2 can be up-regulated by chemical treatment with PMA. In this condition, the neurons from wildtype and GluK1/2$^{-/-}$ hippocampal cultures were incubated for 10 minutes in 1µM PMA prior to antibody treatment and the levels of anti-HA immunoreactivity were compared to a baseline dataset for each wildtype and GluK1/2$^{-/-}$. Wildtype neurons overexpressing HA-KCC2 did not show an increase in surface level expression of anti-HA in response to a 10 minute 1µM PMA treatment (wildtype baseline: 26.1 ± 2.3; n=30 wildtype PMA treatment 26.2 ± 2.9, n= 9; p = 0.136; **Figure 5.4.3.4C$_i$**). This is most likely due to the ceiling effect of overexpressing HA-KCC2. However, GluK1/2$^{-/-}$ neurons experienced an increase in the number of anti-HA punctae after PMA treatment (GluK1/2$^{-/-}$ baseline: 22.3 ± 2.2; GluK1/2$^{-/-}$ PMA treatment 30.3 ± 3.2; n= 9; p <0.001; **Figure 5.4.3.4A, C$_{ii}$**). Together, this indicates that HA-KCC2 in the membrane of GluK1/2$^{-/-}$ neurons is subject to upregulation by 1µM PMA treatment. Wildtype neurons, that are most likely already experiencing a ceiling effect in maximal HA-KCC2 surface expression, do not see changes in membrane reactivity of anti-HA-KCC2 in response to 1µM PMA treatment.

5.5 Conclusions

In conclusion, I examined the expression levels and cell surface stability of KCC2 in wildtype and GluK1/2$^{-/-}$ hippocampal neurons using immunohistochemistry and live cell staining techniques. I found that GluK1/2$^{-/-}$ neurons showed an increase in anti-KCC2 staining in the soma, but displayed a marked decrease in anti-KCC2 staining in their dendritic processes. Furthermore, GluK1/2$^{-/-}$ neurons showed decreased levels of anti-S^{940} KCC2 staining compared to wildtype neurons.

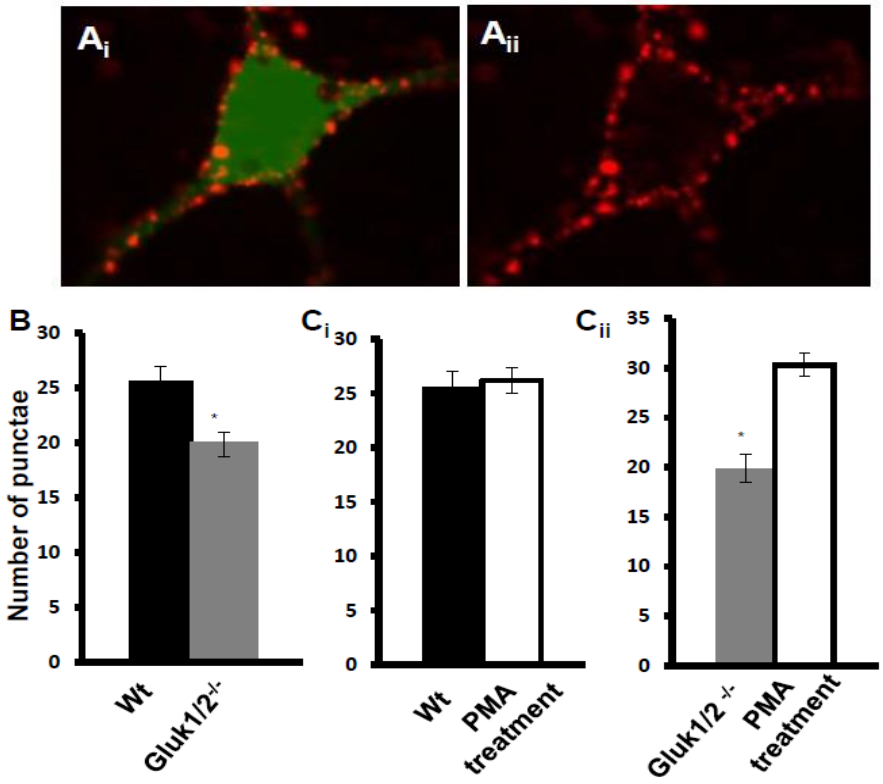

Figure 5.4.3.4. PMA treatment rescues surface stability of HA-KCC2 in GluK1/2$^{-/-}$. **A**. Example image of a GluK1/2$^{-/-}$ neuron expressing HA-KCC2 (GFP overlay, Ai) that has been treated with 1µM PMA for 10 minutes prior to live immunostaining with anti-HA (Cy3, **Aii**). **B**. Baseline levels of anti-HA punctae staining. **C**. Punctae levels after 10 minute 1µM treatment of PMA compared to baseline for wildtype (**Ci**) and GluK1/2$^{-/-}$ (**Cii**). * $p < 0.01$.

Recently, a decrease in KCC2 S^{940} phosphorylation has been linked to the ability of KCC2 to maintain surface expression levels (Lee et al 2011, Lee et al 2007). To test if this was the case, I performed live immunostaining experiments that observed the expression of HA-tagged KCC2 expressed in wildtype and GluK1/2$^{-/-}$ neurons. I found that GluK1/2$^{-/-}$ neurons had a reduced capacity to maintain membrane expression and are more mobile than HA-tagged KCC2 expressed in wildtype neurons.

In the present experiments, the reduction in S^{940} correlated with a decrease in dendritic KCC2 and surface KCC2 levels in GluK1/2$^{-/-}$ neurons. My results corroborate with these findings and provide an insight into the mechanism of the role of GluK1/2 in maintaining proper KCC2 function and maintaining normal, hyperpolarizing GABAergic transmission in the adult hippocampus. The implications of this discovery are discussed in Chapter 6.

Chapter 6: Discussion

6.1 Summary

The mechanisms that regulate the activity of KCC2 remain poorly understood. Here, I have identified the specific 15 amino acid domain of the C-terminus that is responsible for the ability of KCC2 to cotransport K^+Cl^- under basal isotonic conditions allowing it to remain constitutively active to create the steep Cl^- gradient for fast synaptic inhibition. In addition, I have identified a key protein interaction between KCC2 and Neto2 which demonstrates that Neto2, a known KAR auxiliary protein (Zhang et al 2009), can also regulate the activity of the cotransporter. Neto2 is required for neurons to maintain low $[Cl^-]_i$ and strong synaptic inhibition. Finally, I have provided the first evidence that the multi-protein complex including the interactions of KCC2:Neto2:GluK2 work via a PKC-mediated mechanism to maintain the membrane stability of KCC2. These results provide a strong foundation to further explore the synergistic mechanisms of KCC2's regulation. My findings provide a more detailed insight into the mechanisms that regulate the cotransport function of KCC2 in neurons.

Low neuronal $[Cl^-]_i$ results in a hyperpolarized E_{Cl} and a strong postsynaptic inhibitory response. I found that the loss of the native ISO domain and the disruption of the native KCC2:Neto2:GluK2 interaction caused an accumulation in $[Cl^-]_i$ and subsequent depolarization of E_{Cl}. Acute neuronal trauma (Toyoda et al 2003, van den Pol et al 1996), oxygen-glucose deprivation (Galeffi et al 2004) and seizure activity (Galanopoulou 2007) all render E_{Cl} depolarizing and shift GABAergic transmission to become depolarizing and excitatory in action (Fiumelli & Woodin 2007). I have found that the disruption of the GluK2-KCC2 interaction decreases the membrane stability of KCC2. Reduced expression of KCC2 is associated with epileptic seizure activity in the hippocampus (Huberfeld et al 2007, Okabe et al 2003, Rivera et

al 2002, Rivera et al 2005). Thus, my findings suggest three separate mechanisms for maintaining strong synaptic inhibition. Each of these mechanisms point to potential therapeutic targets that may eventually lead to the alleviation of the aforementioned disease states.

6.2 Properties of the KCC2ΔISO domain

I have determined the essential C-terminal domain that is required for KCC2 activity in neurons under normal physiological conditions. This C-terminal domain is a 15 amino acid sequence termed the ISO domain, so named for its ability to confer isotonic transport. By overexpressing KCC2ΔISO, which removes the ability of this transporter to extrude Cl^- under isotonic conditions, I have demonstrated a molecular determinant that makes KCC2 unique from its family members. When the ISO domain is replaced with the analogous region in KCC4, the chimeric protein is devoid of transport until activated by cell swelling. Finally, I demonstrate that in addition to being necessary for isotonic transport, the KCC2 ISO domain is also sufficient to drive transport when the ISO domain is inserted into KCC4 under conditions of elevated neuronal Cl^-.

When the ISO domain of KCC2 was inserted into KCC4, I was able to restore isotonic Cl^- transport when we elevated intracellular Cl^- through the patch pipette, but not when neuronal Cl^- levels were closer to single digit concentrations that are more routinely observed in mature CNS neurons. Increased intracellular Cl^- is likely required to demonstrate the sufficiency of the ISO domain for conferring KCC4 with isotonic transport because K^+Cl^- cotransporter activity (including KCC4) is increased at higher $[Cl^-]_i$ (Bergeron et al 2006, Gillen & Forbush 1999). This finding, demonstrating the sufficiency of the ISO domain, is supported by results obtained

in *Xenopus* oocytes where the same chimeric construct (KCC4-ISO) was sufficient to mediate constitutive activity of the transport (Mercado et al 2006a).

KCC2 shows minimal or reduced swelling-activated cotransport compared to the other KCCs (Payne 1997, Song et al 2002), suggesting that its function under isotonic conditions is specific to basal conditions and for setting the Cl^- gradient for synaptic inhibition. The present study in neurons and previous findings by our collaborators (Mercado et al 2006a) concur that KCC2 mediates equivalent K^+Cl^- cotransport when exposed to hypotonic conditions that activate cell swelling in HEK293 cells. These results point to the importance of investigating the role of KCC2 at excitatory snyapses in the regulation of cell volume. KCC2 is known to play a role at excitatory synapses (Li et al 2007), where fast neural transmission creates a temporary imbalance of osmotic gradients. To date, the role of KCC2 is thought to be structural and independent of Cl^- transport (Chamma et al 2012, Fiumelli et al 2013, Gauvain et al 2011, Li et al 2007). My current work provides the tools (the KCC2ΔISO chimeric construct that does not cotransport K^+Cl^- under isotonic conditions and the KCC4ΔISO chimeric construct that cotransports K^+Cl^- only under swelling-activation or high $[Cl^-]_i$ conditions) for dissociating the Cl^- transport and transport-independent roles of KCC2 in neurons. Examining the role of K^+Cl^- cotransport at the excitatory synapse is a logical topic for future investigation.

Interestingly, all of the chimeric KCC constructs used in the present study displayed similar increases in swelling-activated K^+Cl^- cotransport (**Figure 3.4.4.1B**), except KCC2. The experimental design required the overexpression of each cDNA construct in neurons and therefore, it is most likely that the overexpression of KCC2 creates a ceiling effect where more cotransport upon hypotonic extracellular perfusion is simply not possible because $[Cl^-]_i$ is so low to begin with. Swelling-induced activation is comparable between at least KCC2 and KCC4

(Mercado et al 2006a). The swelling activation of all four KCCs is dependent on serine-threonine phosphatase activity (Mercado et al 2000, Mercado et al 2005, Song et al 2002, Strange et al 2000, Su et al 1999). There is some evidence that the same regulatory kinases SPAK and WNK4 that activate swelling-induced cotransport also play a reciprocal role in regulating constitutive transport of KCC2 (Gagnon et al 2006). Further work is required to identify the domain(s) responsible for the swelling-activated function of the KCCs.

This work focuses on the importance of the C-terminal domain of KCC2, although the role of N-terminus is emerging as an important regulator of other CCCs. The N-terminal domain of NKCC1 contains an interaction motif for PP1 (Darman et al 2001) and for SPAK (Piechotta et al 2002). The N-terminus of NKCC1 also contains threonine sites for activation of the transporter (Darman & Forbush 2002, Flemmer et al 2002). For KCC2, it is known that alternative splicing of the N-terminus results in an additional isoform of the cotransporter (KCC2a)(Uvarov et al 2007). This bears the question: what other regulatory sites on the N-terminal may contribute to the regulation of KCC2?

The exact mechanism for how this short ISO domain of the C-terminal portion of KCC2 maintains cotransport is yet to be determined. However, the lack of this domain does not affect its expression at the plasma membrane (**Figure 3.4.3.3**) and has been confirmed by our collaborators (Mercado et al 2006a). Therefore, it is unlikely that the ISO domain is involved in the trafficking or the membrane stability of the protein. It is well known that KCC2 function is dependent on both phosphorylation state (Lee et al 2007, Rinehart et al 2009, Strange et al 2000, Wake et al 2007a, Watanabe et al 2009) and oligomerization (Blaesse et al 2006, Uvarov et al 2009, Watanabe et al 2009). Within the 15 amino acid sequence of the ISO domain, 3 serines (S^{1022}, S^{1025}, and S^{1034}) are predicted to be kinase substrates (Blom et al 1999, Mercado et al

2006a). These are important regulatory sites for further investigation. It will be interesting to examine whether theses posttranslational modifications regulate transporter activity through an interaction with the ISO domain.

In summary, I have identified that the unique C-terminal ISO domain is required for isotonic KCC2-mediated Cl^- extrusion in neurons. Furthermore, I demonstrate that there are separate molecular determinants of swelling-activated and isotonic KCC2 cotransport in neurons. The identification of the essential ISO domain in neurons is fundamental for two primary reasons. First, because this domain defines what confers KCC2 with its unique ability to extrude Cl^- from neurons at the structural level, allowing this cotransporter to perform its essential physiological role in neuronal Cl^- regulation. Second, by identifying the domain required for isotonic KCC2 function, we have revealed a previously unknown target for the development of prevention strategies and therapeutic treatments directed toward neurological disorders associated with disrupted neuronal Cl^- regulation and the resulting loss of inhibitory tone.

6.3 The Neto2:KCC2 interaction is Required for Synaptic Inhibition

I demonstrated that Neto2 is a KCC2 interacting protein that is required for proper KCC2-mediated Cl^- extrusion in hippocampal neurons. Neto2 regulates KCC2 in a twofold manner, by maintaining its abundance, and by enhancing its efficacy to extrude Cl^- through binding to the active oligomeric form of KCC2. Consequently, the Neto2:KCC2 interaction is required for proper inhibition; Neto2 maintains normal neuronal Cl^- homeostasis in the brain thus, maintaining normal levels of synaptic inhibition.

The identification of the Neto2:KCC2 interaction represents the discovery of a protein that interacts with KCC2 *in vivo* and is critically required for normal neuronal Cl^- homeostasis in

the mature CNS. Before this, only a few KCC2 interactions had been determined, and most of these were demonstrated in either nonneuronal cells or were shown to be nonspecific to KCC2: (i) brain-type creatine kinase was shown to associate with KCC2 in vitro and increase KCC2 activity in heterologous HEK-293 cells (Inoue et al 2004b, Inoue et al 2006a); (ii) protein associated with Myc (Garbarini & Delpire 2008); and iii) cation chloride cotransporter interacting protein 1 (CIP1) (Wenz et al 2009) were determined to interact with KCC2 by measuring 86Rb/K^+ uptake assays in heterologous HEK-293 cells, and in the case of CIP1 the interaction was not limited to KCC2 (36). KCC2 also interacts with a member of the Na^+-K^+-ATPase family, Atp1a2 (Ikeda et al 2004); however, this regulation may be limited to the respiratory center of the brainstem (Hubner et al 2001), because neuronal expression of Atp1α2 dramatically decreases during maturation of the CNS (Herrera et al 1994). Recently, it has been shown that NL2, a protein that is known to play a role in cell adhesion regulating GABAergic synaptogenesis, also regulates the expression of KCC2 (Sun et al 2013). When NL2 is knocked down, KCC2 expression levels are decreased and E_{GABA} depolarizes. No direct interaction between NL2 and KCC2 has been determined. Last, KCC2 interacts to the cytoskeleton-associated protein 4.1N, but this interaction does not regulate KCC2-mediated Cl^- extrusion, but rather functions to promote spine development (Li et al 2007). Thus, our data demonstrate the existence of a KCC2 interacting protein that is required for proper neuronal Cl^- regulation in the mature CNS.

The ability of KCC2 to interact with the cytoskeleton-associated protein 4.1N (Gauvain et al 2011, Li et al 2007), and the requirement for KCC2 in the morphological maturation of cortical neurons (Cancedda et al 2007), indicates that KCC2 plays important roles in neuronal morphology. However, these roles may be independent of KCC2's ability to extrude Cl^-

(Gauvain et al 2011, Li et al 2007). In the present study, I found that Neto2 deficiency did not affect basic neuronal morphology (**Figure 4.4.7.1**), suggesting that the primary role of Neto2 in regulating KCC2 is restricted to its Cl^- extrusion function, and is likely independent of its morphological role.

During embryonic development, NKCC1 is highly expressed in the membrane, and as a result GABA acts as an excitatory neurotransmitter (Plotkin et al 1997, Xu et al 1994). However, during the first few weeks of postnatal development, there is a significant increase in KCC2 expression that results in a hyperpolarizing shift in E_{Cl} (Blaesse et al 2009, Claudio Rivera 1999). Thus, the switch from GABAergic excitation to inhibition results from a postnatal developmental increase in KCC2. For Neto2 to play an important role in KCC2 regulation, I would expect that Neto2 be expressed in a similar time course. In fact, Neto2 mRNA expression is first detected at embryonic day 15, and increased its expression between postnatal day 5 (P5) and P21 (Michishita et al 2004). This expression pattern closely parallels the expression of KCC2 during the same developmental period.

Our collaborators have discovered that Neto2 regulates KCC2-mediated Cl^- homeostasis through two essential mechanisms. First, our biochemical and immunofluorescence data reveal that Neto2 is required for maintaining KCC2 in the neuronal membrane. The reduction of KCC2 in the membrane that occurs in Neto2-null mice led us to consider whether the KCC2 that remained was still capable of efficient Cl^- extrusion. I obtained several lines of converging evidence in support of decreased Cl^- extrusion in Neto2-null mice (electrophysiological data in Chapter 4).

Initially, $Neto2^{-/-}$ neurons demonstrated E_{Cl} values that were on average 20mVs more depolarized than wildtype neurons when recordings were made with gramicidin perforated patch,

providing the first indication that Neto2 plays an important role in maintaining KCC2 cotransport function (**Figure 4.4.1.1**). When Neto2$^{-/-}$ neurons were perfused with an antagonist specific to KCC2, these neurons did not undergo any additional depolarization of E_{Cl} indicating that K^+Cl^- cotransport was already diminished in Neto2$^{-/-}$ neurons (**Figure 4.4.3.1**). The role of Neto2 in maintaining a strong inhibitory response in neurons is further corroborated by my findings that the full length Neto2 rescues E_{Cl} in Neto2$^{-/-}$ neurons (**Figure 4.4.4.1**) and that this same depolarized E_{Cl} phenotype could be created in wildtype neurons by selectively silencing Neto2 (**Figures 4.4.5.1**).

Calcium imaging was performed on Neto2$^{-/-}$ and wildtype hippocampal cultures to assay the levels of activity at three time points in development (**Figure 4.4.2.1**). There was no difference in the activity levels of these neurons from DIV3-DIV11, indicating that wildtype and Neto2$^{-/-}$ neurons undergo similar levels of spontaneous neuronal activity in culture. This is an important finding because if Neto2$^{-/-}$ neurons were more active, the reduction in the strength of inhibitory transmission observed in these neurons may be due to homeostatic plasticity. Homeostatic plasticity is the ability of neurons to regulate their own excitability relative to network activity, a compensatory adjustment that occurs over the timescale of days (Turrigiano et al 1998, Wenner 2011, Wenner 2013). However, because there is no difference in the activity levels of Neto2$^{-/-}$ and wildtype neurons, it can be assumed that the loss of Neto2 does not alter the ability of Neto2$^{-/-}$ neurons to respond to GABA by changes in intrinsic excitability.

It has been determined biochemically that Neto2 preferentially interacts with oligomerized KCC2. KCC2 oligomerization, which depends on tyrosine phosphorylation of the C-terminus (Watanabe et al 2009), correlates with the maturation of inhibitory neurotransmission in the CNS (Blaesse et al 2006), and is believed to play a major role in the change from the

inactive to the active state of this transporter (Blaesse et al 2009, Uvarov et al 2009). In addition to the reduced oligomeric state of KCC2 found when the Neto2:KCC2 interaction is disrupted in Neto2-null neurons, I demonstrated electrophysiologically that Neto2-null neurons are unable to extrude a Cl^- load, indicating that the function of the remaining levels of neuronal KCC2 in Neto2-null neurons is severely compromised (**Figure 4.4.6.1**). Remarkably, the decrease in KCC2 function in Neto2-null neurons can be such that intracellular Cl^- levels rise to the point where GABAergic transmission becomes excitatory (**Table 2**). Thus, the second essential function of Neto2 is its ability to bind to the active oligomeric form of KCC2 and allow KCC2 to extrude Cl^- more efficiently. These two functions of the Neto2:KCC2 interaction are so fundamental that the loss of Neto2 causes the neuronal Cl^- gradient to collapse. Thus, I have discovered that Neto2 interacts with the key protein that regulates the strength of inhibitory synaptic transmission in the CNS.

Our collaborators initially identified the Neto2:KCC2 interaction using the Neto2 cytoplasmic tail, but then later demonstrated that it is the extracellular CUB domains and not the cytoplasmic tail that are required for the interaction in heterologous HEK293 cells. This suggests that in our initial screen our collaborators likely pulled out KCC2 in a multiprotein complex. This possibility was strengthened by my finding that I could rescue the depolarization in E_{Cl} in Neto2-null neurons using the cytoplasmic tail alone (**Figure 4.4.4.2**). The identification of the additional protein(s) in this Neto2:KCC2 multiprotein complex is an important direction of future research, given the importance of this complex in regulating inhibitory synaptic transmission. Unpublished data from our group reveals that the KAR subunit GluK2, Neto2 and KCC2 coexist in a macromolecular complex, and are colocalized in hippocampal and cortical

neurons (Mahadevan, unpublished). This is currently the subject of ongoing investigation by our group.

In summary, I have identified Neto2 as a regulator of KCC2 transporter activity. Moreover, because Neto2 also binds to KARs, I have demonstrated that Neto2 is a multifunctional protein that can modulate the activity of both ion channels and cotransporters. By regulating proteins involved in both excitatory (KARs) and inhibitory (KCC2) neurotransmission, Neto2 is uniquely positioned to fine-tune synaptic activity on both neuronal and network levels. This finding raises the possibility that other CUB domain-containing proteins may function in a similar manner to regulate more than one class of membrane protein. This study sheds new light on the postsynaptic mechanisms responsible for the regulation of inhibitory synapses, unveiling a novel protein interactor of KCC2 and providing new insight on how additional proteins may alter the strength of inhibition at the synapse.

6.4 Genetic Ablation of GluK1/2 Disrupts the Expression and Regulation of KCC2

Neto2 is a transmembrane protein that is both an auxiliary subunit for the KAR subunit GluK2, and for the K^+Cl^- cotransporter KCC2 (Ivakine et al 2013, Zhang et al 2009). Neto2 interacts with both GluK2 and KCC2 through its extracellular CUB domains (Ivakine et al 2013, Tang et al 2011). This allows for the possibility that either two separate populations of Neto2 bind GluK2 and KCC2, or that these three proteins are in the same macromolecular complex. Unpublished data from our group reveals that these three proteins coexist in a macromolecular complex, and are colocalized in hippocampal and cortical neurons (Mahadevan and Pressey, unpublished). This data also reveals that inhibiting GluK2 depolarizes the E_{Cl}, indicating that

KAR signaling maintains KCC2 function and is essential for maintaining the tone of synaptic inhibition (Mahadevan and Pressey, unpublished).

In light of these findings, I asked what is the mechanism for the Neto2:GluK2:KCC2 interaction that maintains $[Cl^-]_i$ and normal levels of mature synaptic inhibition? To address this, I examined the expression pattern and cell surface stability of KCC2 in wildtype and GluK1/2$^{-/-}$ hippocampal neurons using immunohistochemistry and live cell imaging techniques. I found that GluK1/2$^{-/-}$ neurons showed an increase in anti-KCC2 staining in the soma, but displayed a marked decrease in anti-KCC2 staining in their dendritic processes (**Figure 5.4.1.1**). This immunoreactivity pattern of anti-KCC2 suggests that a large pool of KCC2 expressed in GluK1/2$^{-/-}$ neurons remains cytoplasmic. In my next experiment, I found that GluK1/2$^{-/-}$ neurons displayed decreased levels of anti-S^{940} KCC2 staining compared to wildtype neurons (**Figure 5.4.2.1**).

Recently, a decrease in KCC2 S^{940} phosphorylation has been linked to the inability of KCC2 to maintain surface expression levels (Lee et al 2011, Lee et al 2007). To test if this was the case, I performed live immunostaining experiments that observed the expression of HA-tagged KCC2 expressed in wildtype and GluK1/2$^{-/-}$ neurons. I found that GluK1/2$^{-/-}$ neurons have a reduced capacity to maintain membrane expression and overexpressed HA-KCC2 in these neurons are more mobile than HA-KCC2 expressed in wildtype neurons.

Many studies support the notion that phosphorylation of KCC2 regulates its activity and modulates the efficacy of its K^+Cl^- cotransport in neuronal membranes, but there is considerable debate about whether phosphorylation activates or deactivates KCC2. Similar transmembrane proteins cycle almost continuously between phosphorylation and dephosphorylation (Groth et al 2003, Malinow et al 1988, Mulkey et al 1993, Santos et al 2009). Thus, it is unlikely that KCC2

is uniformly phosphorylated or dephosphorylated at any one point in time, a fact that likely contributes to the difficulty in determining the new effect of kinase and phosphatase activity.

This present study supports the hypothesis that PKC activates KCC2 function. I found that in wildtype neurons, there was more phosphorylated S^{940} KCC2 than in GluK1/2$^{-/-}$ neurons and that this correlated with an increase in surface level expression of overexpressed HA-KCC2. Further, the GluK1/2$^{-/-}$ membrane expression phenotype could be rescued when treated with PMA, a putative PKC agonist (**Figure 5.4.3.4**). Recently, another group has shown that PKC directly enhances KCC2 function by direct S^{940} phosphorylation (Banke & Gegelashvili 2008, Lee et al 2007, Sarkar et al 2011). This results in an increased in KCC2 surface expression caused by a decrease in the internalization rate of KCC2 at the membrane. This same group later showed that phosphorylation of KCC2 at S^{940} was decreased by activation of PP1 causing Ca^{2+} influx through NMDARs (Lee et al 2011). Here, the reduction in S^{940} resulted in a quick decrease of total and surface KCC2 levels. The literature supports the hypothesis that the decrease in KCC2 function results in first the decrease in KCC2 surface expression followed by protein degradation (Kitamura et al 2008, Lee et al 2011, Wake et al 2007b, Wardle & Poo 2003) and KCC2 contains two predicted PEST domains (proline, glutamate, serine, threonine) (Mercado et al 2006a) which are thought to signal protein degradation (Rechsteiner & Rogers 1996, Rogers et al 1986) and are likely involved in lysosomal degradation (Lee et al 2010). As mentioned, there is still a debate about the net effect of PKC on KCC2 function. Two initial studies contradict the finding that PKC activates KCC2, indicating that PKC-mediated actions are responsible for downregulating KCC2 function (Bergeron et al 2006, Fiumelli et al 2005). It is important to note that these initial studies failed to address the direct role of PKC in regulating KCC2.

Interestingly, KARs associate with the neuronal scaffolding protein 4.1N (Copits & Swanson 2013), a protein that has previously been identified as a KCC2 interactor at excitatory synapses (Li et al 2007). The 4.1N-KAR interaction is critical for the surface expression of KARs and is proposed to regulate their endocytosis. Copits et al. (2013) determined that 4.1N is critical for the stabilization of KARs but the process also depends on additional protein-protein interactions in the postsynaptic density. Similar to how endocytosis of AMPARs is required for LTP at extrasynaptic sites (Lu et al 2007, Park et al 2004), these authors propose that 4.1N-mediated KAR regulation is important for KAR-dependent synaptic plasticity. This leads to the obvious question: what is the role of the KCC2-4.1N interaction in the regulation of KARs and is 4.1N is part of the multi-protein complex that identified the Neto2-KCC2-GluK2 interaction?

Does the ability of GluK1/2 to maintain KCC2 function and surface stability occur via the classic GluK2 ionotropic current, or via metabotropic signaling (Lerma 1998, Melyan Z 2002 , Melyan et al 2002)? This is an important question for future study. The Neto2:GluK2 interaction increases the GluK2 current decay constant which produces a tonic GluK2 current. Tonic currents generate a near-constant influx of ions that can increase osmolarity. Because KCC2 is the only cotransporter that can extrude Cl^- to maintain neuronal osmolarity isotonically (Acton et al 2012), I speculate that the colocalization of KCC2 to GluK2-containing synapses may be to maintain neuronal osmolarity, particularly during conditions of elevated glutamatergic transmission.

The data presented here could be strengthened by two specific experiments. First, the membrane expression imaging could be supplemented by a biotinylation experiment to quantify the proportion of surface versus total protein levels in each the wildtype and the GluK1/2$^{-/-}$ neurons. Second, the role of S^{940} has not been determined in these experiments, it has only been

shown that S^{940} is reduced in the GluK1/2$^{-/-}$ and this is hypothesized to underly other phenotypes observed in these neurons. By using KCC2 constructs that include S^{940}A and S^{940}D substitutions, the direct role of this phosphorylation site could be examined in each of the present experiments. These are important experiments for the future of understanding the mechanisms underlying the phenotypes presented here.

In summary, this study contributes to the growing body of evidence that postsynaptic mechanisms are in large part responsible for maintaining and regulating inhibitory synaptic transmission. Here, I demonstrated that a novel protein regulator of KCC2 is required for membrane stability of the cotransporter, providing new insight on how additional proteins and downstream pathways may alter the strength of inhibition at the synapse.

6.4.5 Conclusion and Summary

This thesis outlines three distinct mechanisms that regulate the activity of KCC2, a topic that remains poorly understood in the field today. Here, I have assayed the cotransport function of KCC2 under isotonic conditions and determined the 15 amino acid molecular domain of the cotransporter required for constitutive Cl^- transport (Acton et al 2012) (**Figure 6.4.5.1.A$_i$**). This C-terminal domain is responsible for the ability of KCC2 to cotransport K^+Cl^- under basal isotonic conditions, allowing it to remain constitutively active to create the steep Cl^- gradient across the neuronal membrane required for fast synaptic inhibition. Secondly, I have investigated a novel KCC2-interacting protein, Neto2 and determined its critical effect on the postsynaptic action of GABA (Ivakine et al 2013) **(Figure 6.4.5.1.A$_{ii}$**). I have identified a key protein interaction between KCC2 and Neto2 which demonstrates that Neto2, a known KAR

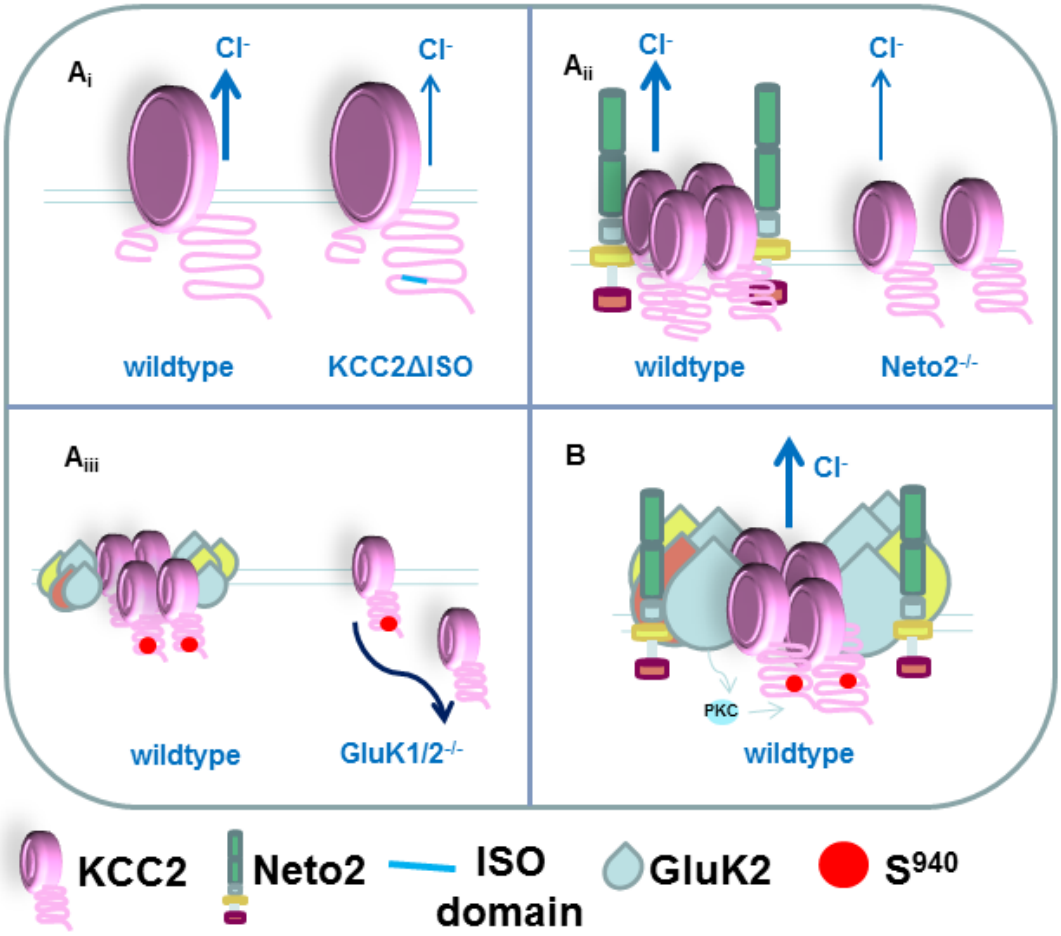

Figure 6.5.1.1. Summary schematic of the mechanisms of KCC2 regulation outlined in this thesis **Ai**. KCC2 requires the ISO domain of the C-terminus for K^+Cl^- cotransport function **Aii**. The Neto2:KCC2 interaction is required for K^+Cl^- cotransport function of KCC2 **Aiii.** Membrane surface stability and S^{940} phosphorylation of KCC2 requires the presence of GluK2. **B**. Synergistic schematic of the effect of all three mechanisms (**Ai-Aiii**) on the K^+Cl^- cotransport ability of KCC2.

auxiliary protein, can also regulate the activity of the cotransporter. Neto2 is required for neurons to maintain low $[Cl^-]_i$ and strong synaptic inhibition. My last finding further explores Neto2 as a KAR auxiliary protein and the effect of this interaction with KCC2 on the expression pattern and membrane stability of the cotransporter. Finally, I have provided the first evidence that the multi-protein complex including the interactions of Neto2-KCC2-GluK2 may work via a PKC-mediated mechanism to maintain the membrane stability of KCC2 (**Figure 6.4.5.1A$_{iii}$**). These three mechanisms of KCC2 regulation exert synergistic effects that maintain physiological K^+Cl^- cotransport levels (**Figure 6.4.5.1B**). The results described in this thesis provide a strong foundation to further explore the mechanism of action of KCC2 in its critical role in both excitatory and inhibitory transmission in the hippocampus.

References

A. I. Gulyas AS, J. A. Payne, K. Kaila and T. F. Freund. 2001. The KCl cotransporter, KCC2, is highly expressed in the vicinity of excitatory synapses in the rat hippocampus. *European Journal of Neuroscience,* 13: 2205-17

Acton BA, Mahadevan V, Mercado A, Uvarov P, Ding Y, et al. 2012. Hyperpolarizing GABAergic transmission requires the KCC2 C-terminal ISO domain. *J Neurosci* 32: 8746-51

Aguado F, Carmona MA, Pozas E, Aguilo A, Martinez-Guijarro FJ, et al. 2003. BDNF regulates spontaneous correlated activity at early developmental stages by increasing synaptogenesis and expression of the K+/Cl- co-transporter KCC2. *Development* 130: 1267-80

Akerman CJ, Cline HT. 2006. Depolarizing GABAergic conductances regulate the balance of excitation to inhibition in the developing retinotectal circuit in vivo. *J Neurosci* 26: 5117-30

Amaral DG, Witter MP. 1989. The three-dimensional organization of the hippocampal formation: a review of anatomical data. *Neuroscience* 31: 571-91

Amiry-Moghaddam M, Ottersen OP. 2003. The molecular basis of water transport in the brain. *Nat Rev Neurosci* 4: 991-1001

Anand KS, Dhikav V. 2012. Hippocampus in health and disease: An overview. *Ann Indian Acad Neurol* 15: 239-46

Andrew RD, Labron MW, Boehnke SE, Carnduff L, Kirov SA. 2007. Physiological evidence that pyramidal neurons lack functional water channels. *Cereb Cortex* 17: 787-802

Balena T, Acton BA, Koval D, Woodin MA. 2008. Extracellular potassium regulates the chloride reversal potential in cultured hippocampal neurons. *Brain Res* 1205: 12-20

Balena T, Woodin MA. 2008. Coincident pre- and postsynaptic activity downregulates NKCC1 to hyperpolarize E(Cl) during development. *Eur J Neurosci* 27: 2402-12

Banke TG, Gegelashvili G. 2008. Tonic activation of group I mGluRs modulates inhibitory synaptic strength by regulating KCC2 activity. *J Physiol* 586: 4925-34

Belelli D, Harrison NL, Maguire J, Macdonald RL, Walker MC, Cope DW. 2009. Extrasynaptic GABAA receptors: form, pharmacology, and function. *J Neurosci* 29: 12757-63

Ben-Ari Y. 2002. Excitatory actions of gaba during development: the nature of the nurture. *Nat Rev Neurosci* 3: 728-39

Ben-Ari Y, Khalilov I, Kahle KT, Cherubini E. 2012a. The GABA excitatory/inhibitory shift in brain maturation and neurological disorders. *Neuroscientist* 18: 467-86

Ben-Ari Y, Woodin MA, Sernagor E, Cancedda L, Vinay L, et al. 2012b. Refuting the challenges of the developmental shift of polarity of GABA actions: GABA more exciting than ever! *Front Cell Neurosci* 6: 35

Benarroch EE. 2012. GABAB receptors: structure, functions, and clinical implications. *Neurology* 78: 578-84

Bergeron MJ, Frenette-Cotton R, Carpentier GA, Simard MG, Caron L, Isenring P. 2009. Phosphoregulation of K(+)-Cl(-) cotransporter 4 during changes in intracellular Cl(-) and cell volume. *J Cell Physiol* 219: 787-96

Bergeron MJ, Gagnon E, Caron L, Isenring P. 2006. Identification of key functional domains in the C terminus of the K+-Cl- cotransporters. *J Biol Chem* 281: 15959-69

Bettler B, Boulter J, Hermans-Borgmeyer I, O'Shea-Greenfield A, Deneris ES, et al. 1990. Cloning of a novel glutamate receptor subunit, GluR5: expression in the nervous system during development. *Neuron* 5: 583-95

Bianchi MT, Haas KF, Macdonald RL. 2002. Alpha1 and alpha6 subunits specify distinct desensitization, deactivation and neurosteroid modulation of GABA(A) receptors containing the delta subunit. *Neuropharmacology* 43: 492-502

Blaesse P, Airaksinen MS, Rivera C, Kaila K. 2009. Cation-chloride cotransporters and neuronal function. *Neuron* 61: 820-38

Blaesse P, Guillemin I, Schindler J, Schweizer M, Delpire E, et al. 2006. Oligomerization of KCC2 correlates with development of inhibitory neurotransmission. *J Neurosci* 26: 10407-19

Blom N, Gammeltoft S, Brunak S. 1999. Sequence and structure-based prediction of eukaryotic protein phosphorylation sites. *J Mol Biol* 294: 1351-62

Bloom FE, Iversen LL. 1971. Localizing 3H-GABA in nerve terminals of rat cerebral cortex by electron microscopic autoradiography. *Nature* 229: 628-30

Boettger T, Rust MB, Maier H, Seidenbecher T, Schweizer M, et al. 2003. Loss of K-Cl co-transporter KCC3 causes deafness, neurodegeneration and reduced seizure threshold. *Embo J* 22: 5422-34

Bork P, Beckmann G. 1993. The CUB domain. A widespread module in developmentally regulated proteins. *J Mol Biol* 231: 539-45

Bos R, Sadlaoud K, Boulenguez P, Buttigieg D, Liabeuf S, et al. 2013. Activation of 5-HT2A receptors upregulates the function of the neuronal K-Cl cotransporter KCC2. *Proc Natl Acad Sci U S A* 110: 348-53

Boulenguez P, Liabeuf S, Bos R, Bras H, Jean-Xavier C, et al. 2010. Down-regulation of the potassium-chloride cotransporter KCC2 contributes to spasticity after spinal cord injury. *Nat Med* 16: 302-7

Bregestovski P, Bernard C. 2012. Excitatory GABA: How a Correct Observation May Turn Out to be an Experimental Artifact. *Front Pharmacol* 3: 65

Cancedda L, Fiumelli H, Chen K, Poo MM. 2007. Excitatory GABA action is essential for morphological maturation of cortical neurons in vivo. *J Neurosci* 27: 5224-35

Carmona MA, Pozas E, Martinez A, Espinosa-Parrilla JF, Soriano E, Aguado F. 2006. Age-dependent spontaneous hyperexcitability and impairment of GABAergic function in the hippocampus of mice lacking trkB. *Cereb Cortex* 16: 47-63

Caron L, Rousseau F, Gagnon E, Isenring P. 2000. Cloning and functional characterization of a cation-Cl-cotransporter-interacting protein. *J Biol Chem* 275: 32027-36

Castillo PE, Malenka RC, Nicoll RA. 1997. Kainate receptors mediate a slow postsynaptic current in hippocampal CA3 neurons. *Nature* 388: 182-6

Castillo PE MR, Nicoll RA. 1997. Kainate receptors mediate a slow postsynaptic current in hippocampal CA3 neurons. *Nature* 388: 182-6.

Chamma I, Chevy Q, Poncer JC, Levi S. 2012. Role of the neuronal K-Cl co-transporter KCC2 in inhibitory and excitatory neurotransmission. *Front Cell Neurosci* 6: 5

Chao DL, Ma L, Shen K. 2009. Transient cell-cell interactions in neural circuit formation. *Nat Rev Neurosci* 10: 262-71

Chittajallu R VM, Dev KK, Barnes JM, Collingridge GL, Henley JM. 1996. Regulation of glutamate release by presynaptic kainate receptors in the hippocampus. *Nature.* 379():78-81: 78-81

Claudio Rivera JV, John A. Payne, Eva Ruusuvuori, Hannele Lahtinen, Karri Lamsa, Ulla Pirvola, Mart Saarma & Kai Kaila. 1999. TheK+/Cl- co-transporter KCC2 renders GABA hyperpolarizing during neuronal maturation. *Nature* 397: 251-55

Cohen I, Navarro V, Clemenceau S, Baulac M, Miles R. 2002. On the origin of interictal activity in human temporal lobe epilepsy in vitro. *Science* 298: 1418-21

Conn PJ, Pin JP. 1997. Pharmacology and functions of metabotropic glutamate receptors. *Annu Rev Pharmacol Toxicol* 37: 205-37

Connors BW, Long MA. 2004. Electrical synapses in the mammalian brain. *Annu Rev Neurosci* 27: 393-418

Contractor A, Mulle C, Swanson GT. 2011. Kainate receptors coming of age: milestones of two decades of research. *Trends Neurosci* 34: 154-63
Copits BA, Swanson GT. 2012. Dancing partners at the synapse: auxiliary subunits that shape kainate receptor function. *Nat Rev Neurosci* 13: 675-86
Copits BA, Swanson GT. 2013. Kainate receptor post-translational modifications differentially regulate association with 4.1N to control activity-dependent receptor endocytosis. *J Biol Chem* 288: 8952-65
Coull JA, Beggs S, Boudreau D, Boivin D, Tsuda M, et al. 2005. BDNF from microglia causes the shift in neuronal anion gradient underlying neuropathic pain. *Nature* 438: 1017-21
Coull JA, Boudreau D, Bachand K, Prescott SA, Nault F, et al. 2003. Trans-synaptic shift in anion gradient in spinal lamina I neurons as a mechanism of neuropathic pain. *Nature* 424: 938-42
Crable SC, Hammond SM, Papes R, Rettig RK, Zhou GP, et al. 2005. Multiple isoforms of the KC1 cotransporter are expressed in sickle and normal erythroid cells. *Exp Hematol* 33: 624-31
Crawford RM, Ranki HJ, Botting CH, Budas GR, Jovanovic A. 2002. Creatine kinase is physically associated with the cardiac ATP-sensitive K+ channel in vivo. *Faseb J* 16: 102-4
Darman RB, Flemmer A, Forbush B. 2001. Modulation of ion transport by direct targeting of protein phosphatase type 1 to the Na-K-Cl cotransporter. *J Biol Chem* 276: 34359-62
Darman RB, Forbush B. 2002. A regulatory locus of phosphorylation in the N terminus of the Na-K-Cl cotransporter, NKCC1. *J Biol Chem* 277: 37542-50
Delgado-Lezama R, Loeza-Alcocer E, Andres C, Aguilar J, Guertin PA, Felix R. 2013. Extrasynaptic GABAA Receptors in the Brainstem and Spinal Cord: Structure and Function. *Curr Pharm Des* 19: 4485-97
Delpire E. 2000. Cation-Chloride Cotransporters in Neuronal Communication. *News Physiol Sci* 15: 309-12
Delpire E, Baranczak A, Waterson AG, Kim K, Kett N, et al. 2012. Further optimization of the K-Cl cotransporter KCC2 antagonist ML077: development of a highly selective and more potent in vitro probe. *Bioorg Med Chem Lett* 22: 4532-5
Dingledine R, Borges K, Bowie D, Traynelis SF. 1999. The glutamate receptor ion channels. *Pharmacological reviews* 51: 7-61
Dunham PB, Ellory JC. 1981. Passive potassium transport in low potassium sheep red cells: dependence upon cell volume and chloride. *J Physiol* 318: 511-30
Dzhala V, Valeeva G, Glykys J, Khazipov R, Staley K. 2012. Traumatic alterations in GABA signaling disrupt hippocampal network activity in the developing brain. *J Neurosci* 32: 4017-31
Dzhala VI, Talos DM, Sdrulla DA, Brumback AC, Mathews GC, et al. 2005. NKCC1 transporter facilitates seizures in the developing brain. *Nat Med* 11: 1205-13
Farrant M, Nusser Z. 2005. Variations on an inhibitory theme: phasic and tonic activation of GABA(A) receptors. *Nat Rev Neurosci* 6: 215-29
Finelli P, Sirchia SM, Masciadri M, Crippa M, Recalcati MP, et al. 2012. Juxtaposition of heterochromatic and euchromatic regions by chromosomal translocation mediates a heterochromatic long-range position effect associated with a severe neurological phenotype. *Mol Cytogenet* 5: 16
Fiumelli H, Briner A, Puskarjov M, Blaesse P, Belem BJ, et al. 2013. An ion transport-independent role for the cation-chloride cotransporter KCC2 in dendritic spinogenesis in vivo. *Cereb Cortex* 23: 378-88
Fiumelli H, Cancedda L, Poo MM. 2005. Modulation of GABAergic transmission by activity via postsynaptic Ca2+-dependent regulation of KCC2 function. *Neuron* 48: 773-86
Fiumelli H, Woodin MA. 2007. Role of activity-dependent regulation of neuronal chloride homeostasis in development. *Curr Opin Neurobiol* 17: 81-6
Flatman PW. 2008. Cotransporters, WNKs and hypertension: an update. *Curr Opin Nephrol Hypertens* 17: 186-92

Flemmer AW, Gimenez I, Dowd BF, Darman RB, Forbush B. 2002. Activation of the Na-K-Cl cotransporter NKCC1 detected with a phospho-specific antibody. *J Biol Chem* 277: 37551-8

Gagnon E, Bergeron MJ, Brunet GM, Daigle ND, Simard CF, Isenring P. 2004. Molecular mechanisms of Cl- transport by the renal Na(+)-K(+)-Cl- cotransporter. Identification of an intracellular locus that may form part of a high affinity Cl(-)-binding site. *J Biol Chem* 279: 5648-54

Gagnon KB, England R, Delpire E. 2006. Volume sensitivity of cation-Cl- cotransporters is modulated by the interaction of two kinases: Ste20-related proline-alanine-rich kinase and WNK4. *Am J Physiol Cell Physiol* 290: C134-42

Galanopoulou AS. 2007. Developmental patterns in the regulation of chloride homeostasis and GABA(A) receptor signaling by seizures. *Epilepsia* 48 Suppl 5: 14-8

Galeffi F, Sah R, Pond BB, George A, Schwartz-Bloom RD. 2004. Changes in intracellular chloride after oxygen-glucose deprivation of the adult hippocampal slice: effect of diazepam. *J Neurosci* 24: 4478-88

Gamba G. 1999. Molecular biology of distal nephron sodium transport mechanisms. *Kidney Int* 56: 1606-22

Gamba G. 2005. Molecular physiology and pathophysiology of electroneutral cation-chloride cotransporters. *Physiol Rev* 85: 423-93

Gamba G, Saltzberg SN, Lombardi M, Miyanoshita A, Lytton J, et al. 1993. Primary structure and functional expression of a cDNA encoding the thiazide-sensitive, electroneutral sodium-chloride cotransporter. *Proc Natl Acad Sci U S A* 90: 2749-53

Ganguly K, Schinder AF, Wong ST, Poo M. 2001. GABA itself promotes the developmental switch of neuronal GABAergic responses from excitation to inhibition. *Cell* 105: 521-32

Garbarini N, Delpire E. 2008. The RCC1 domain of protein associated with Myc (PAM) interacts with and regulates KCC2. *Cell Physiol Biochem* 22: 31-44

Garzon-Muvdi T, Pacheco-Alvarez D, Gagnon KB, Vazquez N, Ponce-Coria J, et al. 2007. WNK4 kinase is a negative regulator of K+-Cl- cotransporters. *Am J Physiol Renal Physiol* 292: F1197-207

Gauvain G, Chamma I, Chevy Q, Cabezas C, Irinopoulou T, et al. 2011. The neuronal K-Cl cotransporter KCC2 influences postsynaptic AMPA receptor content and lateral diffusion in dendritic spines. *Proc Natl Acad Sci U S A* 108: 15474-9

Gillen CM, Forbush B, 3rd. 1999. Functional interaction of the K-Cl cotransporter (KCC1) with the Na-K-Cl cotransporter in HEK-293 cells. *Am J Physiol* 276: C328-36

Glykys J, Mody I. 2007. Activation of GABAA receptors: views from outside the synaptic cleft. *Neuron* 56: 763-70

Gonzalez-Islas C, Chub N, Garcia-Bereguiain MA, Wenner P. 2010. GABAergic synaptic scaling in embryonic motoneurons is mediated by a shift in the chloride reversal potential. *J Neurosci* 30: 13016-20

Gonzalez-Islas C, Chub N, Wenner P. 2009. NKCC1 and AE3 appear to accumulate chloride in embryonic motoneurons. *J Neurophysiol* 101: 507-18

Greengard P. 2001. The neurobiology of slow synaptic transmission. *Science* 294: 1024-30

Grégory Gauvain IC, Quentin Chevy, Carolina Cabezas, Theano Irinopoulou, Natalia Bodrug, Michèle Carnaud, Sabine Lévi, and Jean Christophe Poncer. 2011 The neuronal K-Cl cotransporter KCC2 influences postsynaptic AMPA receptor content and lateral diffusion in dendritic spines. *PNAS* 108 15474-79

Groth RD, Dunbar RL, Mermelstein PG. 2003. Calcineurin regulation of neuronal plasticity. *Biochem Biophys Res Commun* 311: 1159-71

Grunder S, Thiemann A, Pusch M, Jentsch TJ. 1992. Regions involved in the opening of CIC-2 chloride channel by voltage and cell volume. *Nature* 360: 759-62

Gulyas AI, Sik A, Payne JA, Kaila K, Freund TF. 2001. The KCl cotransporter, KCC2, is highly expressed in the vicinity of excitatory synapses in the rat hippocampus. *Eur J Neurosci* 13: 2205-17

Haas KF, Macdonald RL. 1999. GABAA receptor subunit gamma2 and delta subtypes confer unique kinetic properties on recombinant GABAA receptor currents in mouse fibroblasts. *J Physiol* 514 (Pt 1): 27-45

Hartmann AM, Blaesse P, Kranz T, Wenz M, Schindler J, et al. 2009. Opposite effect of membrane raft perturbation on transport activity of KCC2 and NKCC1. *J Neurochem* 111: 321-31

Hasbargen T, Ahmed MM, Miranpuri G, Li L, Kahle KT, et al. 2010. Role of NKCC1 and KCC2 in the development of chronic neuropathic pain following spinal cord injury. *Ann N Y Acad Sci* 1198: 168-72

He Z, Tessier-Lavigne M. 1997. Neuropilin is a receptor for the axonal chemorepellent Semaphorin III. *Cell* 90: 739-51

Hekmat-Scafe DS, Lundy MY, Ranga R, Tanouye MA. 2006. Mutations in the K+/Cl- cotransporter gene kazachoc (kcc) increase seizure susceptibility in Drosophila. *J Neurosci* 26: 8943-54

Herrera VL, Cova T, Sassoon D, Ruiz-Opazo N. 1994. Developmental cell-specific regulation of Na(+)-K(+)-ATPase alpha 1-, alpha 2-, and alpha 3-isoform gene expression. *Am J Physiol* 266: C1301-12

Hollmann M, Heinemann S. 1994. Cloned glutamate receptors. *Annu Rev Neurosci* 17: 31-108

Holmgren CD, Mukhtarov M, Malkov AE, Popova IY, Bregestovski P, Zilberter Y. 2010. Energy substrate availability as a determinant of neuronal resting potential, GABA signaling and spontaneous network activity in the neonatal cortex in vitro. *J Neurochem* 112: 900-12

Huang WC, Xiao S, Huang F, Harfe BD, Jan YN, Jan LY. 2012. Calcium-activated chloride channels (CaCCs) regulate action potential and synaptic response in hippocampal neurons. *Neuron* 74: 179-92

Huberfeld G, Wittner L, Clemenceau S, Baulac M, Kaila K, et al. 2007. Perturbed chloride homeostasis and GABAergic signaling in human temporal lobe epilepsy. *J Neurosci* 27: 9866-73

Hubner CA, Stein V, Hermans-Borgmeyer I, Meyer T, Ballanyi K, Jentsch TJ. 2001. Disruption of KCC2 reveals an essential role of K-Cl cotransport already in early synaptic inhibition. *Neuron* 30: 515-24

Hyde TM, Lipska BK, Ali T, Mathew SV, Law AJ, et al. 2011. Expression of GABA signaling molecules KCC2, NKCC1, and GAD1 in cortical development and schizophrenia. *J Neurosci* 31: 11088-95

Ikeda K, Onimaru H, Yamada J, Inoue K, Ueno S, et al. 2004. Malfunction of respiratory-related neuronal activity in Na+, K+-ATPase alpha2 subunit-deficient mice is attributable to abnormal Cl- homeostasis in brainstem neurons. *J Neurosci* 24: 10693-701

Ikeda M, Toyoda H, Yamada J, Okabe A, Sato K, et al. 2003. Differential development of cation-chloride cotransporters and Cl- homeostasis contributes to differential GABAergic actions between developing rat visual cortex and dorsal lateral geniculate nucleus. *Brain Res* 984: 149-59

Inglefield JR, Schwartz-Bloom RD. 1998. Activation of excitatory amino acid receptors in the rat hippocampal slice increases intracellular Cl- and cell volume. *J Neurochem* 71: 1396-404

Inoue H, Okada Y. 2007. Roles of volume-sensitive chloride channel in excitotoxic neuronal injury. *J Neurosci* 27: 1445-55

Inoue K, Furukawa T, Kumada T, Yamada J, Wang T, et al. 2012. Taurine inhibits K+-Cl- cotransporter KCC2 to regulate embryonic Cl- homeostasis via with-no-lysine (WNK) protein kinase signaling pathway. *J Biol Chem* 287: 20839-50

Inoue K, Ueno S, Fukuda A. 2004a. Interaction of neuron-specific K+-Cl- cotransporter, KCC2, with brain-type creatine kinase. *FEBS Lett* 564: 131-5

Inoue K, Ueno S, Fukuda A. 2004b. Interaction of neuron-specific K+-Cl− cotransporter, KCC2, with brain-type creatine kinase. *FEBS Lett* 564: 131-35

Inoue K, Yamada J, Ueno S, Fukuda A. 2006a. Brain-type creatine kinase activates neuron-specific K+-Cl- co-transporter KCC2. *J Neurochem* 96: 598-608

Inoue K, Yamada J, Ueno S, Fukuda A. 2006b. Brain-type creatine kinase activates neuron-specific K+-Cl- co-transporter KCC2. *J Neurochem* 96: 598-608

Ivakine EA, Acton BA, Mahadevan V, Ormond J, Tang M, et al. 2013. Neto2 is a KCC2 interacting protein required for neuronal Cl- regulation in hippocampal neurons. *Proc Natl Acad Sci U S A* 110: 3561-6

Jarolimek W, Lewen A, Misgeld U. 1999. A furosemide-sensitive K+-Cl- cotransporter counteracts intracellular Cl- accumulation and depletion in cultured rat midbrain neurons. *J Neurosci* 19: 4695-704

Jean-Xavier C, Mentis GZ, O'Donovan MJ, Cattaert D, Vinay L. 2007. Dual personality of GABA/glycine-mediated depolarizations in immature spinal cord. *Proc Natl Acad Sci U S A* 104: 11477-82

Jentsch TJ, Stein V, Weinreich F, Zdebik AA. 2002. Molecular structure and physiological function of chloride channels. *Physiol Rev* 82: 503-68

Jourdain P, Pavillon N, Moratal C, Boss D, Rappaz B, et al. 2011. Determination of transmembrane water fluxes in neurons elicited by glutamate ionotropic receptors and by the cotransporters KCC2 and NKCC1: a digital holographic microscopy study. *J Neurosci* 31: 11846-54

Kahle KT, Rinehart J, de Los Heros P, Louvi A, Meade P, et al. 2005. WNK3 modulates transport of Cl- in and out of cells: implications for control of cell volume and neuronal excitability. *Proc Natl Acad Sci U S A* 102: 16783-8

Kahle KT, Rinehart J, Lifton RP. 2010. Phosphoregulation of the Na-K-2Cl and K-Cl cotransporters by the WNK kinases. *Biochimica et biophysica acta* 1802: 1150-8

Kahle KT, Staley KJ, Nahed BV, Gamba G, Hebert SC, et al. 2008. Roles of the cation-chloride cotransporters in neurological disease. *Nat Clin Pract Neurol* 4: 490-503

Kaila K. 1994. Ionic basis of GABAA receptor channel function in the nervous system. *Prog Neurobiol* 42: 489-537

Kalkman HO. 2011. Alterations in the expression of neuronal chloride transporters may contribute to schizophrenia. *Prog Neuropsychopharmacol Biol Psychiatry* 35: 410-4

Kandel ER, Spencer WA. 1961. Electrophysiology of hippocampal neurons. II. After-potentials and repetitive firing. *J Neurophysiol* 24: 243-59

Karadsheh MF, Byun N, Mount DB, Delpire E. 2004. Localization of the KCC4 potassium-chloride cotransporter in the nervous system. *Neuroscience* 123: 381-91

Karadsheh MF, Delpire E. 2001. Neuronal restrictive silencing element is found in the KCC2 gene: molecular basis for KCC2-specific expression in neurons. *J Neurophysiol* 85: 995-7

Kennedy MB. 2000. Signal-processing machines at the postsynaptic density. *Science* 290: 750-4

Khirug S, Huttu K, Ludwig A, Smirnov S, Voipio J, et al. 2005. Distinct properties of functional KCC2 expression in immature mouse hippocampal neurons in culture and in acute slices. *Eur J Neurosci* 21: 899-904

Kitamura A, Ishibashi H, Watanabe M, Takatsuru Y, Brodwick M, Nabekura J. 2008. Sustained depolarizing shift of the GABA reversal potential by glutamate receptor activation in hippocampal neurons. *Neurosci Res* 62: 270-7

Kuntz A, Clement HW, Lehnert W, van Calker D, Hennighausen K, et al. 2004. Effects of secretin on extracellular amino acid concentrations in rat hippocampus. *J Neural Transm* 111: 931-9

Kyrozis A, Reichling DB. 1995. Perforated-patch recording with gramicidin avoids artifactual changes in intracellular chloride concentration. *J Neurosci Methods* 57: 27-35

Lauf PK, Adragna NC. 2004. Twenty-five years of K-Cl cotransport: from stimulation by a thiol reaction to cloning of the full-length KCCs. *Adv Exp Med Biol* 559: 11-28

Lauf PK, Bauer J. 1987a. Direct evidence for chloride-dependent volume reduction in macrocytic sheep reticulocytes. *Biochem Biophys Res Commun* 144: 849-55

Lauf PK, Bauer J. 1987b. Direct evidence for chloride-dependent volume reduction in macrocytic sheep reticulocytes. *Biochem Biophys Res Commun* 144: 849-55
Lauf PK, Perkins CM, Adragna NC. 1985. Cell volume and metabolic dependence of NEM-activated K+-Cl- flux in human red blood cells. *Am J Physiol* 249: C124-8
Lauf PK, Theg BE. 1980. A chloride dependent K+ flux induced by N-ethylmaleimide in genetically low K+ sheep and goat erythrocytes. *Biochem Biophys Res Commun* 92: 1422-8
Lauf PK, Zhang J, Delpire E, Fyffe RE, Mount DB, Adragna NC. 2001. K-Cl co-transport: immunocytochemical and functional evidence for more than one KCC isoform in high K and low K sheep erythrocytes. *Comp Biochem Physiol A Mol Integr Physiol* 130: 499-509
Lee H, Chen CX, Liu YJ, Aizenman E, Kandler K. 2005a. KCC2 expression in immature rat cortical neurons is sufficient to switch the polarity of GABA responses. *Eur J Neurosci* 21: 2593-9
Lee H, Chen CX, Liu YJ, Aizenman E, Kandler K. 2005b. KCC2 expression in immature rat cortical neurons is sufficient to switch the polarity of GABA responses. *Eur J Neurosci* 21: 2593-9
Lee HH, Deeb TZ, Walker JA, Davies PA, Moss SJ. 2011. NMDA receptor activity downregulates KCC2 resulting in depolarizing GABAA receptor-mediated currents. *Nat Neurosci* 14: 736-43
Lee HH, Jurd R, Moss SJ. 2010. Tyrosine phosphorylation regulates the membrane trafficking of the potassium chloride co-transporter KCC2. *Mol Cell Neurosci* 45: 173-9
Lee HH, Walker JA, Williams JR, Goodier RJ, Payne JA, Moss SJ. 2007. Direct protein kinase C-dependent phosphorylation regulates the cell surface stability and activity of the potassium chloride cotransporter KCC2. *J Biol Chem* 282: 29777-84
Leitch E, Coaker J, Young C, Mehta V, Sernagor E. 2005. GABA type-A activity controls its own developmental polarity switch in the maturing retina. *J Neurosci* 25: 4801-5
Lenertz LY, Lee BH, Min X, Xu BE, Wedin K, et al. 2005. Properties of WNK1 and implications for other family members. *J Biol Chem* 280: 26653-8
Lerma AR-MaJ. 1998. Kainate Receptor Modulation of GABA Release Involves a Metabotropic Function. *Neuron*
20: 1211-18
Lerma J. 2006. Kainate receptor physiology. *Curr Opin Pharmacol* 6: 89-97
Li H, Khirug S, Cai C, Ludwig A, Blaesse P, et al. 2007. KCC2 interacts with the dendritic cytoskeleton to promote spine development. *Neuron* 56: 1019-33
Li H, Tornberg J, Kaila K, Airaksinen MS, Rivera C. 2002. Patterns of cation-chloride cotransporter expression during embryonic rodent CNS development. *Eur J Neurosci* 16: 2358-70
Lindau M, Fernandez JM. 1986. A patch-clamp study of histamine-secreting cells. *J Gen Physiol* 88: 349-68
Loscher W, Puskarjov M, Kaila K. 2013. Cation-chloride cotransporters NKCC1 and KCC2 as potential targets for novel antiepileptic and antiepileptogenic treatments. *Neuropharmacology* 69: 62-74
Lu J, Helton TD, Blanpied TA, Racz B, Newpher TM, et al. 2007. Postsynaptic positioning of endocytic zones and AMPA receptor cycling by physical coupling of dynamin-3 to Homer. *Neuron* 55: 874-89
Ludwig A, Li H, Saarma M, Kaila K, Rivera C. 2003. Developmental up-regulation of KCC2 in the absence of GABAergic and glutamatergic transmission. *Eur J Neurosci* 18: 3199-206
Ludwig A, Uvarov P, Pellegrino C, Thomas-Crusells J, Schuchmann S, et al. 2011a. Neurturin evokes MAPK-dependent upregulation of Egr4 and KCC2 in developing neurons. *Neural Plast* 2011: 1-8
Ludwig A, Uvarov P, Soni S, Thomas-Crusells J, Airaksinen MS, Rivera C. 2011b. Early growth response 4 mediates BDNF induction of potassium chloride cotransporter 2 transcription. *J Neurosci* 31: 644-9

Mahajan VB, Pai KS, Lau A, Cunningham DD. 2000. Creatine kinase, an ATP-generating enzyme, is required for thrombin receptor signaling to the cytoskeleton. *Proc Natl Acad Sci U S A* 97: 12062-7

Malinow R, Madison DV, Tsien RW. 1988. Persistent protein kinase activity underlying long-term potentiation. *Nature* 335: 820-4

Man Tang EI, Vivek Mahadevan, Michael W. Salter, Roderick R. McInnes. 2012. Neto2 Interacts with the Scaffolding Protein GRIP and Regulates Synaptic Abundance of Kainate Receptors. *PLoS One* 7

McEntee WJ, Crook TH. 1993. Glutamate: its role in learning, memory, and the aging brain. *Psychopharmacology (Berl)* 111: 391-401

Melyan Z WH, Lancaster B. 2002 Metabotropic-mediated kainate receptor regulation of IsAHP and excitability in pyramidal cells. *Neuron.* 34: 107-14

Melyan Z, Wheal HV, Lancaster B. 2002. Metabotropic-mediated kainate receptor regulation of IsAHP and excitability in pyramidal cells. *Neuron* 34: 107-14

Mercado A, Broumand V, Zandi-Nejad K, Enck AH, Mount DB. 2006a. A C-terminal domain in KCC2 confers constitutive K+-Cl- cotransport. *J Biol Chem* 281: 1016-26

Mercado A, Broumand V, Zandi-Nejad K, Enck AH, Mount DB. 2006b. A C-terminal domain in KCC2 confers constitutive K+-Cl- cotransport. *J Biol Chem* 281: 1016-26

Mercado A, Mount DB, Gamba G. 2004. Electroneutral cation-chloride cotransporters in the central nervous system. *Neurochem Res* 29: 17-25

Mercado A, Song L, Vazquez N, Mount DB, Gamba G. 2000. Functional comparison of the K+-Cl- cotransporters KCC1 and KCC4. *J Biol Chem* 275: 30326-34

Mercado A, Vazquez N, Song L, Cortes R, Enck AH, et al. 2005. NH2-terminal heterogeneity in the KCC3 K+-Cl- cotransporter. *Am J Physiol Renal Physiol* 289: F1246-61

Michishita M, Ikeda T, Nakashiba T, Ogawa M, Tashiro K, et al. 2003. A novel gene, Btcl1, encoding CUB and LDLa domains is expressed in restricted areas of mouse brain. *Biochem Biophys Res Commun* 306: 680-86

Michishita M, Ikeda T, Nakashiba T, Ogawa M, Tashiro K, et al. 2004. Expression of Btcl2, a novel member of Btcl gene family, during development of the central nervous system. *Brain Res Dev Brain Res* 153: 135-42

Morgado C, Pinto-Ribeiro F, Tavares I. 2008. Diabetes affects the expression of GABA and potassium chloride cotransporter in the spinal cord: a study in streptozotocin diabetic rats. *Neurosci Lett* 438: 102-6

Mount DB, Delpire E, Gamba G, Hall AE, Poch E, et al. 1998. The electroneutral cation-chloride cotransporters. *J Exp Biol* 201: 2091-102

Mount DB, Mercado A, Song L, Xu J, George AL, Jr., et al. 1999. Cloning and characterization of KCC3 and KCC4, new members of the cation-chloride cotransporter gene family. *J Biol Chem* 274: 16355-62

Mulkey RM, Herron CE, Malenka RC. 1993. An essential role for protein phosphatases in hippocampal long-term depression. *Science* 261: 1051-5

Neher E, Sakmann B, Steinbach JH. 1978. The extracellular patch clamp: a method for resolving currents through individual open channels in biological membranes. *Pflugers Arch* 375: 219-28

Ng D, Pitcher GM, Szilard RK, Sertie A, Kanisek M, et al. 2009. Neto1 is a novel CUB-domain NMDA receptor-interacting protein required for synaptic plasticity and learning. *PLoS Biol* 7: e41

Nicoll RA, Tomita S, Bredt DS. 2006. Auxiliary subunits assist AMPA-type glutamate receptors. *Science* 311: 1253-6

O'Kane G, Kensinger EA, Corkin S. 2004. Evidence for semantic learning in profound amnesia: an investigation with patient H.M. *Hippocampus* 14: 417-25

Okabe A, Yokokura M, Toyoda H, Shimizu-Okabe C, Ohno K, et al. 2003. Changes in chloride homeostasis-regulating gene expressions in the rat hippocampus following amygdala kindling. *Brain Res* 990: 221-6

Otis TS, Staley KJ, Mody I. 1991. Perpetual inhibitory activity in mammalian brain slices generated by spontaneous GABA release. *Brain Res* 545: 142-50

Owens DF, Boyce LH, Davis MB, Kriegstein AR. 1996. Excitatory GABA responses in embryonic and neonatal cortical slices demonstrated by gramicidin perforated-patch recordings and calcium imaging. *J Neurosci* 16: 6414-23

Pan D, Kalfa TA, Wang D, Risinger M, Crable S, et al. 2011. K-Cl cotransporter gene expression during human and murine erythroid differentiation. *J Biol Chem* 286: 30492-503

Park M, Penick EC, Edwards JG, Kauer JA, Ehlers MD. 2004. Recycling endosomes supply AMPA receptors for LTP. *Science* 305: 1972-5

Pathak HR, Weissinger F, Terunuma M, Carlson GC, Hsu FC, et al. 2007. Disrupted dentate granule cell chloride regulation enhances synaptic excitability during development of temporal lobe epilepsy. *J Neurosci* 27: 14012-22

Payne JA. 1997. Functional characterization of the neuronal-specific K-Cl cotransporter: implications for [K+]o regulation. *Am J Physiol* 273: C1516-25

Payne JA, Rivera C, Voipio J, Kaila K. 2003. Cation–chloride co-transporters in neuronal communication, development and trauma. *Trends Neurosci* 26: 199-206

Payne JA, Stevenson TJ, Donaldson LF. 1996. Molecular characterization of a putative K-Cl cotransporter in rat brain. A neuronal-specific isoform. *J Biol Chem* 271: 16245-52

Perrais D, Veran J, Mulle C. 2010. Gating and permeation of kainate receptors: differences unveiled. *Trends Pharmacol Sci* 31: 516-22

Piechotta K, Lu J, Delpire E. 2002. Cation chloride cotransporters interact with the stress-related kinases Ste20-related proline-alanine-rich kinase (SPAK) and oxidative stress response 1 (OSR1). *J Biol Chem* 277: 50812-9

Plotkin MD, Snyder EY, Hebert SC, Delpire E. 1997. Expression of the Na-K-2Cl cotransporter is developmentally regulated in postnatal rat brains: a possible mechanism underlying GABA's excitatory role in immature brain. *J Neurobiol* 33: 781-95

Pouille F, Scanziani M. 2001. Enforcement of temporal fidelity in pyramidal cells by somatic feed-forward inhibition. *Science* 293: 1159-63

Price TJ, Cervero F, Gold MS, Hammond DL, Prescott SA. 2009. Chloride regulation in the pain pathway. *Brain Res Rev* 60: 149-70

Puskarjov M, Ahmad F, Kaila K, Blaesse P. 2012. Activity-dependent cleavage of the K-Cl cotransporter KCC2 mediated by calcium-activated protease calpain. *J Neurosci* 32: 11356-64

Reali C, Fernandez A, Radmilovich M, Trujillo-Cenoz O, Russo RE. 2011. GABAergic signalling in a neurogenic niche of the turtle spinal cord. *J Physiol* 589: 5633-47

Rechsteiner M, Rogers SW. 1996. PEST sequences and regulation by proteolysis. *Trends Biochem Sci* 21: 267-71

Rettig J, Neher E. 2002. Emerging roles of presynaptic proteins in Ca++-triggered exocytosis. *Science* 298: 781-5

Rinehart J, Maksimova YD, Tanis JE, Stone KL, Hodson CA, et al. 2009. Sites of regulated phosphorylation that control K-Cl cotransporter activity. *Cell* 138: 525-36

Rivera C, Li H, Thomas-Crusells J, Lahtinen H, Viitanen T, et al. 2002. BDNF-induced TrkB activation down-regulates the K+-Cl- cotransporter KCC2 and impairs neuronal Cl- extrusion. *J Cell Biol* 159: 747-52

Rivera C, Voipio J, Kaila K. 2005. Two developmental switches in GABAergic signalling: the K+-Cl- cotransporter KCC2 and carbonic anhydrase CAVII. *J Physiol* 562: 27-36

Rivera C, Voipio J, Payne JA, Ruusuvuori E, Lahtinen H, et al. 1999. The K+/Cl- co-transporter KCC2 renders GABA hyperpolarizing during neuronal maturation. *Nature* 397: 251-5
Rivera C, Voipio J, Thomas-Crusells J, Li H, Emri Z, et al. 2004. Mechanism of activity-dependent downregulation of the neuron-specific K-Cl cotransporter KCC2. *J Neurosci* 24: 4683-91
Rodriguez-Moreno A, Sihra TS. 2007. Kainate receptors with a metabotropic modus operandi. *Trends Neurosci* 30: 630-7
Rogers S, Wells R, Rechsteiner M. 1986. Amino acid sequences common to rapidly degraded proteins: the PEST hypothesis. *Science* 234: 364-8
Rushmore J, Luebke J, Galler JR. 1998. Electrophysiological properties of rat hippocampal principal cells are unaltered by prenatal protein malnutrition. *Hippocampus* 8: 380-9
Russell JM. 2000. Sodium-potassium-chloride cotransport. *Physiol Rev* 80: 211-76
Saier MH, Jr. 2003. Tracing pathways of transport protein evolution. *Mol Microbiol* 48: 1145-56
Salin-Cantegrel A, Shekarabi M, Holbert S, Dion P, Rochefort D, et al. 2008. HMSN/ACC truncation mutations disrupt brain-type creatine kinase-dependant activation of K+/Cl- co-transporter 3. *Hum Mol Genet* 17: 2703-11
Salin PA, Prince DA. 1996. Spontaneous GABAA receptor-mediated inhibitory currents in adult rat somatosensory cortex. *J Neurophysiol* 75: 1573-88
Sallinen R, Tornberg J, Putkiranta M, Horelli-Kuitunen N, Airaksinen MS, Wessman M. 2001. Chromosomal localization of SLC12A5/Slc12a5, the human and mouse genes for the neuron-specific K(+)-Cl(-) cotransporter (KCC2) defines a new region of conserved homology. *Cytogenet Cell Genet* 94: 67-70
Santos SD, Carvalho AL, Caldeira MV, Duarte CB. 2009. Regulation of AMPA receptors and synaptic plasticity. *Neuroscience* 158: 105-25
Sarkar J, Wakefield S, MacKenzie G, Moss SJ, Maguire J. 2011. Neurosteroidogenesis is required for the physiological response to stress: role of neurosteroid-sensitive GABAA receptors. *J Neurosci* 31: 18198-210
Saxena NC, Macdonald RL. 1994. Assembly of GABAA receptor subunits: role of the delta subunit. *J Neurosci* 14: 7077-86
Scher MS, Painter MJ. 1989. Controversies concerning neonatal seizures. *Pediatr Clin North Am* 36: 281-310
Schomberg SL, Su G, Haworth RA, Sun D. 2001. Stimulation of Na-K-2Cl cotransporter in neurons by activation of Non-NMDA ionotropic receptor and group-I mGluRs. *J Neurophysiol* 85: 2563-75
Schroeder BC, Cheng T, Jan YN, Jan LY. 2008. Expression cloning of TMEM16A as a calcium-activated chloride channel subunit. *Cell* 134: 1019-29
Scoville WB, Milner B. 1957. Loss of recent memory after bilateral hippocampal lesions. *J Neurol Neurosurg Psychiatry* 20: 11-21
Segal M. 1983. Rat hippocampal neurons in culture: responses to electrical and chemical stimuli. *J Neurophysiol* 50: 1249-64
Sernagor E, Young C, Eglen SJ. 2003. Developmental modulation of retinal wave dynamics: shedding light on the GABA saga. *J Neurosci* 23: 7621-9
Sheng M, Kim MJ. 2002. Postsynaptic signaling and plasticity mechanisms. *Science* 298: 776-80
Shimell MJ, Ferguson EL, Childs SR, O'Connor MB. 1991. The Drosophila dorsal-ventral patterning gene tolloid is related to human bone morphogenetic protein 1. *Cell* 67: 469-81
Shulga A, Blaesse A, Kysenius K, Huttunen HJ, Tanhuanpaa K, et al. 2009. Thyroxin regulates BDNF expression to promote survival of injured neurons. *Mol Cell Neurosci* 42: 408-18
Soltesz I, Roberts JD, Takagi H, Richards JG, Mohler H, Somogyi P. 1990. Synaptic and Nonsynaptic Localization of Benzodiazepine/GABAA Receptor/Cl- Channel Complex Using Monoclonal Antibodies in the Dorsal Lateral Geniculate Nucleus of the Cat. *Eur J Neurosci* 2: 414-29

Somogyi P, Takagi H, Richards JG, Mohler H. 1989. Subcellular localization of benzodiazepine/GABAA receptors in the cerebellum of rat, cat, and monkey using monoclonal antibodies. *J Neurosci* 9: 2197-209

Song L, Mercado A, Vazquez N, Xie Q, Desai R, et al. 2002. Molecular, functional, and genomic characterization of human KCC2, the neuronal K-Cl cotransporter. *Brain Res Mol Brain Res* 103: 91-105

Staley K. 1994. The role of an inwardly rectifying chloride conductance in postsynaptic inhibition. *J Neurophysiol* 72: 273-84

Starke LC, Jennings ML. 1993. K-Cl cotransport in rabbit red cells: further evidence for regulation by protein phosphatase type 1. *Am J Physiol* 264: C118-24

Stein V, Hermans-Borgmeyer I, Jentsch TJ, Hubner CA. 2004. Expression of the KCl cotransporter KCC2 parallels neuronal maturation and the emergence of low intracellular chloride. *J Comp Neurol* 468: 57-64

Stohr H, Berger C, Frohlich S, Weber BH. 2002. A novel gene encoding a putative transmembrane protein with two extracellular CUB domains and a low-density lipoprotein class A module: isolation of alternatively spliced isoforms in retina and brain. *Gene* 286: 223-31

Strange K, Singer TD, Morrison R, Delpire E. 2000. Dependence of KCC2 K-Cl cotransporter activity on a conserved carboxy terminus tyrosine residue. *Am J Physiol Cell Physiol* 279: C860-7

Straub C, Tomita S. 2012. The regulation of glutamate receptor trafficking and function by TARPs and other transmembrane auxiliary subunits. *Curr Opin Neurobiol* 22: 488-95

Straub C, Zhang W, Howe JR. 2011. Neto2 modulation of kainate receptors with different subunit compositions. *J Neurosci* 31: 8078-82

Su G, Kintner DB, Sun D. 2002. Contribution of Na(+)-K(+)-Cl(-) cotransporter to high-[K(+)](o)- induced swelling and EAA release in astrocytes. *Am J Physiol Cell Physiol* 282: C1136-46

Su W, Shmukler BE, Chernova MN, Stuart-Tilley AK, de Franceschi L, et al. 1999. Mouse K-Cl cotransporter KCC1: cloning, mapping, pathological expression, and functional regulation. *Am J Physiol* 277: C899-912

Sullivan JE, Witte MK, Yamashita TS, Myers CM, Blumer JL. 1996. Pharmacokinetics of bumetanide in critically ill infants. *Clin Pharmacol Ther* 60: 405-13

Sun C, Zhang L, Chen G. 2013. An unexpected role of neuroligin-2 in regulating KCC2 and GABA functional switch. *Mol Brain* 6: 23

Swanson GT, Sakai R. 2009. Ligands for ionotropic glutamate receptors. *Progress in molecular and subcellular biology* 46: 123-57

Tang M, Ivakine E, Mahadevan V, Salter MW, McInnes RR. 2012. Neto2 interacts with the scaffolding protein GRIP and regulates synaptic abundance of kainate receptors. *PloS one* 7: e51433

Tang M, Pelkey KA, Ng D, Ivakine E, McBain CJ, et al. 2011. Neto1 is an auxiliary subunit of native synaptic kainate receptors. *J Neurosci* 31: 10009-18

Tao R, Li C, Newburn EN, Ye T, Lipska BK, et al. 2012. Transcript-specific associations of SLC12A5 (KCC2) in human prefrontal cortex with development, schizophrenia, and affective disorders. *J Neurosci* 32: 5216-22

Thiemann A, Grunder S, Pusch M, Jentsch TJ. 1992. A chloride channel widely expressed in epithelial and non-epithelial cells. *Nature* 356: 57-60

Titz S, Hans M, Kelsch W, Lewen A, Swandulla D, Misgeld U. 2003. Hyperpolarizing inhibition develops without trophic support by GABA in cultured rat midbrain neurons. *J Physiol* 550: 719-30

Toyoda H, Ohno K, Yamada J, Ikeda M, Okabe A, et al. 2003. Induction of NMDA and GABAA receptor-mediated Ca2+ oscillations with KCC2 mRNA downregulation in injured facial motoneurons. *J Neurophysiol* 89: 1353-62

Treiman DM. 1990. The role of benzodiazepines in the management of status epilepticus. *Neurology* 40: 32-42

Tu CF, Yan YT, Wu SY, Djoko B, Tsai MT, et al. 2008. Domain and functional analysis of a novel platelet-endothelial cell surface protein, SCUBE1. *J Biol Chem* 283: 12478-88

Turrigiano GG, Leslie KR, Desai NS, Rutherford LC, Nelson SB. 1998. Activity-dependent scaling of quantal amplitude in neocortical neurons. *Nature* 391: 892-6

Uvarov P, Ludwig A, Markkanen M, Pruunsild P, Kaila K, et al. 2007. A novel N-terminal isoform of the neuron-specific K-Cl cotransporter KCC2. *J Biol Chem* 282: 30570-6

Uvarov P, Ludwig A, Markkanen M, Rivera C, Airaksinen MS. 2006. Upregulation of the neuron-specific K+/Cl- cotransporter expression by transcription factor early growth response 4. *J Neurosci* 26: 13463-73

Uvarov P, Ludwig A, Markkanen M, Soni S, Hubner CA, et al. 2009. Coexpression and heteromerization of two neuronal K-Cl cotransporter isoforms in neonatal brain. *J Biol Chem* 284: 13696-704

van den Pol AN, Obrietan K, Chen G. 1996. Excitatory actions of GABA after neuronal trauma. *J Neurosci* 16: 4283-92

Vu TQ, Payne JA, Copenhagen DR. 2000. Localization and developmental expression patterns of the neuronal K-Cl cotransporter (KCC2) in the rat retina. *J Neurosci* 20: 1414-23

Vukicevic M, Kellenberger S. 2004. Modulatory effects of acid-sensing ion channels on action potential generation in hippocampal neurons. *Am J Physiol Cell Physiol* 287: C682-90

Wake H, Watanabe M, Moorhouse AJ, Kanematsu T, Horibe S, et al. 2007a. Early changes in KCC2 phosphorylation in response to neuronal stress result in functional downregulation. *J Neurosci* 27: 1642-50

Wake H, Watanabe M, Moorhouse AJ, Kanematsu T, Horibe S, et al. 2007b. Early changes in KCC2 phosphorylation in response to neuronal stress result in functional downregulation. *J Neurosci* 27: 1642-50

Walz W. 1989. Role of glial cells in the regulation of the brain ion microenvironment. *Prog Neurobiol* 33: 309-33

Wang C, Shimizu-Okabe C, Watanabe K, Okabe A, Matsuzaki H, et al. 2002. Developmental changes in KCC1, KCC2, and NKCC1 mRNA expressions in the rat brain. *Brain Res Dev Brain Res* 139: 59-66

Wardle RA, Poo MM. 2003. Brain-derived neurotrophic factor modulation of GABAergic synapses by postsynaptic regulation of chloride transport. *J Neurosci* 23: 8722-32

Watanabe M, Wake H, Moorhouse AJ, Nabekura J. 2009. Clustering of neuronal K+-Cl- cotransporters in lipid rafts by tyrosine phosphorylation. *J Biol Chem* 284: 27980-8

Wei B, Kumada T, Furukawa T, Inoue K, Watanabe M, et al. 2013. Pre- and post-synaptic switches of GABA actions associated with Cl- homeostatic changes are induced in the spinal nucleus of the trigeminal nerve in a rat model of trigeminal neuropathic pain. *Neuroscience* 228: 334-48

Wenner P. 2011. Mechanisms of GABAergic homeostatic plasticity. *Neural Plast* 2011: 489470

Wenner P. 2013. Homeostatic synaptic plasticity in developing spinal networks driven by excitatory GABAergic currents. *Neuropharmacology*

Wenz M, Hartmann AM, Friauf E, Nothwang HG. 2009. CIP1 is an activator of the K+-Cl- cotransporter KCC2. *Biochem Biophys Res Commun* 381: 388-92

Williams JR, Sharp JW, Kumari VG, Wilson M, Payne JA. 1999. The neuron-specific K-Cl cotransporter, KCC2. Antibody development and initial characterization of the protein. *J Biol Chem* 274: 12656-64

Wisden W, Parker EM, Mahle CD, Grisel DA, Nowak HP, et al. 1993. Cloning and characterization of the rat 5-HT5B receptor. Evidence that the 5-HT5B receptor couples to a G protein in mammalian cell membranes. *FEBS Lett* 333: 25-31

Woo NS, Lu J, England R, McClellan R, Dufour S, et al. 2002. Hyperexcitability and epilepsy associated with disruption of the mouse neuronal-specific K-Cl cotransporter gene. *Hippocampus* 12: 258-68

Woodin MA, Ganguly K, Poo M-m. 2003. Coincident Pre- and Postsynaptic Activity Modifies GABAergic Synapses by Postsynaptic Changes in Cl− Transporter Activity. *Neuron* 39: 807-20

Wyss M, Kaddurah-Daouk R. 2000. Creatine and creatinine metabolism. *Physiol Rev* 80: 1107-213

Xu B, English JM, Wilsbacher JL, Stippec S, Goldsmith EJ, Cobb MH. 2000. WNK1, a novel mammalian serine/threonine protein kinase lacking the catalytic lysine in subdomain II. *J Biol Chem* 275: 16795-801

Xu JC, Lytle C, Zhu TT, Payne JA, Benz E, Jr., Forbush B, 3rd. 1994. Molecular cloning and functional expression of the bumetanide-sensitive Na-K-Cl cotransporter. *Proc Natl Acad Sci U S A* 91: 2201-5

Yan D, Tomita S. 2012. Defined criteria for auxiliary subunits of glutamate receptors. *J Physiol* 590: 21-31

Zadran S, Jourdi H, Rostamiani K, Qin Q, Bi X, Baudry M. 2010. Brain-derived neurotrophic factor and epidermal growth factor activate neuronal m-calpain via mitogen-activated protein kinase-dependent phosphorylation. *J Neurosci* 30: 1086-95

Zhang RW, Wei HP, Xia YM, Du JL. 2010. Development of light response and GABAergic excitation-to-inhibition switch in zebrafish retinal ganglion cells. *J Physiol* 588: 2557-69

Zhang W, St-Gelais F, Grabner CP, Trinidad JC, Sumioka A, et al. 2009. A transmembrane accessory subunit that modulates kainate-type glutamate receptors. *Neuron* 61: 385-96

Zheng Y, Mellem JE, Brockie PJ, Madsen DM, Maricq AV. 2004. SOL-1 is a CUB-domain protein required for GLR-1 glutamate receptor function in C. elegans. *Nature* 427: 451-7

Zhou HY, Chen SR, Byun HS, Chen H, Li L, et al. 2012. N-methyl-D-aspartate receptor- and calpain-mediated proteolytic cleavage of K+-Cl- cotransporter-2 impairs spinal chloride homeostasis in neuropathic pain. *J Biol Chem* 287: 33853-64

Zhu L, Lovinger D, Delpire E. 2005. Cortical neurons lacking KCC2 expression show impaired regulation of intracellular chloride. *J Neurophysiol* 93: 1557-68

Zilberter Y, Zilberter T, Bregestovski P. 2010. Neuronal activity in vitro and the in vivo reality: the role of energy homeostasis. *Trends Pharmacol Sci* 31: 394-401

Zuniga L, Niemeyer MI, Varela D, Catalan M, Cid LP, Sepulveda FV. 2004. The voltage-dependent ClC-2 chloride channel has a dual gating mechanism. *J Physiol* 555: 671-82